A suite of mathematical models to simulate the water and salt circulation in the Vaal river water supply system

C. E. Herold

A SUITE OF MATHEMATICAL MODELS TO SIMULATE THE WATER AND SALT CIRCULATION IN THE VAAL RIVER WATER SUPPLY SYSTEM

by

Christopher Edward Herold

A thesis submitted to the Faculty of Engineering, University of the Witwatersrand, Johannesburg, for the degree of Doctor of Philosophy

September, 1981.

DECLARATION

I, the undersigned, declare that this thesis is entirely my own work and has not been submitted for degree purposes to any other university.

C E Herold

DEDICATION

To the memory of my late father, Edward, whose great courage in the face of adversity inspired me to persevere; to my mother, Esther, who encouraged me by patiently tolerating my long silences and to my God Who created an ordered universe and endowed me with an inquisitive mind with which to explore its exciting mysteries.

ABSTRACT

The Pretoria-Witwatersrand-Vereeniging (PWV) complex relies for water supply on the resources of the Vaal basin, supplemented by importation from the Tugela river. Most of the water supplied to the region is abstracted from the Vaal Barrage, which is also the sink for much of the water-borne pollution generated in the southern portion of the PWV complex. This feature of the system has led to an ever-increasing build-up of total dissolved solids (TDS) in the water supplies, resulting in substantial economic loss to consumers. Increasing mineralization is ascribable mainly to return of effluents to the Vaal Barrage where the concentrated salts are re-introduced to the Rand Water Board distribution system. The problem is exacerbated by the washoff, during the wet season, of enormous diffuse-source salt loads, leading to intolerably high peak TDS concentrations.

A suite of deterministic mathematical models has been developed, and successfully tested, with the aim of predicting the anticipated severity of mineralization problems of the future and of facilitating objective comparison of the merits of various ameliorative measures.

The first of the suite is the daily washoff model, designed to simulate daily catchment runoffs and associated daily diffuse-source salt washoff. Basic input is daily meteorological data. In the model account is taken of both surface and sub-surface flow processes. Calibration of the model parameters for each of the twelve sub-catchments comprising the southern PWV region was effected with records of discharge and water quality at key monitoring points. A relationship was established between industrial water consumption and diffuse-source salt generation rates by means of which pollution levels likely to arise in the future could be predicted.

Daily fluctuations of discharge and salt concentration at any point in the tributaries of the southern PWV region and in the Vaal Barrage, as well as water and salt storages in the major impoundments of the Vaal basin are simulated by means of the daily feed-back model. A feed-back element is incorporated which accounts for the mixing of water distributed to each of 27 sub-regions of the southern PWV catchment, the addition of salts through usage and the routing of effluents, together with diffuse-source washoff generated by the first model, through the tributary system back into the Barrage. The transmission of pollutants through the Barrage is simulated by means of a one-dimensional, cell-type level-pool model. This model was used to check the reliability of calibrated parameter values used in the daily washoff model by comparing simulated daily salt concentrations in the Vaal Barrage with those observed at the Rand Water Board Barrage intakes.

The third model, a simplified version of the daily feed-back model designed to operate at a monthly computational time step, was developed to facilitate preliminary comparisons of the various options. This coarse time-step model is relatively cheaper to run and makes possible the testing of each option with several different hydrological sequences. Economic factors relating salt concentration in water supply to costs to consumers have also been incorporated.

The two feed-back models were designed in such a way that a wide variety of planning and management options could be modelled with the minimum of programming changes.

Procedures for comparing, with the aid of the models, the merits of various planning and management options to improve water quality have been evolved and are illustrated by way of example.

PREFACE

The thesis has for the sake of clarity been divided into three parts, each dealing with one of the major elements of the Pretoria-Witwatersrand-Vereeniging (PWV) model.

Part I describes the development of a model which, having meteorological data as basic input, simulates on a daily basis the runoff of water and associated salt loads from the catchment. This model is referred to as the daily washoff model.

Part II describes a model which can be used to simulate, on a daily basis, the circulation of both water and salt throughout the PWV complex. Provision is made for modelling the feed-back effect whereby the salts discharged with effluents from sewage treatment works, industries and mines, are recycled in the water supply system via Vaal Barrage. This model is referred to as the daily feed-back model.

Described in part III is a simplified version of the daily feed-back model, operating at monthly computational time step. This is called the monthly feed-back model.

The suite of models is designed for optimising the broad planning and management of water supplies within the Vaal basin. The role of each model is elucidated in the text. For the sake of brevity computer program listings and program user manuals have been omitted. These are documented in full in the reports of the Hydrological Research Unit to which reference is made in the introduction to each Part in the thesis.

ACKNOWLEDGEMENTS

This work is the fruit of a research project sponsored by the Water Research Commission and would not be complete without some mention of the far-sightedness displayed by this exemplary body in authorising the study. Little could have been achieved without the enthusiastic support of the staff of the Hydrological Research Unit and in particular its director, Professor D C Midgley, whose guidance and encouragement were invaluable. It has indeed been a privilege to work under this great doyen of hydrological research. Special credit is due to Dr. W V Pitman whose watershed model provided the foundation upon which the first part of this thesis is based.

My gratitude is extended also to members of staff of the Rand Water Board, the Directorate of Water Affairs, the Transvaal Provincial Administration, Johannesburg Municipality, the National Institute for Water Research of the CSIR, my employers, Messrs. Stewart, Sviridov and Oliver, and many others who have assisted me in this work.

I am conscious of the fact that my research did not take place in a vacuum. I am indebted to countless researchers, both local and abroad, upon whose work I have built and I trust that others will in turn follow to carry forward the growing edge of our knowledge to yet more distant frontiers and use this knowledge to the advantage of mankind.

PART I

THE DAILY WASHOFF MODEL

TABLE OF CONTENTS

TABLE OF CONTENTS - cont.

LIST OF FIGURES

LIST OF FIGURES - cont.

LIST OF FIGURES - cont.

LIST OF FIGURES - cont.

LIST OF FIGURES - cont.

LIST OF FIGURES - cont.

LIST OF FIGURES - cont

LIST OF FIGURES - cont

LIST OF TABLES

LIST OF TABLES - cont.

SYNOPSIS

This report describes a numerical model designed to generate, route and aggregate daily catchment runoffs, along with associated loadings of total dissolved solids derived from both point and diffuse sources.

Inputs to the model comprise calibration parameters, physical features of the catchment and of the channel reaches, point source effluents, daily rainfall and daily or average monthly potential evaporation.

The model element that generates daily catchment runoffs is an adaptation of the model developed by Pitman (1976), to which water quality parameters have been added. Salts are assumed to accumulate gradually on catchment surfaces from where they are washed off during rainfall events. Pervious catchment surfaces are dealt with separately from impervious surfaces and both surface and subsurface salt movements are modelled.

The channel routing component of the model routes the output from the catchment model, together with point source inputs, through a system of interconnected channel reaches. Irrigation, evaporation and bed seepage losses are accounted for and provision is made for simulating the behaviour of the extensive reed beds in the system.

Sensitivity analyses of the model parameters were performed and the model was tested on twelve catchments with satisfactory results. A strong correlation between industrial water supply and calibrated salt generation was established.

Guidelines to calibration procedures as well as worked examples are provided and the report contains a comprehensive user manual for the relevant computer programs.

CHAPTER 1 INTRODUCTION

1.1 Motivation

In 1975 the Water Research Commission initiated a study of the Pretoria-Witwatersrand-Vereeniging (PWV) Complex in regard to existing and incipient problems of water supply, waste water management and pollution control. Increasing mineral pollution of the water resources of this highly urbanised region was from the start recognised as a major problem. Of particular concern to the water supply authorities has been the increasingly frequent occurrence of transient TDS peaks at the RWB Vaal Barrage intakes. These peaks are usually of one or more days' duration and occur during the wet (summer) season when the tributaries of the southern PWVS catchment are in spate, giving rise to a pronounced "first flush" effect when salts stored on the catchment are washed out. These salts are derived from both point and diffuse sources. The major point injections are effluent returns from sewage works and groundwater pumped from mines. These can be readily identified and the flows and total salt loads can be estimated with reasonable accuracy.

Many studies have indicated, however, that a significant proportion of water pollutants of all categories are derived from nonpoint sources (Ackerman et al., 1978), (Council on Enviromental Quality, 1972), (Vitale and Spey, 1974), (Whipple et al., 1971), (Bryan, 1971), (Weibel et al., 1964), (Lester, 1975). For the southern PWVS region in particular it was found that more than 50 percent of the dissolved solids entering the Vaal Barrage via the tributaries during the hydrological year 1977/78 were derived from nonpoint sources (Herold et al., 1980).

Diffuse source pollutant loads cannot be measured directly and have to be estimated by subtracting known point source loadings from the total measured loads at stream monitoring points. Most of the streamflow gauges in the heavily polluted tributaries draining the southern PWV catchment are, however, rated only for low flows and records are both short and intermittent. Furthermore, prior to September 1977, only weekly (in some cases monthly)

grab samples of the tributary water were analysed. A means of patching and extending the available record was sought, in the first instance, in order to establish salt concentration frequency distributions and annual salt loadings at key points in the catchment so that problem areas could be identified. The patched data could then be used to simulate the effect on the system of various management and planning options for the abatement of water pollution.

The mathematical catchment model developed by Pitman (1976) presented a ready means of patching and extending the runoff records using available meteorological data. The Pitman model was developed specifically to suit the climatic conditions of Southern Africa. It has been extensively used with success and has gained wide acceptance.

Introduction of a water quality component to the model, however, required a fresh approach. A water quality model capable of simulating the behaviour of both point and nonpoint source dissolved solids was needed. Statistical models were rejected as inappropriate in view of the paucity of data and the complex interrelationship between the behaviour of the many tributaries and that of the major impoundments. Such models employ parameters that are devoid of any physical meaning, and therefore it is impossible to draw conclusions as to cause and effect; these models are thus incapable of predicting the consequences of adopting many of the management options that may be open. A deterministic model seemed the only acceptable alternative.

A vast array of deterministic water quality models are available, but none was found to be appropriate to the problem at hand. In the literature a great deal of emphasis has been placed upon the urban environment, with particular reference to the storm water management problems associated with combined sewer systems. These models, of which SWMM (Metcalf and Eddy, 1971) is perhaps the best known, are usually designed to operate at extremely short time steps (of the order of minutes) and require vast quantities of highly detailed input data. The enormous data preparation and computer costs involved in applying such detailed models to the complex PWVS region would be quite prohibitive.

SWMM is moreover an event-orientated model, not intended to be used for continuous long-term simulations. Some models, such as STORM (Army Corps of Engineers, 1975) and HSP (Hydrocomp, 1975) are continuous simulation models, but neither adequately represents the processes occurring in the pervious parts of a catchment. Although most of the pollutants are usually generated in urban areas, it is highly simplistic to assume that they are confined within the boundaries of the paved portions of the catchment.

Much of the generated pollution can be expected to be deposited on pervious catchment surfaces, particularly in the case of conservative pollutants derived from atmospheric fall-out. The importance of this largely overlooked process is highlighted in the case of the tributaries draining the southern PWVS region where it is found that several of the floods subsequent to the first flood of the wet season continue to exhibit high salinities throughout the season. Fig. 3.29 of section 3.2.2 which depicts streamflows and salinities at monitoring point N8 on the Natalspruit illustrates the point very well. The 1977/78 season was an above-average wet year, yet even the flood in February, a full five months into the wet season and immediately following the biggest flood of the season in late January, produced salinities approaching 1000 mg/ℓ.

This persistence in the pollutographs is most likely due to the effects of salts stored in the soil moisture and in the groundwater, because gutters and parking lots in the urban areas would by this stage have been well and truly flushed. There was to be found in the literature no model that paid sufficient attention to these important processes. *

---

* One of the most nearly applicable models that could be traced was the Nonpoint Source (NPS) model (Donigian and Crawford, 1976) but this model, although it takes account of sub-surface processes to model streamflow, does not take these processes into consideration when modelling the movement of pollutants. Sediment and sediment-like material are used as the basic indicators of nonpoint pollutants (Litwin and Donigian, 1978); in other words, washoff is treated as a purely surface phenomenon. This assumption is reasonable for particulate matter such as B.O.D., but is completely inappropriate for soluble salts.

The result was a decision to proceed with the development of a water quality model that could take due cognisance of sub-surface processes.

1.2 Program NACLØ1

The size of the catchments concerned (231 to 1119 km^2) indicated that a model operating at a time step of the order of one day would be most appropriate. Examination of available hydrographs and pollutographs at key points confirmed that most of the flood events and peak salt loadings were of more than one day duration. Data limitations in any case prescribed the daily time step as being the finest time resolution that could practically be adopted. The Pitman model (Pitman, 1976), which had already proved its capabilities, therefore became the obvious choice for adaptation into a water quality model both in terms of its proven reliability and in view of the author's familiarity with it.

The Pitman model uses meteorological data (rainfall and evaporation) discretised at daily intervals, and incorporates analogues to describe sub-surface processes. Conservative pollutant water quality processes were included in the model and the modifications are described in section 2.2.

1.3 Program NACLØ2

A channel routing model was developed to route the output from the washoff model along with known point-source effluents through the tributary system. Particular attention had to be given to the routing of water and salts through the extensive vlei (reed bed) systems of the upper Klip and Suikerbosrand rivers (some of these reed beds are over 50 km^2 in extent and play an important role in the routing process). This model is discussed in section 2.3.

Criteria used to test the model are discussed in section 3.1 while section 3.2 gives details of the tests performed. Section 3.3 deals with the correlation between calibrated diffuse source

salt generation rates and several catchment characteristics. The verification of calibrated model parameters for the twelve test catchments is described in section 3.4.

The sensitivity of modelled output to changes in the calibration parameters is discussed in Chapter 4 and Chapter 5 gives guidelines for calibration of the model.

Details of the data used as input to the model and a comprehensive users' manual for computer programs are given in HRU report No. 3/81 (Herold, 1981).

1.4 Programs NACLØ3 and NACL23

NACLØ3 is a program to produce a line-printer plot of observed and modelled daily discharges, salt concentrations and salt loads, while NACL23 produces an equivalent plot using a CALCOMP plotter.

1.5 Programs RANKØ1, RANKØ2 and RANKØ3

RANKØ1 is a program to produce a line-printer plot of duration curves of observed and modelled daily discharges, salt concentrations and salt loads, while RANKØ2 produces an equivalent plot using a CALCOMP plotter. RANKØ3 processes the output from NACLØ2 into a form suitable for use as input to RANKØ2.

All programs are written in FORTRAN IV and have been developed for an IBM 360 or 370 system.

CHAPTER 2 THE DAILY WASHOFF MODEL

2.1 Introduction

In this chapter the mathematical analogues representing the hydrological cycle and the movements of dissolved solids through the catchment environment are presented.

Rainfall-runoff processes and the accumulation, storage and release of salts in the catchment are described in section 2.2 while the channel routing model is described in section 2.3.

2.2 Structure of program NACLØ1

2.2.1 Catchment runoff modelling

That portion of program NACLØ1 which generates the daily catchment runoff from meteorological data is based on the Pitman model. Input comprises daily precipitation and monthly (or daily) potential evaporation. The initial soil moisture state is specified and the soil moisture and groundwater storage budget is maintained throughout the simulation.

Interception losses are subtracted from the daily precipitation. Depression storage does not constitute a specific component of the daily model; depression storage effects are taken care of in the assumed spatial distribution of catchment permeability.

Rainfall excess on impervious surfaces that are in direct communication with the drainage lines becomes surface runoff. On pervious surfaces, part of the rainfall excess enters soil moisture storage where it is subjected to evapotranspiration, and the remainder becomes surface runoff.

A portion of the water in the soil moisture percolates to groundwater storage. Water in groundwater storage is not subject to evapotranspiration but contributes to streamflow. A function is included in the model to allow for losses to deep-seated groundwater.

Fig. 2.1 depicts the operation of the model. Model processes are in most instances identical to those used by Pitman (1976). For the sake of completeness the salien. features of each are discussed here. Attention is drawn to the modifications that have been made by the author; these are described in detail.

a) Precipitation

For rainless days a computation time step of one day is used. On rain-days the rainfall duration is estimated by the equation derived by Pitman (1976)

$$\text{Duration (h)} = AA + BB \times \text{rainfall (mm)} \quad \ldots\ldots\ldots \quad (2.1)$$

where AA and BB are constants.

The duration as determined by equation 2.1 is rounded to the nearest whole number of hours. Pitman (1976) found, after analysing a plot of daily rainfall against duration for an autographic rainfall recorder at Pretoria, that values of 0,96 and 0,14 for AA and BB respectively fitted the observed data. Values suited to conditions elsewhere can be derived from analyses of local autographic rainfall records.

After the rainfall duration has been calculated, the daily rainfall total is disaggregated into hourly values. The assumption is made that the onset of rain coincides with the beginning of the day. After cessation of the storm a single time step of n hours is used, where n = 24-(rainfall duration).

The distribution of the rainfall within the estimated rainfall duration period is calculated assuming an S-shaped mass curve of rainfall as indicated in Fig. 2.2.

From the relationship derived by Pitman the mass curve can be represented by:

$$y = \frac{x^2}{x^2+(1-x)^2} \quad \ldots\ldots\ldots\ldots (2.2)$$

where $y = \dfrac{\text{cumulative precipitation}}{\text{total precipitation}}$

$x = \dfrac{\text{cumulative time}}{\text{total time}}$

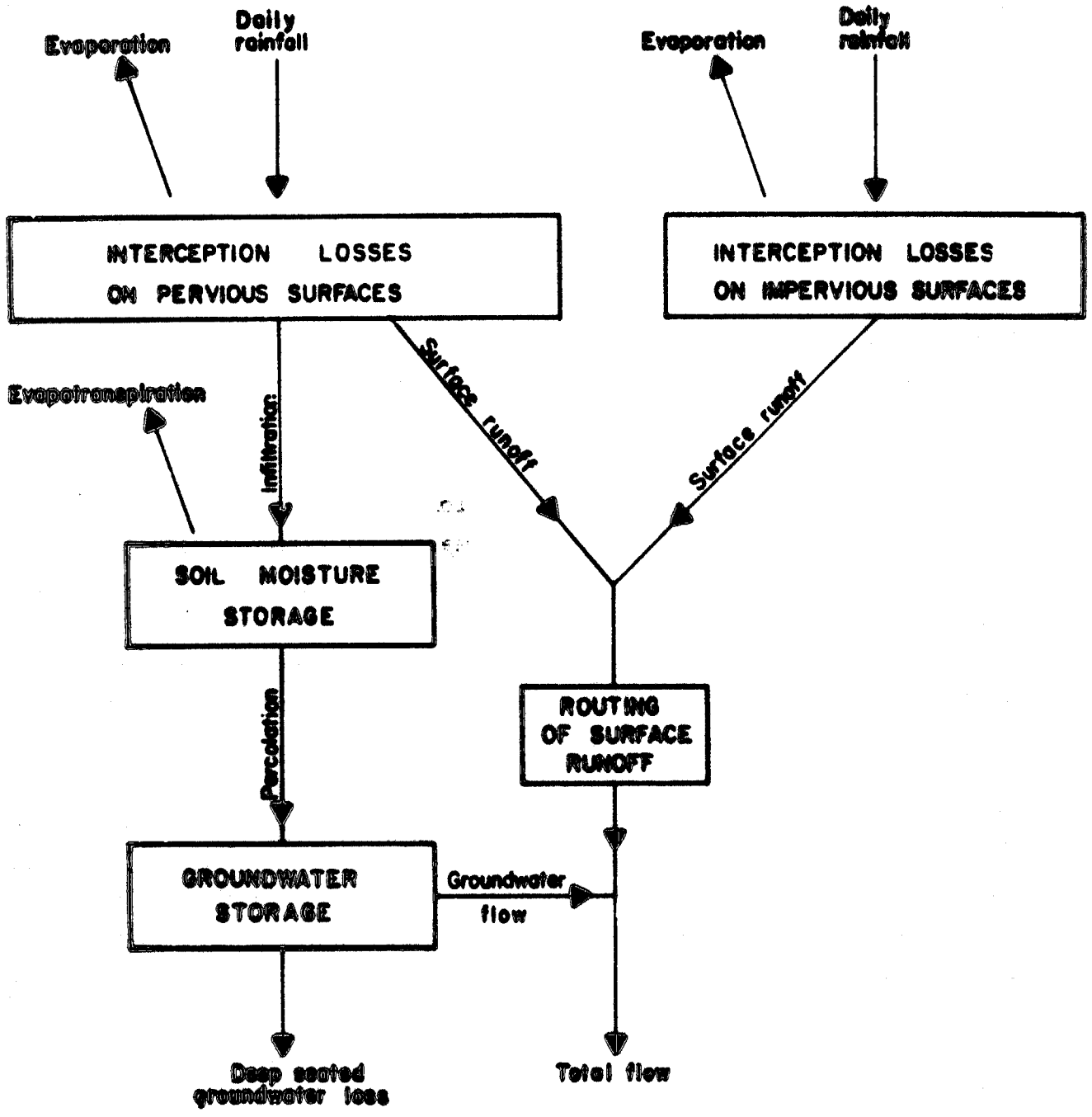

Fig. 2.1: Diagram depicting operation of the runoff component of program NACL01.

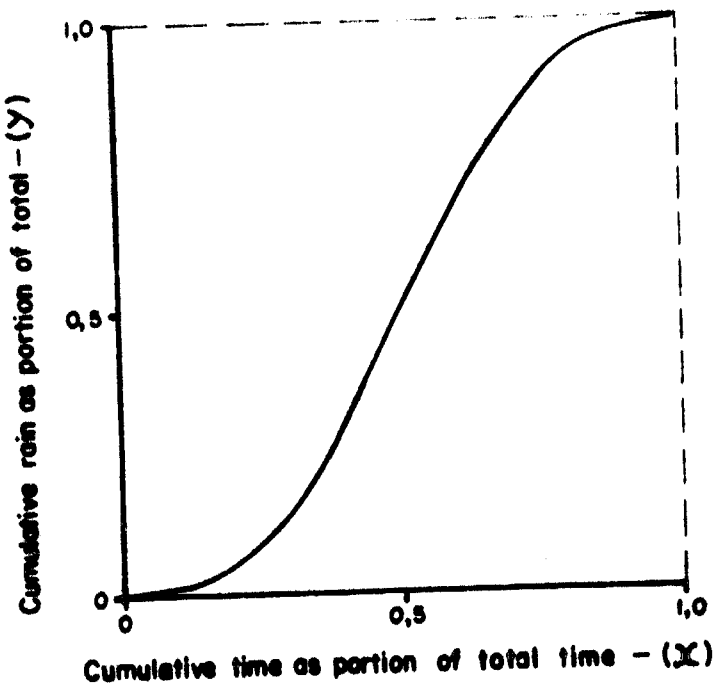

Fig. 2.2: Assumed typical mass curve for rainfall.

Subtraction of successive cumulative hourly rainfalls from one another yields the hourly rainfalls to be used in each computational time step. Equation 2.2 is used for rainfall durations in excess of 2 hours. For a two-hour duration storm the hourly falls are taken to be 20% and 80% respectively of the total rainfall. Pitman's equation 2.2 was also derived from his autographic rainfall records (Pitman, 1976).

The assumption that rainfall always commences at the beginning of the day is obviously simplistic, but the only alternative is to include a random distribution component to disaggregate the rainfall into hourly events. This, however, would make the model more cumbersome and render calibration extremely difficult. How, for instance, could the user evaluate the effect of a parameter value change if successive simulations, even with identical parameter values, produce different flood peaks due to dissimilar dissaggregation of daily rainfalls? There would appear to be little justification for changing Pitman's assumptions.

b) Interception

Before runoff or infiltration can occur, vegetation and soil surfaces must first be wetted. Pitman's assumption was that a small, constant interception storage (PI) must be filled before either infiltration or runoff can occur and that interception storage is depleted at potential evapotranspiration rate.

c) Infiltration and surface runoff

All rainfall in excess of that required to fill interception storage on the impervious portion of the catchment (AI) is assumed to contribute to surface runoff. AI is defined as that portion of the catchment which is both impervious and in direct communication with the watercourses.

Cognisance is taken of the fact that permeability and hence infiltration rate vary spatially, even for the most nearly uniform of catchments (Pitman, 1976). Infiltration rates over the pervious portion of the catchment must therefore be assumed to follow a frequency distribution. A triangular distribution identical to that adopted by Pitman (1976) is postulated, as represented in Fig. 2.3a, in which:

Z_1 = minimum infiltration rate (mm/h)

Z_3 = maximum infiltration rate (mm/h)

Z_2 = mean infiltration rate (mm/h)
= $\frac{1}{2}(Z_1+Z_3)$

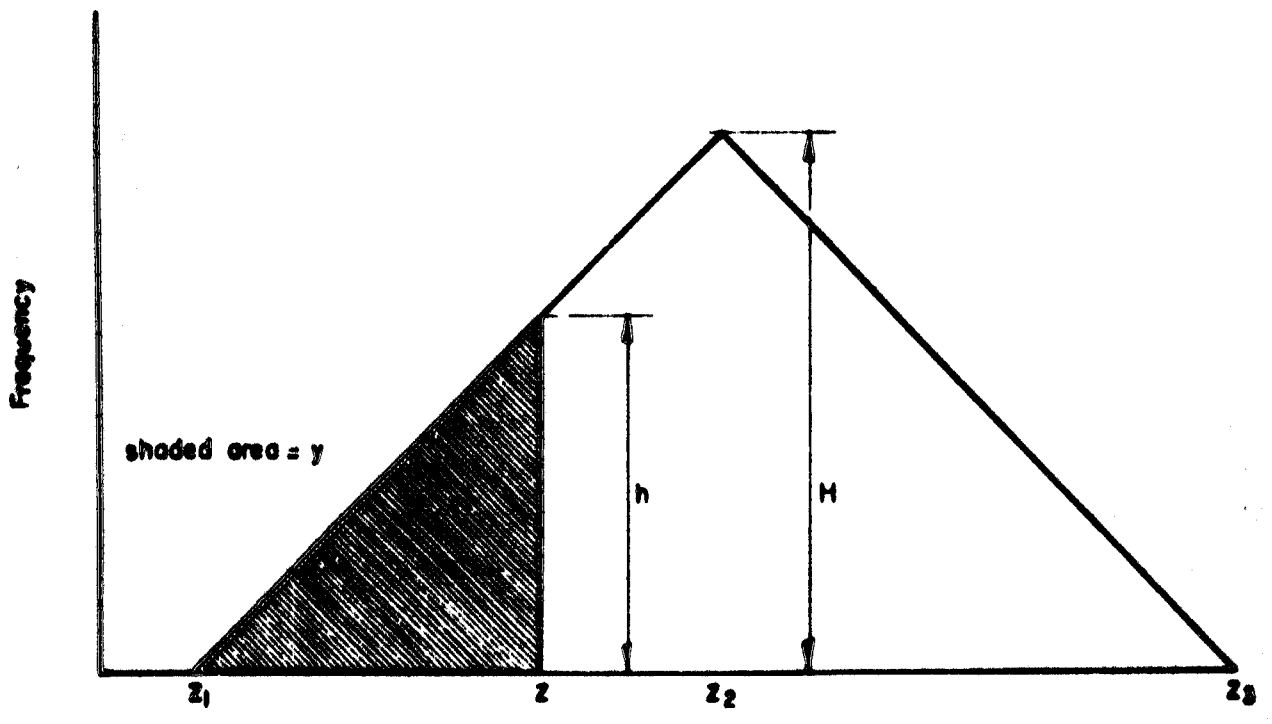

Fig. 2.3a. Assumed frequency distribution of catchment infiltration rate Z.

Fig. 2.3b is the corresponding cumulative frequency curve.

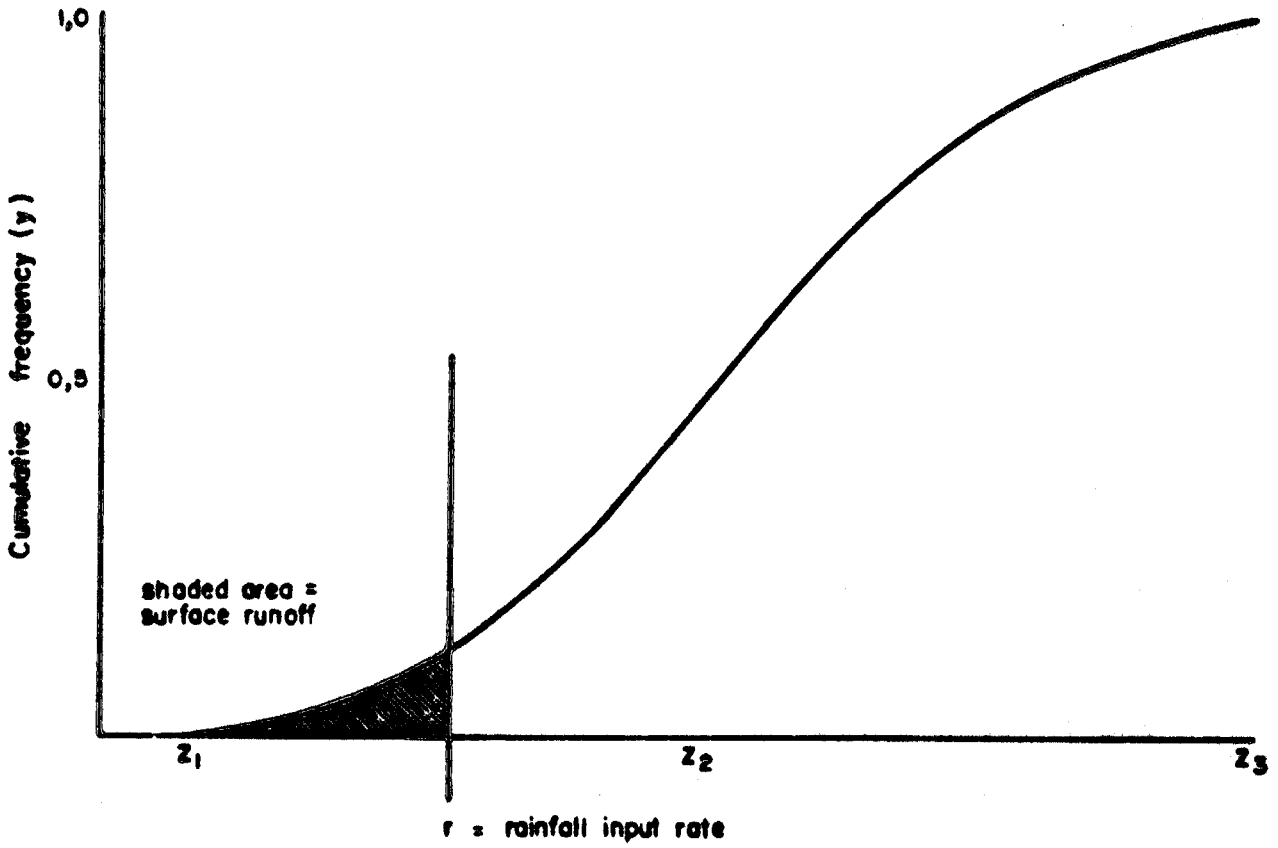

Fig. 2.3b Cumulative frequency curve

Recognising that the area subtended by the frequency curve must equal unity it may be seen from Fig. 2.3a that:

$$H = 2/(Z_3-Z_1).$$

The cumulative probability y of any absorption rate Z is given by the shaded area in Fig. 2.3a. From the geometry, y is given by:

$$y = 2(Z-Z_1)^2/(Z_3-Z_1)^2 \qquad (\text{for } Z \leq Z_2)$$

and $$y = 1 - \frac{2(Z_3-Z)^2}{(Z_3-Z_1)^2} \qquad (\text{for } Z \geq Z_2)$$

For any given excess rainfall input rate REFF the surface runoff rate QVELD is represented by the shaded area in Fig. 2.3b.

Hence for $Z_1 \leq$ REFF $\leq Z_2$

$$\text{QVELD} = \int_{Z_1}^{\text{REFF}} 2(Z-Z_1)^2/(Z_3-Z_1)^2 . dZ$$

$$\text{i.e. QVELD} = \frac{2}{3}\,\frac{(\text{REFF}-Z_1)^3}{(Z_3-Z_1)^2} \qquad \text{.....(2.3)}$$

Thus, when REFF = Z_2,

$$\text{QVELD} = \frac{1}{12}\,(Z_3-Z_1)$$

Hence from symmetry in Fig. 2.3b:

for $Z_2 \leq \text{REFF} \leq Z_3$,

$$\text{QVELD} = \frac{1}{12}\,(Z_3-Z_1)+(\text{REFF}-Z_2)-\left\{\frac{1}{12}(Z_3-Z_1)-\frac{2}{3}\,\frac{(Z_3-\text{REFF})^3}{(Z_3-Z_1)^2}\right\}$$

$$\text{i.e.} \qquad \text{QVELD} = \text{REFF} - \tfrac{1}{2}(Z_1+Z_3) + \frac{2\,(Z_3-\text{REFF})^3}{3\,(Z_3-Z_1)^2} \qquad \text{..... (2.4)}$$

and for REFF > Z_3,

QVELD = REFF minus average catchment infiltration rate

$$\text{i.e.} \qquad \text{QVELD} = \text{REFF} - \tfrac{1}{2}\,(Z_1+Z_3) \qquad \text{..... (2.5)}$$

Thus, for any given rainfall input rate, the corresponding surface runoff is determined by the minumum and maximum infiltration rates Z_1 and Z_3. Z_1 and Z_3, however, will be influenced by the wetness of the catchment. Infiltration rates generally decrease with increasing duration of rain.

The functions used by Pitman (1976) to relate infiltration rates to soil moisture storage have been adopted:

$$Z_3 = 4.\text{ZMAXN}.2^{-(2\cdot S/ST)} \qquad \text{.....(2.6)}$$

and

$$Z_1 = \frac{\text{ZMINN}}{\text{ZMAXN}}\,.Z_3 \qquad \text{.....(2.7)}$$

where ZMAXN = nominal maximum infiltration rate (mm/h)
ZMINN = nominal minimum infiltration rate (mm/h)
S = soil moisture storage (mm)
ST = soil moisture capacity (mm)

The assumption implicit in equation 2.7 is that the ratio $Z_3 : Z_1$ remains constant for all soil moisture storage states.

On pervious areas all precipitation in excess of the interception storage that does not give rise to surface runoff enters the soil moisture storage.

Equation 2.6 is represented in Fig. 2.4

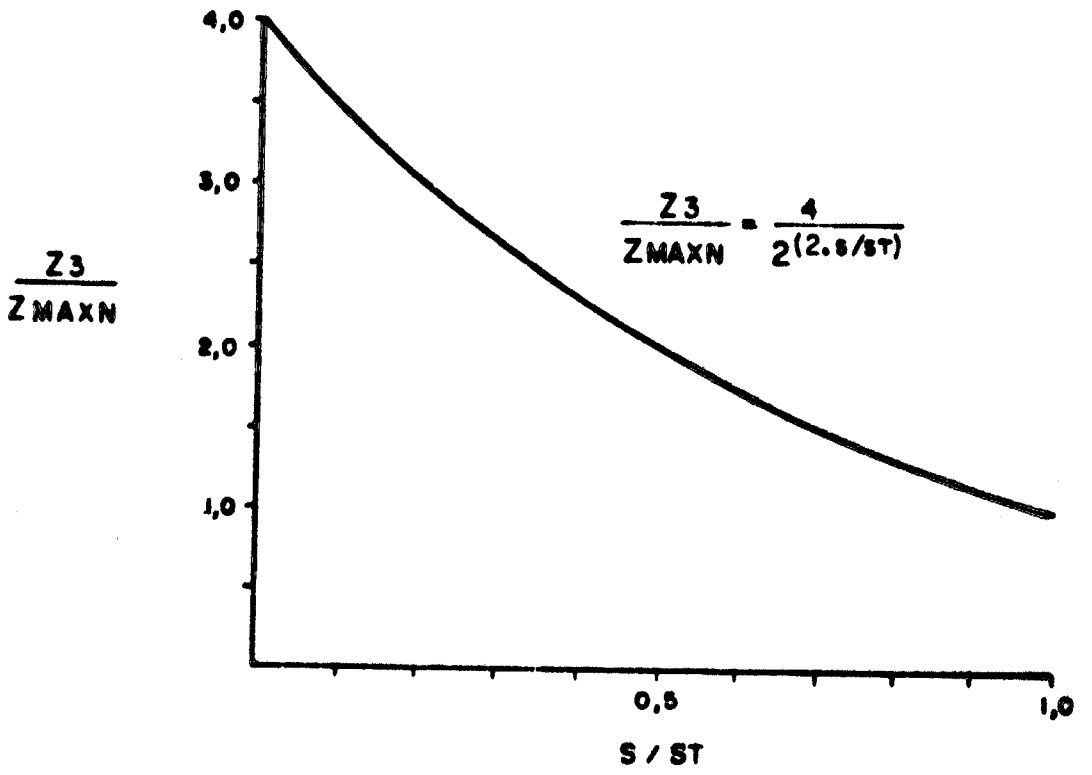

Fig. 2.4. Relationship between infiltration capacity and soil moisture.

Infiltration rates and surface runoffs are computed on an hourly basis.

d) Interflow

Studies by Fritz et al. (1976) and Sklash (1978) of the movement of isotope tracers have revealed that a large proportion of storm runoff is attributable to a rapid groundwater response. It is not clear whether this rapid response is due to the process postulated by Sklash and Farvolden (1979) in which partially saturated soils become quickly saturated thereby causing a 'groundwater ridge' with a consequent near instantaneous response of ground-

water already in a 'discharge position', or the effect of the rapid conveyance of infiltrating water through cracks and fissures where salts present in the soil moisture, or previously deposited in the soil matrix, are transported laterally to re-appear as surface runoff, as suggested by Kennedy (1977). More than likely both of these mechanisms are at work. What appears certain, however, is that some form of interflow or rapid groundwater response must make a significant contribution to the salt load present in surface runoff. In the southern PWVS region, for example, by far the greater proportion of the rainfall becomes infiltration while only a small fraction gives rise to surface runoff. If the washoff salt load is divided in these same proportions then most of the salts should end up in the groundwater resulting in groundwater and baseflow salinities several times higher than those observed, unless there is some mechanism by which these salts can be flushed from the soil during storms. *

In view of these findings an interflow process has been introduced into the Pitman model whereby it is assumed that a proportion of all surface runoff from pervious surfaces is derived from interflow. Sklash and Varvolden (1979) found in their study catchments that for a very wet basin both overland flow and stream flow were dominated by groundwater, while for a dry basin runoff was dominated by rain water.

It is therefore assumed that when the soil moisture storage, S is at full storage capacity ST the interflow component QINT is equal to a maximum proportion PINTM of the surface runoff QVELD, and that the interflow component decreases linearly to zero when the soil moisture storage is empty. This assumed relationship is represented in Fig. 2.5. The controlling equation is thus:

---

* Earlier versions of the washoff model did not take account of interflow and, as a result, salts tended to accumulate in the soil moisture and groundwater storages, leading to unacceptably high modelled salinities. The small baseflows did not provide sufficient through-flow to reduce salinities to observed values. It is also unrealistic to assume that the surface flow component carries with it a disproportionally higher share of the load than that infiltrating to the soil moisture as both are drawing salts from a common source.

$$QINT = \frac{1}{2} \cdot \frac{(S+S')}{ST} \cdot PINTM.QVELD \qquad \ldots\ldots\ldots\ldots\ldots\ldots (2.8)$$

where S = soil moisture storage at start of time step Δt

S′= soil moisture storage at end of time step Δt

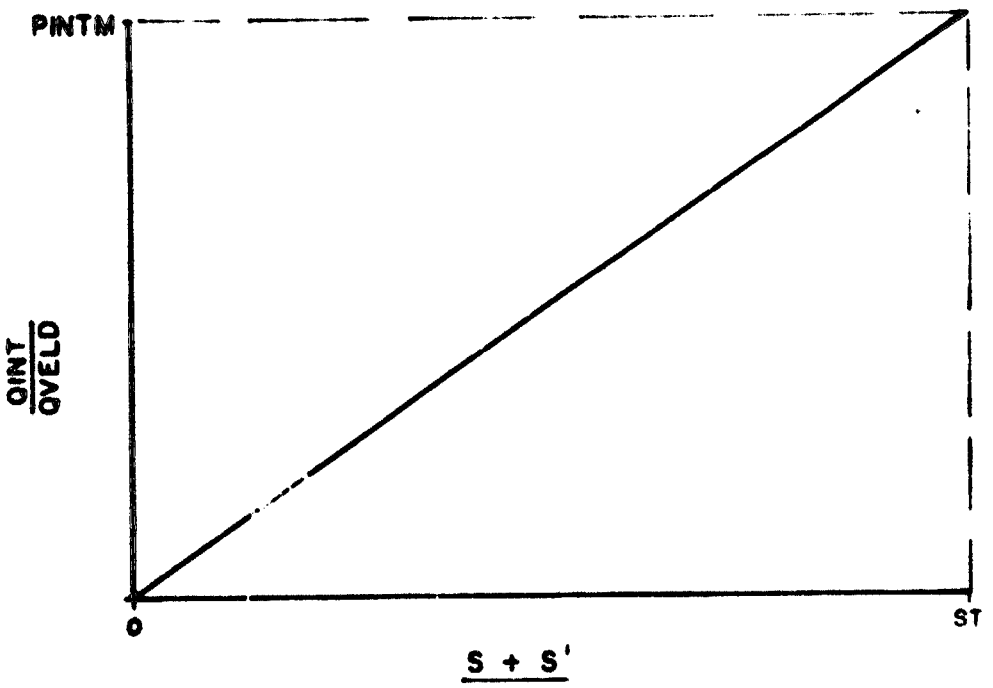

Fig. 2.5. Relationship between interflow, surface runoff and soil mixture

e) Potential evapotranspiration

Lake evaporation is calculated from Symons pan evaporation data. Based on studies made by Kriel (1963) and Barker (1965), Pitman (1973) concluded that lake evaporation could be estimated from Symons pan data as follows: for the period July-October a pan coefficient of 0,8 would be acceptable, while for the period November-June the coefficient would be practically unity. The model has been written in such a way that Symons pan evaporation values are automatically adjusted by these factors.

The original Pitman model uses mean monthly evaporation data as input. This has been modified to allow either mean monthly or observed daily Symons pan evaporation values to be used. In the latter case mean monthly pan evaporations, averaged over the catchment, are still read in as well as mean monthly evaporations for the reference gauge used. This permits the daily pan evapo-

rations for the reference gauge to be weighted according to the mean monthly catchment and reference gauge evaporations.

If so desired, the daily evaporations from several Symons pans within the catchment can be averaged and fed in as the daily evaporation input to the model. In such event the mean monthly catchment and reference gauge evaporations should be set equal to each other, thereby effectively setting the weighting factor to unity.

As a rule, however, evaporation stations having sufficiently long daily evaporation records are scarce and one is obliged to use average values.

f) Evaporation from the soil moisture

The relationship used by Pitman was modified by the introduction of soil moisture storage SE below which evaporation is assumed to cease. This additional feature was included in order to maintain realistic soil moisture salinities towards the end of the dry season, when modelled base flows would otherwise tend to rise to unacceptably high values. The relationship between soil moisture storage and evaporation from the soil moisture is depicted in Fig. 2.6. Soil moisture evaporation is assumed to take place at the potential lake evaporation rate PE when the soil moisture S is at full capacity ST. The potential evaporation rate PE is either obtained from a data file of daily potential evaporation or calculated from mean monthly evaporation values, depending upon the data input option chosen.

The function controlling soil moisture evaporation E is as follows:

$$ESOIL = PE \frac{(S-SE)}{(ST-SE)} \quad \ldots\ldots\ldots\ldots\ldots \quad (2.9)$$

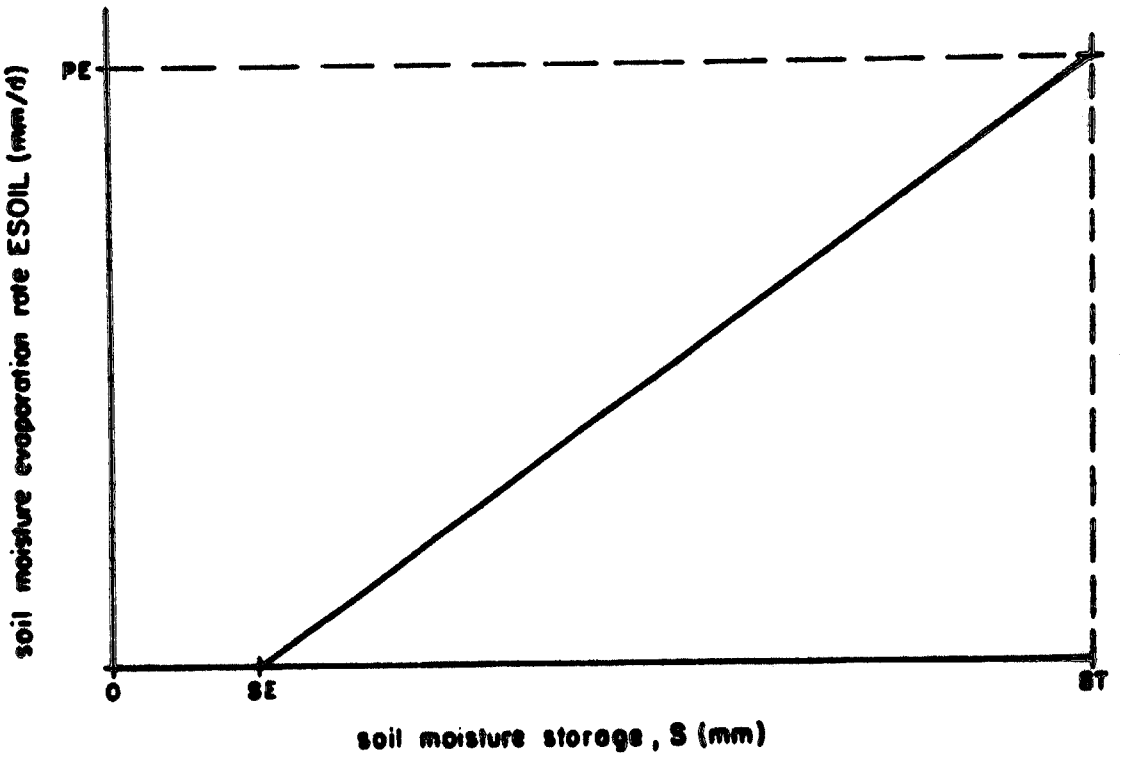

Fig. 2.6. Soil moisture - evaporation relationship.

g) Percolation of soil moisture to groundwater storage

Pitman's simple power curve is adopted to relate percolation QPERC to soil moisture conditions:

$$QPERC = A(S-3L)^{POW} \quad \ldots\ldots\ldots (2.10)$$

where SL = soil moisture storage below which no percolation occurs (mm)

ST = soil moisture capacity (mm)

POW = power of the QPERC-S curve

A = constant

This relationship is represented in Fig. 2.7.

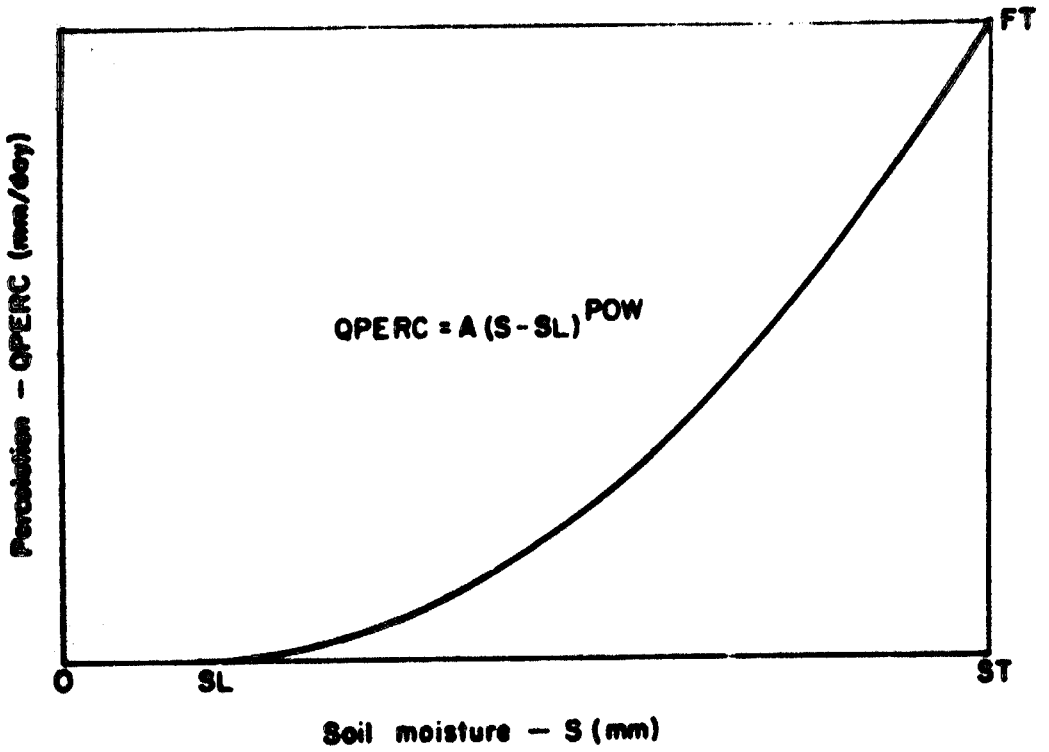

Fig.2.7: Soil moisture - percolation relationship.

Defining FT as the percolation at soil moisture capacity and substituting QPERC = FT at S = ST in equation 2.10 yields:

$$A = \frac{FT}{(ST-SL)^{POW}}$$

Thus equation 2.10 becomes:

$$QPERC = FT \left[\frac{S-SL}{ST-SL}\right]^{POW} \qquad \text{.....(2.11)}$$

When the soil moisture capacity is exceeded, part or all to the excess is added to the groundwater storage GWS. The remainder of the excess is added to the surface runoff.

h) Groundwater discharge and losses to deep groundwater

The assumption is made that the total loss of water from the groundwater storage GWS (i.e. groundwater discharge plus loss to deep-seated groundwater) can be represented by a function similar to that employed by Pitman (1976) to determine groundwater discharge alone. The recession constant Kr is determined by the equation:

$$Kr = GW \sqrt{GWS/ST} \qquad \text{.....(2.12)}$$

where GW is a constant. The model parameter GL is the reciprocal of GW and has the units of days. Equation 2.12 is depicted in Fig. 2.8.

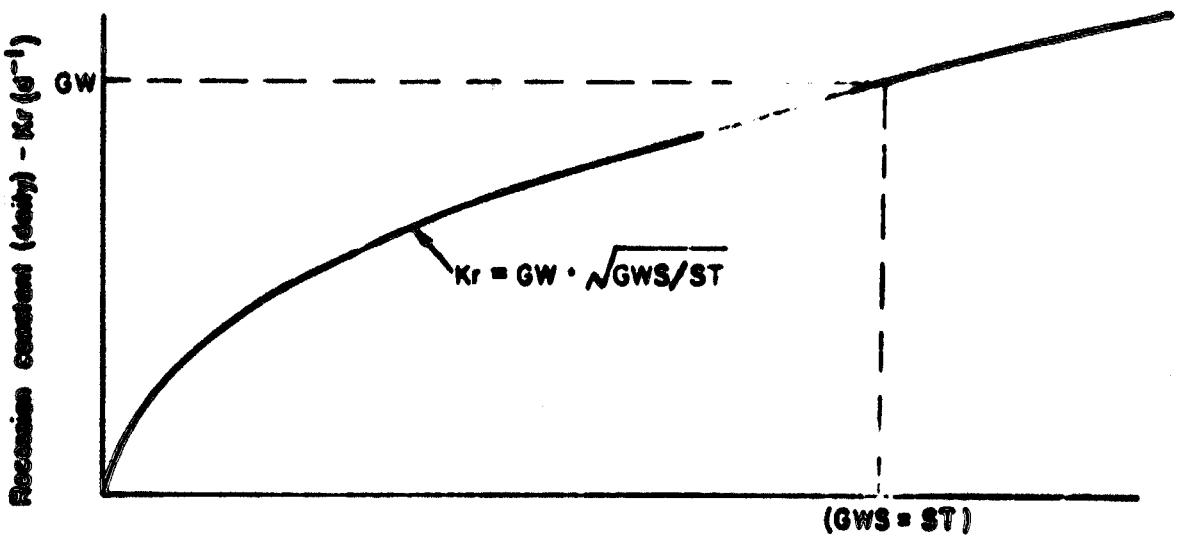

Fig.2.8: Recession constant - groundwater storage relationship.

Total groundwater outflow over a one-day period GWFT is then given by:

$$GWFT = Kr \cdot GWS$$

$$= GW \cdot GWS^{1/2} \cdot ST^{-1/2}$$

$$\text{or} \quad GWFT = GL^{-1} \cdot GWS^{1/2} \cdot ST^{-1/2} \qquad \text{.....(2.13)}$$

No upper limit is placed upon the value of GWS.

The Pitman model was also modified to allow for the loss of water to deep-seated groundwater GWFD. This is determined by the parameter DGL, viz. the proportion of the total groundwater outflow that enters deep groundwater:

$$GWFD = GWFT.DGL \qquad \text{.....(2.14)}$$

The deep-seated groundwater discharge is regarded as having been lost to the system and the concept is applicable in instances where it is known that extensive dewatering is taking place, for example, in association with mining activities.

The groundwater discharge to the drainage system, GWF. is calculated as:

$$GWF = GWFT - GWFD \qquad \text{.....(2.15)}$$

i) Time delay and attenuation of runoff

The calculated instantaneous runoff is lagged by means of the parameter LAG, which has units of days.

Attenuation of surface runoff is achieved by means of the Muskingum equation (U.S. Corps of Engineers, 1936) which can be written as:

$$O_2 = C_o \cdot O_1 + C_1 \cdot I_1 + C_2 \cdot I_2 \qquad \text{.....(2.16)}$$

where $$C_o = \frac{K - K \cdot x - \frac{1}{2}\Delta t}{K - K \cdot x + \frac{1}{2}\Delta t} \qquad \text{..... (2.17)}$$

$$C_1 = \frac{K \cdot x + \frac{1}{2}\Delta t}{K - K \cdot x + \frac{1}{2}\Delta t} \qquad \text{.....(2.18)}$$

$$C_2 = \frac{-K \cdot x + \frac{1}{2}\Delta t}{K - K \cdot x + \frac{1}{2}\Delta t} \qquad \text{.....(2.19)}$$

where O = surface runoff at catchment outlet
I = surface runoff input
Δt = routing period (= 1 day)
K = storage factor
x = weighting factor

Subscripts 1 and 2 to I and O refer to the previous and the current day's runoffs respectively. The storage factor K has the units of time and is denoted by the model parameter TL. The factor x is set to zero for reservoir-type storage attenuation. Hence equations 2.17 to 2.19 become:

$$C_o = \frac{TL - \frac{1}{2}\Delta t}{TL + \frac{1}{2}\Delta t} \qquad \text{.....(2.20)}$$

and $C_1 = \frac{\frac{1}{2}\Delta t}{TL+\frac{1}{2}\Delta t}$ .....(2.21)

In the Pitman model equation 2.16 is used to route instantaneous runoff all the way to the catchment outlet. In the author's mod , on the other hand, routing is accomplished by means of the channel routing model (see section 2.3). In this context therefore equation 2.16 is used only to route runoff as far as the main river channels. For this reason the parameter TL should be smaller than would be the case when using the Pitman model. (If the channel routing step is not used, however, then higher TL values are more appropriate).

2.2.2 Salt washoff modelling

The water quality phase of the model has been introduced specifically to represent the generation, storage and transport of total dissolved solids (TDS) derived from diffuse sources. Although the model was developed primarily to simulate the mass balance and fluctuations of TDS, there is no reason why it should not be employed, if necessary, to model the wash-off of any conservative constituents of polluted streamflow, such as sulphates, chlorides or possibly even sediments.

Precipitation is assumed to have an associated constant background TDS, viz. CONCBG. Conservative pollutants (in particular, dissolved solids) are assumed to accumulate gradually on the catchment surface from where they are removed when runoff occurs. These accumulated salts have been divided for the purposes of modelling into two broad categories: (a) those stored on paved surfaces and (b) those on pervious surfaces. In both cases the pollutant store may be recharged at a rate which may be steady or vary with time.

Salt washed off paved surfaces is assumed to enter the river system directly and is therefore routed with surface runoff. That washed off pervious surfaces is split in proportion to the direct surface runoff, interflow and infiltration components derived in section 2.2.1. Direct surface washoff is routed in the same manner as washoff from paved surfaces, while the remaining washoff load enters the soil moisture storage.

Interflow transports salts back into surface runoff at the current

soil moisture salinity. Salt stored in the soil moisture can also move into groundwater storage and thence to the stream with the groundwater outflow. Provision is made for the gradual leaching of salt into the soil moisture and groundwater from the surrounding soils, and for the deposition of salt in the soil matrix as evaporation depletes the soil moisture storage and subsequent solution of salt as the soil moisture storage increases.

Fig. 2.9 illustrates the processes involved.

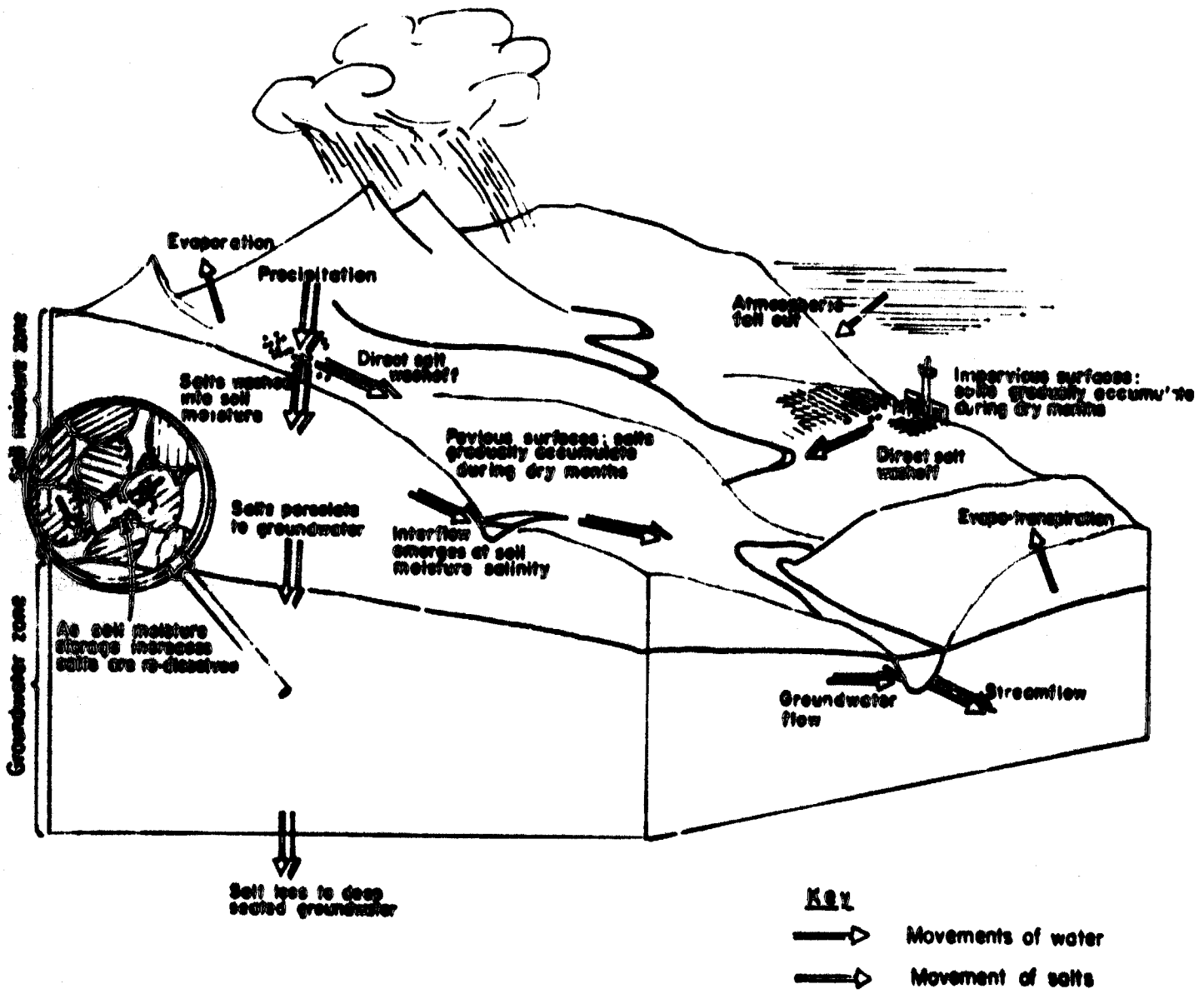

Fig. 2.9: Diagram illustrating the modelled movements of dissolved solids

(a) Wash-off from impervious urbanised surfaces

A basic assumption made here is that the urbanised area of the catchment may be represented by AI, the parameter defining the impervious portion of the catchment. As human activities are known to have a profound impact upon the generation of diffuse-source pollutants, it was considered appropriate to differentiate between pollutants emanating from areas of highly concentrated human activity (urban areas) and those from the remainder of the catchment. Urban areas also warrant special consideration because of their extensive paved surfaces which are linked directly to the drainage system. It is logical to suppose that high runoff efficiencies from such paved surfaces are just as likely to be associated with high pollutant removal efficiencies.

It is assumed that at any instant the pollutant load stored on the urbanised surface (and in the atmosphere immediately above it) and available for removal is equal to SALTU, in t/km^2 of urbanised area.

It may be assumed also that this storage is depleted primarily during those precipitation events which result in runoff from the urbanised surfaces and that during such events the load picked up per unit area, d(SALTU), within time interval dt is proportional to the instantaneous storage SALTU. This gives rise to the first order differential equation:

$$-\frac{d}{dt}\,SALTU = K.SALTU \qquad \text{.....(2.22)}$$

Integration for the interval Δt yields:

$$SALTU - SALTU' = SALTU\cdot(1-\exp(-K\Delta t)) \qquad \text{.....(2.23)}$$

where SALTU$'$ = pollutant stored per unit area at end of time step Δt (t/km^2)

K = constant (d^{-1} when Δt is in days)

With the further assumption that K is proportional to QURBAN, the runoff from the urbanised (impervious) area in mm/d:

$$K = APARU.QURBAN \qquad \text{.....(2.24)}$$

where APARU is a constant of units mm^{-1}

Thus from equations 2.23 and 2.24 the total wash-off of TDS from impervious areas, WASHU, during time step Δt is given by:

$$WASHU = SALTU.AREA.AI.(1-\exp(-APARU.QURBAN.\Delta t)) \quad \ldots\ldots\ldots (2.25)$$

where AREA is the total catchment area in km^2 and WASHU is in ton units.

Equation 2.25 is similar in form to that developed by Metcalf and Eddy (1971) in SWMM (Storm Water Management Model). Equation 2.25 is depicted in Fig. 2.10.

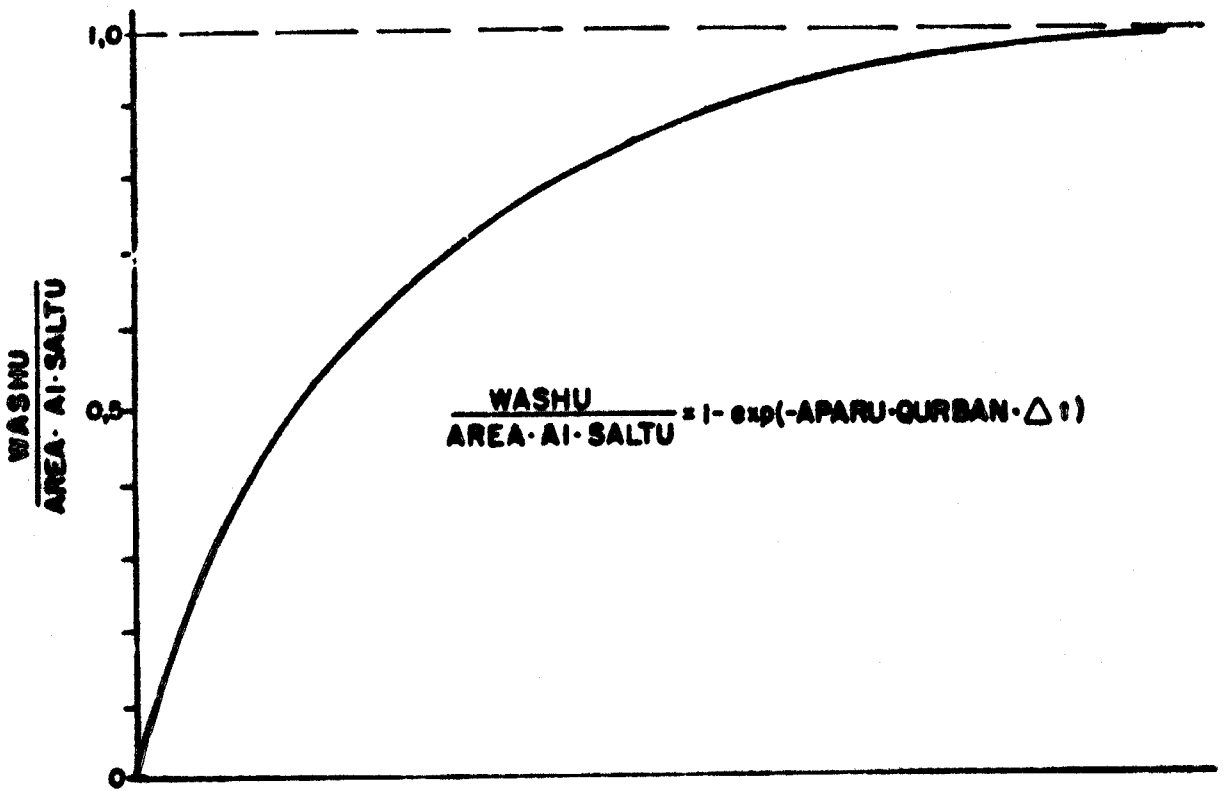

Fig. 2.10: Relationship between load washed off, initial load storage and runoff.

The urban salt storage can be replenished via fall-out from atmospheric pollution, abrasion of surfaces, refuse, faecal deposition etc. During any given calendar year the recharge of the urban salt storage is assumed to be proportional to time. Hence the recharge per unit area, r_u (t/km^2), is given by:

$$r_u = BPARU.\Delta t \quad \ldots\ldots\ldots (2.26)$$

where BPARU = recharge rate ($t/km^2/d$)

The mass balance equation for salts stored on impervious urban surfaces can then be written as:

$$SALTU' = SALTU+BPARU.\Delta t-SALTU.(1-\exp(-APARU.QURBAN.\Delta t)) \quad \ldots(2.27)$$

Equation 2.27 is a valid approximation provided that BPARU << SALTU.

Thus the salt storage builds up gradually during dry spells and is depleted when runoff occurs to a degree dependent upon the magnitude of runoff. The process is illustrated in Fig. 2.11.

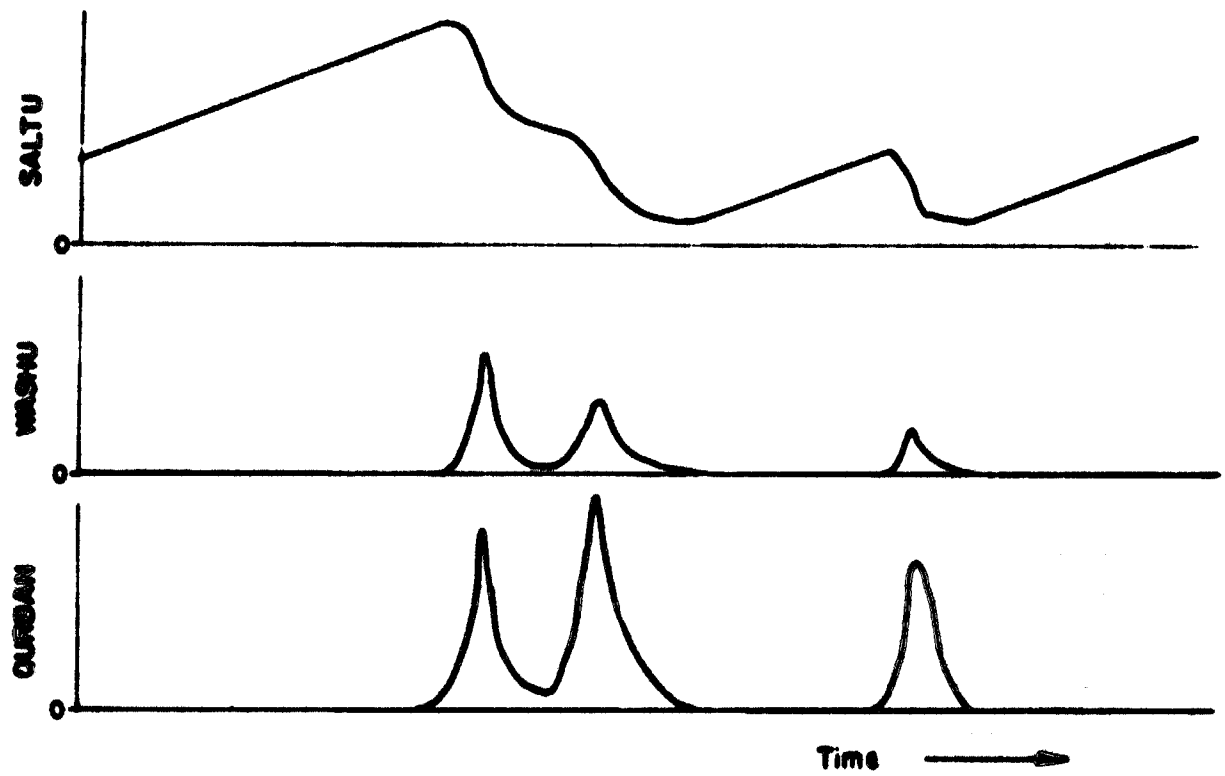

Fig.2.11. Hypothetical example illustrating the variation of salt storage SALTU with time.

The recharge rate BPARU would vary widely depending upon such factors as the nature and degree of industrialisation, density and economic activity of the population and the methods and efficiency of waste disposal.

Dynamic conditions may be simulated by means of a growth index GROW which is specified for each calendar year simulated. The recharge rate applicable to any given year is then computed as:

$$BPARU = BPARUO.\frac{GROW}{GROWO} \quad \ldots\ldots\ldots\ldots(2.28)$$

where BPARUO = urban recharge rate during first year of simulation ($t/km^2/d$)
GROWO = growth factor for first year of simulation
GROW = growth factor for current year of simulation

The growth factor may be any index of the state of development of the catchment that is indicative of the rate at which salts are generated. For the catchments of the southern PWVS region the industrial water supply was found to be the best index of salt generation (see section 3.3).

The entire salt load washed off paved surfaces, together with that associated with the precipitation, is assumed to enter surface runoff.

The total salt load emanating from paved surfaces, SURBAN (t), is thus computed as:

$$SURBAN = WASHU + QURBAN.CONCBG.AREA.10^{-3} \quad .....(2.29)$$

(b) Wash-off from pervious catchment surfaces

Wash-off from pervious catchment surfaces is presumably derived from material stored in the atmosphere above the pervious portion of the catchment, salts stored on foliage and other catchment surfaces, including mine dumps, and in the upper layers of the soil through which interflow occurs, and in dry stream beds.

Salt storage is replenished through weathering of catchment surfaces, agricultural practices, refuse, atmospheric pollution, faecal deposition and so forth.

Equations controlling the wash-off and recharge of salts are assumed to be similar to those for impervious surfaces.

The corresponding wash-off equation for pervious surfaces is:

$$WASHP = SALTP.AREA.(1-\exp(-APARP.REFF.\Delta t) \quad .....(2.30)$$

where SALTP = salt load stored per unit area of pervious catchment at start of time step Δt (t/km^2)

WASHP = salt load washed off pervious surfaces during time step Δt (t)
APARP = constant (mm^{-1})

For AI << AREA, equation 2.30 can be re-written as:

$$WASHP = SALTP.AREA.(1-\exp(-APARR.REFF.\Delta t)) \quad \ldots\ldots\ldots (2.31)$$

The mass balance equation takes the form:

$$SALTP' = SALTP+BPARP.\Delta t - SALTP(1-\exp(-APARP.REFF.\Delta t)) \ldots\ldots (2.32)$$

where SALTP' = salt load stored per unit area of pervious catchment at end of time step Δt (t/km^2)
BPARP = recharge rate ($t/km^2/d$)

For dynamic conditions BPARP is computed for each calendar year in a manner similar to that for impervious surfaces:

$$BPARP = BPARPO.\frac{GROW}{GROWO} \quad \ldots\ldots\ldots\ldots\ldots\ldots (2.33)$$

where BPARPO = pervious surface recharge rate during first year of simulation ($t/km^2/d$)

Using the same growth indices for recharge on both pervious and impervious portions of the catchment implies that the ratio of salts generated on these two categories of catchment surface remains constant with time.

The washoff from pervious catchment surfaces, together with the salt load associated with the background TDS of the precipitation, is split into two components which enter surface runoff and the soil moisture respectively. SINF(t), the portion that enters soil moisture storage, is computed as:

$$SINF = (QINT+QINF).\left(\frac{WASHP}{REFF} + CONCBG.AREA.10^{-3}\right) \quad \ldots\ldots\ldots (2.34)$$

where QINF = net infiltration during time step Δt (mm)
= REFF - QVELD

The salt load that directly enters surface runoff, SVELD(t), is given by:

$$SVELD = (QVELD-QINT).\left(\frac{WASHP}{REFF} + CONCBG.AREA.10^{-3}\right) \quad .....(2.35)$$

c) Salt balance in the soil moisture

It is assumed that salt enters the soil moisture storage via infiltration and interflow and through leaching, and leaves as percolation to groundwater and interflow. Allowance is made for evaporation-induced deposition of salt in the soil matrix and for subsequent re-solution of deposited salt as the soil moisture storage increases. Complete mixing of the soil moisture is assumed.

Salt is assumed to be leached out of the soil matrix at a constant rate per unit of soil moistur storage. The total salt load leached in time Δt, SLEACH(t), is thus assumed to be directly proportional to the soil moisture storage, S:

$$SLEACH = ALEACH.S.AREA.\Delta t \quad ....(2.36)$$

where ALEACH = groundwater salt leaching rate ($t/km^2/mm/d$)

It is also assumed that as water is lost to evapotranspiration, part of the salt load is deposited in the soil matrix and is re-dissolved when the soil moisture storage is increased. The salt load deposited in the soil matrix during time step Δt, SDEP (t), is computed as:

$$SDEP = PDEPS.\left(\frac{ESOIL}{S}\right).SLOAD \quad .....(2.37)$$

where PDEPS = proportion of salt contained in evaporated water which is assumed to be deposited in the soil matrix ($0 \leq PDEPS \leq 1$)

SLOAD = soil moisture salt storage at start of time step Δt (t)

The above relationship is depicted in Fig. 2.12.

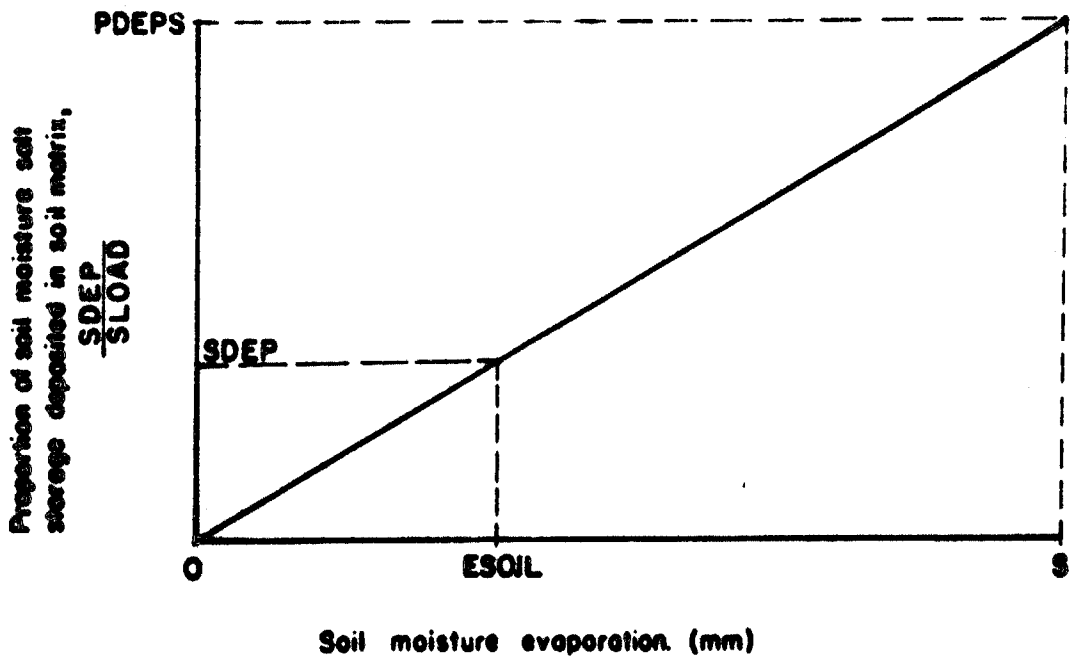

Fig.2.12. Relationship between proportion of soil moisture salt storage deposited and soil moisture evaporation.

The salt load re-dissolved during time step Δt, SDIS(t), is computed as:

$$SDIS = 0 \qquad (S' \leq S) \qquad \text{.....(2.38a)}$$

$$\text{or} \quad SDIS = \frac{S'-S}{ST-S} \cdot SSOIL \qquad (S' > S) \qquad \text{.....(2.38b)}$$

where S' = soil moisture storage at end of time step Δt (mm)
SSOIL = salt storage in the dry portion of the soil at start of time step Δt (t)

The salt mass balance equation for salt stored in the dry portion of the soil is then given by:

$$SSOIL' = SSOIL + SDEP - SDIS \qquad \text{.....(2.39)}$$

where SSOIL' = salt storage in the dry portion of the soil at end of time step Δt (t)

The relationship between the salt load re-dissolved and soil moisture storage is depicted in Fig. 2.13.

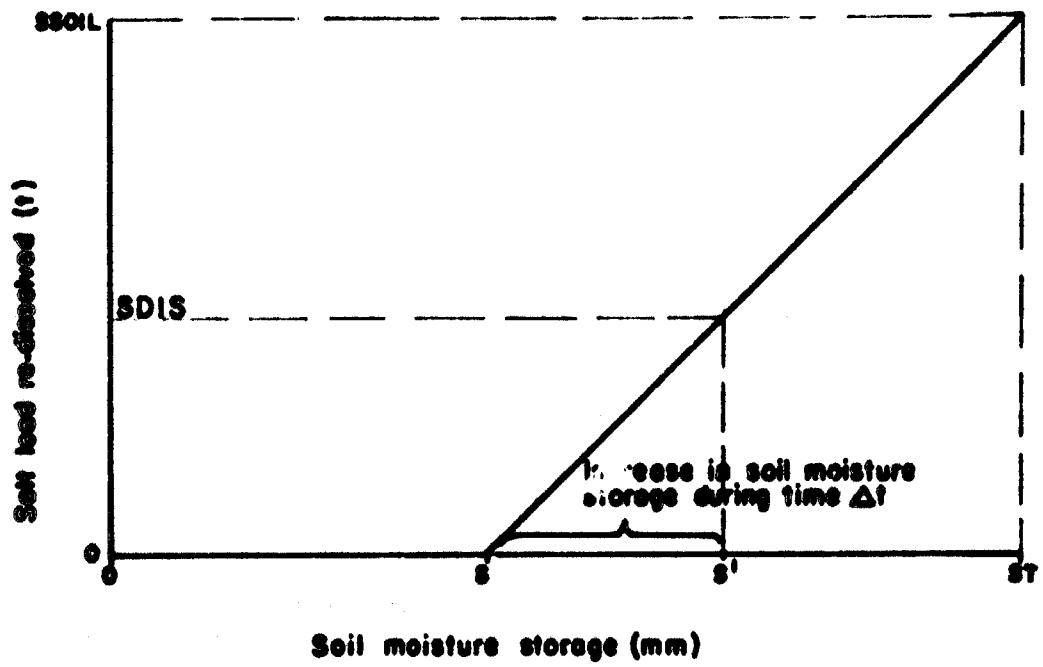

Fig.2.13. Relationship between salt load re-dissolved and soil moisture storage.

The implication of equations 2.38 is that the re-dissolving of salt stored in the dry portion of the soil is directly proportional to the increase in soil moisture storage. It is possible that the re-solution of such salt could be better explained by means of a decay equation similar in form to (2.31) with REFF replaced by (QINT+QINF). The less complex equations 2.38 were used, however, in order to reduce the number of model parameters that have to be calibrated.

The soil moisture salt storage mass balance equation is solved in two steps. All contributions to soil moisture salt storage are first added, then losses are deducted. This is to ensure unconditional stability of the salt balance equations. SLOAD″, the intermediate soil moisture salt storage after adding all salt gains and deducting the deposited salt load, is computed as:

$$SLOAD'' = SLOAD + SINF + SLEACH + SDIS - SDEP \quad \ldots\ldots\ldots (2.40)$$

The salt load returned to surface runoff via interflow, SINT(t), is then computed as:

$$SINT = \frac{QINT \cdot SLOAD''}{S + QINT+QINF-ESOIL} \qquad \text{.....(2.41)}$$

while the salt load transferred to the groundwater via percolation, SPERC (t), is given by:

$$SPERC = \frac{QPERC \cdot SLOAD''}{S+QINT+QINF-ESOIL} \qquad \text{.....(2.42)}$$

The assumption of complete mixing within the soil moisture gains credibility when it is considered that, although water and salts infiltrate in a roughly vertical direction in such a way as might cause vertical stratification, the interflow must migrate more or less horizontally in order to reach the stream. Thus, although the soil moisture itself may not be well mixed, the water entering the stream is likely to be practically fully mixed. The same argument applies to the assumption of complete mixing within the groundwater.

The soil moisture salt storage at the end of time step Δt, $SLOAD'(t)$, is then computed as:

$$SLOAD' = SLAOD'' - SINT - SPERC \qquad \text{.....(2.43)}$$

d) <u>Salt balance in the groundwater</u>

Salt is assumed to enter the groundwater as percolation from the soil moisture and by the leaching of salts from the soil/rock in the groundwater region. Salt leaves the groundwater storage by groundwater outflows to the stream and to deep-seated groundwater. The groundwater is assumed to be completely mixed at the end of each time step.

The salt mass balance is maintained by the equation:

$$GLOAD' = GLOAD+SPERC+GLEACH-SGWF-SGWFD \qquad \text{.....(2.44)}$$

where GLOAD′ = groundwater salt storage at end of time step Δt (t)
GLOAD = groundwater salt storage at start of time step Δt (t)

GLEACH = salt load leached into groundwater during time Δt (t)

$$= ALEACH.GWS.AREA.\Delta t \qquad \text{.....(2.45)}$$

SGWF = salt load entering stream as groundwater outflow during time Δt (t)

$$= \frac{GLOAD.GWF}{GWS} \qquad \text{..... (2.46)}$$

SGWFD = salt load entering deep-seated groundwater during time Δt (t)

$$= \frac{GLOAD.GWFD}{GWS} \qquad \text{..... (2.47)}$$

e) Routing of surface wash-off

As explained in section 2.2.1, surface runoff is attenuated by means of the Muskingum equation:

$$O_2 = C_o O_2 + C_1 I_1 + C_2 I_2 \qquad \text{..... (2.16)}$$

Use of equation 2.16 to route surface water, however, raises the problem of how to route the associated pollutant load. To avoid unduly complicating the model a simple empirical method based on the Muskingum equation has been devised.

Associated with the surface runoff input I (where I = QURBAN + QVELD) on any day, a salinity CI is calculated from the equation:

$$CI = \frac{SURBAN + SVELD + SINT}{(QURBAN+QVELD).AREA} .10^3 \qquad \text{.....(2.48)}$$

Thus the salt concentrations CI_1 and CI_2 (mg/ℓ), corresponding to runoff inputs I_1 and I_2 (where subscripts 1 and 2 refer to the previous and current days), can be calculated from equation 2.48. Further, from previous calculations, CO_1, the salinity of the runoff at the catchment outlet on the previous day, is also known. If it can be assumed that the water leaving the catchment outlet during the current day comprises a mixture of three types of water having salinities CI_1, CI_2 and CO_1, mixed together in the same proportions as I_1, I_2 and O_1 to make up O_2 in equation 2.16, then the following equation will hold:

$$CO_2 = \frac{C_o O_1 CO_1 + C_1 I_1 CI_1 + C_2 I_2 CI_2}{O_2} \qquad \text{.....(2.49)}$$

where CO_2 = salinity of the runoff at the catchment outlet during the current day (mg/ℓ).

Equation 2.49 ensures conservation of mass as C_0, C_1 and C_2 add up to unity. In effect the salt is routed with its associated water. This method of routing can be criticised on the grounds that with channel storage it is possible during any one time interval to have water leaving the lower end of the channel which contains none of the water that entered at the upper end during the same time step. (In other words, under such conditions, the term $C_1 I_1 CI_1$ should be deleted from equation 2.49 and the remaining terms adjusted). When it is considered, however, that equations 2.16 and 2.48 are being used not merely to route water through a channel but across a catchment, the assumption becomes plausible. Obviously, during a given time step, that part of the runoff which is derived from precipitation near the catchment outlet or near the major river channels will indeed leave the catchment within the same time step. In any event, little if any information is available on the exact mechanism and relative lagging of water and pollutant movements across a catchment surface. Even where reasonably precise relationships can be derived they are likely to vary widely with local conditions. The adoption of an equation such as 2.48 would therefore seem to be justified as it is based on assumptions certainly no more sweeping than others that have had to be made.

The final concentration of the water leaving the catchment, COUT, is then calculated by mixing the surface and groundwater flows:

$$COUT = \frac{CO_2.O_2 + SGWF}{O_2 + GWF} \qquad \text{.....(2.50)}$$

2.3 Structure of program NACLØ2

The channel routing model handles channel storage effects and the operating program, NACLØ2, is designed specifically to account for the storage and movement of water and salt through large storage elements such as the extensive reed-beds encountered in the tributaries draining southwards from the Witwatersrand. No attempt is made to model water movements with a high degree of hydraulic accuracy, as the long computational times entailed in so doing

would defeat the objective, which is to simulate long sequences of hydrology and the associated water quality fluctuations. The aim has been to devise a simple but effective empirical model; the data requirements of anything more complex than this would become prohibitive.

Storage effects are handled by introducing one or more interlinked channel reaches which are treated as linear reservoirs. Each reach is assumed to comprise a central channel within a flood plain. Discharges in the channel and through the flood plain are computed according to the Manning formula and provision is made for lateral flow between channel and flood plain. Each reach accepts at its head the outflow from up to three upstream reaches, together with effluent point flows and part of the runoff from the catchment within which the reach is situated. The remainder of the catchment runoff enters the river reach laterally via the flood plain.

That portion of the inflow which enters the upstream end of the channel section of the reach is aggregated to form a new cell. These cells are then advected through the reach. At the downstream end of the reach the cells are progressively destroyed, their contents then contributing towards the input to the following reach.

Lateral flows to and from the channel are fed into, or removed from, each cell in proportion to the cell volumes (i.e. the channel is assumed to be uniform in cross-section). Allowance is made for bed seepage losses, irrigation abstractions and return seepage, as well as evaporation from free water surfaces and evapotranspiration from reed beds.

It is hypothesized that due to evapotranspiration salt accumulates in the sponge-like root zone of those parts of the flood plain that are covered by reed beds and that the accumulated salt is flushed out during floods. This process could be particularly important in instances where the flood plain is not perennially covered by water. A salt "sponge" storage function was therefore introduced.

Apart from a list of model parameters, input to the model comprises an output file from program NACLØ1 containing mean monthly potential evaporation and daily runoffs with their salt concentrations, and average effluent point flows (with salinities) entering the upstream end of each reach. If desired, monthly values of effluent flows and salinities may be given.

One or more catchments, each containing one or more river reaches, can be modelled.

2.3.1 Channel routing model : Water mass balance

a) Channel geometry

Each river reach is assumed to have a uniform cross-section. BC and BT, the channel and total breadths respectively, are specified for various depths of flow, H. Breadths at intermediate depths are interpolated linearly. The depth-breadth relationship is illustrated in Fig. 2.14.

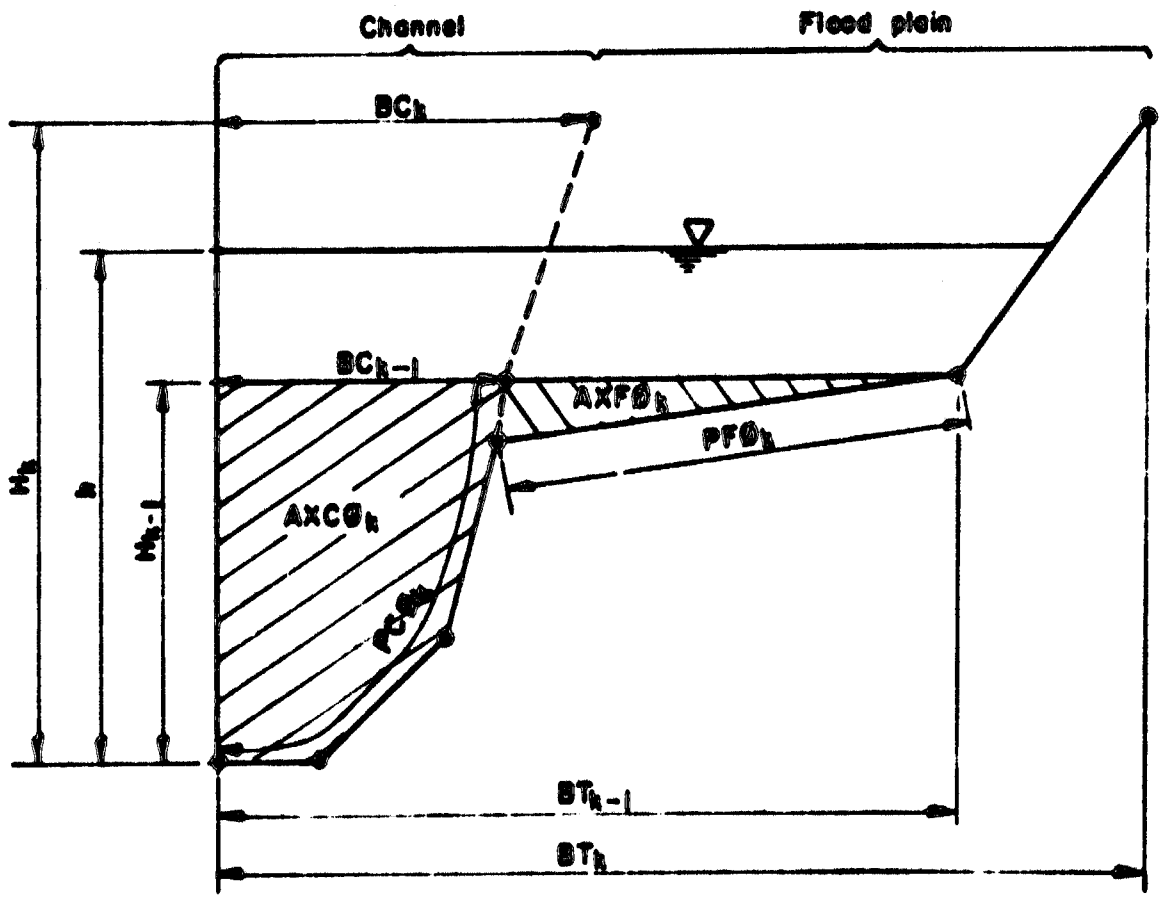

Fig. 2.14: Breadth-depth relationship for a typical river reach.

(b) Inflow from upstream reaches

Each river reach may be connected at its upstream end to as many as three river reaches. The calculated volume of outflow from each of these reaches during time step Δt is simply added to the storage of the reach under consideration.

(c) Effluent point flows

All effluent point-flows entering the river system are aggregated as inflows entering the upstream end of the relevant reaches. These values are supplied externally to the model.

(d) Catchment runoff directly into reach

Each river reach must be situated entirely within a catchment which has been modelled using program NACLØ1, but more than one reach may be defined within each such catchment. Each reach within the catchment then derives catchment runoff in proportion to the percentage of the catchment area draining directly into the reach. Of the runoff entering the reach directly, part will enter the reach at its upstream end and the remainder laterally.

The catchment runoff entering the reach at its upstream end during time step Δt, QCATU ($m^3 \times 10^6$), is then given by:

$$QCATU = \frac{PLAT.QCAT.CUMEC}{NSTEP} \qquad \text{.....(2.51)}$$

where PLAT = proportion of catchment draining to upstream end of river reach
QCAT = catchment outflow as calculated in program NACLØ1 (m^3/s)
CUMEC = constant
= 0,0864
NSTEP = number of computational time steps per day

QLAT ($m^3 \times 10^6$), the catchment runoff entering the reach laterally during time step Δt is computed as:

$$QLAT = \frac{PUP.QCAT.CUMEC}{NSTEP} \qquad \text{.....(2.52)}$$

where PUP = proportion of catchment draining laterally to the river reach

Fig. 2.15 serves to clarify the definitions of PLAT and PUP. In the diagram, for reach number 1, PLAT = $\frac{70}{220}$ = 0,318 and PUP = $\frac{40}{220}$ = 0,182.

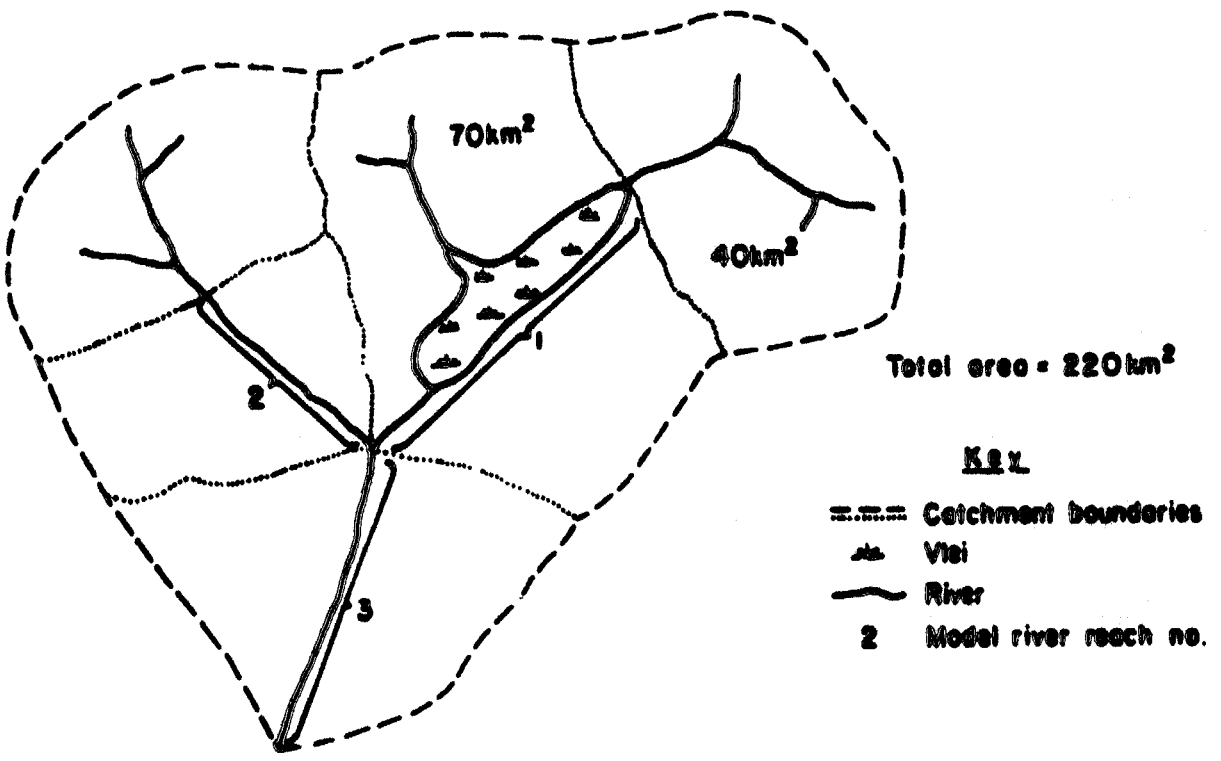

Fig.2.15: Illustration of the definitions of PLAT and PUP

(e) Evaporation losses

Net evaporation losses are calculated on a daily basis from the mean monthly potential evaporation and the daily rainfall. The potential evaporation, PE(mm/d), is multiplied by a monthly evaporation factor FEVAP in order to account for the reduction or increase in evaporation as the result of the influence of the extensive reed beds covering large areas of some of the reaches. The equations governing evaporation are:

$$EVAPV = (PE.FEVAP - RCAT).\frac{AT.10^{-3}}{NSTEP} \quad (m^3x10^6) \text{ .....(2.53)}$$

where RCAT = rainfall during day (mm)
AT = average total water surface area during time step Δt (km^2).

AT can be re-written in terms of h_1 and h_2, the depths of flow at the start and end of time step Δt respectively, to yield:

$$AT = ATH1 + ATH2 \cdot \tfrac{1}{2}(h_1 + h_2) \quad \text{.....(2.54)}$$

From the geometry, for $H_{k-1} \leq \tfrac{1}{2}(h_1+h_2) \leq H_k$, ATH1 and ATH2 are given by:

$$ATH1 = \left[BT_{k-1} - \frac{(BT_k - BT_{k-1})}{(H_k - H_{k-1})}\right]. CHAIN.10^{-3} \quad \text{.....(2.55)}$$

and
$$ATH2 = \frac{(BT_k - BT_{k-1})}{(H_k - H_{k-1})}. CHAIN.10^{-3} \quad \text{.....(2.56)}$$

where CHAIN = length of river reach (km).

AC, the corresponding channel water surface area, is computed by equations identical in form to 2.54 - 2.55 with ATH1, ATH2, BT_k and BT_{k-1} replaced by ACH1, ACH2, BC_k and BC_{k-1}.

Equation 2.53 can be re-written as:

$$EVAPV = ET1 + ET2 \cdot h_2 \quad \text{.....(2.57)}$$

where
$$ET1 = \frac{(PE.FEVAP-RCAT)}{NSTEP \cdot 10^3} .(ATH1+\tfrac{1}{2}.ATH2.h_1)$$

$$ET2 = \frac{(PE.FEVAP-RCAT)}{NSTEP \cdot 10^3} .(\tfrac{1}{2}ATH2)$$

Transpiration loss from the reeds and other swamp vegetation is computed as:

$$QTG = (PE.FTRANS-RCAT) \cdot \frac{AVLEI.10^{-3}}{NSTEP} \quad (m^3 x 10^6) \quad \text{.....(2.58)}$$

where FTRANS = seasonal transpiration factor
AVLEI = vlei area (km^2)

(f) **Bed losses**

A constant potential bed loss rate is specified per reach. The actual bed loss applied during any time step is adjusted according to the availability of water in the reach.

(g) **Irrigation losses**

The assumption is made that the crop demand during time step Δt, QCD ($m^3 x 10^6$), is directly proportional to the potential evaporation.
Hence:

$$QCD = \frac{AIRRIG.FIRRIG.PE.10^{-3}}{NSTEP} \qquad \ldots\ldots\ldots\ldots (2.59)$$

where AIRRIG = area of land under irrigation (km^2)
FIRRIG = seasonal irrigation demand factor.

This demand is then met by precipitation and irrigation. The irrigation demand during time step Δt, QIRRIG ($m^3 x 10^6$), is then given by:

$$QIRRIG = (PE \cdot FIRRIG - RCAT) \cdot \frac{AIRRIG}{NSTEP} .10^{-3} \qquad \ldots\ldots\ldots\ldots (2.60)$$

When equation 2.60 becomes negative QIRRIG is set equal to zero.

Allowance is made for irrigation return flows. It is assumed that a constant proportion, RETURN, of the irrigation demand returns to the stream. The irrigation return flow during time step Δt, QIR ($m^3 x 10^6$), is given by:

$$QIR = RETURN \cdot QIRRIG \qquad \ldots\ldots\ldots\ldots (2.61)$$

(h) **Outflow from downstream end**

Outflow from each reach is assumed to be controlled by the Manning equation. Discharge from the central channel during time step Δt, QOUTC ($m^3 x 10^6$), is thus computed as:

$$QOUTC = \frac{AXC \cdot CUMEC}{AMANC \cdot NSTEP} \cdot \left(\frac{AXC}{PC}\right)^{2/3} \cdot SLOPE^{1/2} \qquad \ldots\ldots\ldots\ldots (2.62)$$

where AXC = average wetted cross-sectional area of channel during time step Δt (m^2)

AMANC = Manning n factor for channel

PC = average wetted perimeter of channel during time step Δt (m)

SLOPE = channel slope,

while the discharge from the flood plain, QOUTF ($m^3 \times 10^6$), is given by:

$$QOUTF = \frac{AXF.CUMEC}{AMANF.NSTEP} \cdot \left[\frac{AXF}{PF}\right]^{2/3} . SLOPE^{1/2} \quad .....(2.63)$$

where AXF = average wetted cross-sectional area of flood plain during time step Δt (m^2)

AMANF = Manning n factor for flood plain

PF = average wetted perimeter of channel during time step Δt (m).

The implicit assumption behind equations 2.62 and 2.63 is that the outflow at the lower end of each reach is independent of the influence of storages in downstream reaches. Care should therefore be taken to choose river reaches in such a way as to make these equations as nearly valid as possible. A weir or outlet from a lake or vlei would thus form an ideal river reach boundary.

From the geometry, for $H_{k-1} \leq \frac{1}{2}(h_1+h_2) \leq H_k$, AXC can be expressed as:

$$AXC = AXCH1 + AXCH2 \cdot \tfrac{1}{2}(h_1+h_2) + AXCH3 \cdot (\tfrac{1}{2}(h_1+h_2))^2 \quad .....(2.64)$$

where AXCH1 = wetted cross-sectional area below depth H_{k-1} (m^2)

$$AXCH2 = BC_{k-1} - H_{k-1} \cdot \frac{(BC_k - BC_{k-1})}{(H_k - H_{k-1})} \quad .....(2.65)$$

and $$AXCH3 = \frac{1}{2} \cdot \frac{(BC_k - BC_{k-1})}{(H_k - H_{k-1})} \quad .....(2.66)$$

Similarly PC can be expressed as:

$$PC = PCH1 + PCH2 \cdot \tfrac{1}{2}(h_1+h_2) \qquad \text{.....(2.67)}$$

where PCH1 = wetted perimeter below depth H_{k+1} (m)

$$PCH2 = 2 \cdot \left[\left\{ \frac{(BC_k - BC_{k-1})}{2 \cdot (H_k - H_{k-1})} \right\}^2 + 1 \right] \qquad \text{.....(2.68)}$$

AXF and PF can similarly be expressed in terms of h_1 and h_2 as:

$$AXF = AXFH1+AXFH2 \cdot \tfrac{1}{2}(h_1+h_2) + AXCH3 \cdot \left\{ \tfrac{1}{2}(h_1+h_2) \right\}^2 \qquad \text{....(2.69)}$$

and

$$PF = PFH1 + PFH2 \cdot \tfrac{1}{2}(h_1+h_2) \qquad \text{.....(2.70)}$$

where coefficients AXFH1, ASFH2, AXFH3, PFH1 and PFH2 are derived in the same way as AXCH1-3, PCH1 and PCH2.

(i) <u>Overall water mass balance</u>

The continuity equation for any river reach may be written as:

$$VOL' = VOL + \sum_{i=1}^{m} QOUT_i + QEFF + QCATU + QLAT - EVAPV - QTG - GLOSS - QIRRIG + QIR - QOUTC - QOUTF \qquad \text{.....(2.71)}$$

where VOL′ = storage at end of time step Δt ($m^3 \times 10^6$)

VOL = storage at start of time step Δt ($m^3 \times 10^6$)

m = number of river reaches connected to upstream end of reach

$QOUT_i$ = outflow from ith upstream reach during time step Δt ($m^3 \times 10^6$)

QEFF = effluent point flow into reach during time step Δt ($m^3 \times 10^6$)

GLOSS = bed loss during time step Δt ($m^3 \times 10^6$)

For $H_{k-1} \leq h_2 \leq H_k$, VOL′ is given by:

$$VOL' = (AXC + AXF) \cdot CHAIN \cdot 10^{-3}$$

$$= VTH1 + VTH2 \cdot h_2 + VTH3 \cdot h_2^2 \qquad \text{.....(2.72)}$$

where $VTH1 = (AXCH1 + AXFH1) \cdot CHAIN \cdot 10^{-3}$

$VTH2 = (AXCH2 + AXFH2) \cdot CHAIN \cdot 10^{-3}$

and $VTH3 = (AXCH3 + AXFH3) \cdot CHAIN \cdot 10^{-3}$

Although output from program NACLØ2 is at a daily time step, equ. 2.71 is solved NSTEP times (where NSTEP is user-defined) per day. Two methods are used to solve equation 2.71, the first being the Newton-Rhapson convergence procedure.

The continuity equation (2.71) can be re-written as:

$$f(h_2) = 0 = CONST - EVAPV - QOUTC - QOUTF - VOL' \quad \ldots\ldots\ldots (2.73)$$

where $CONST = VOL + \sum_{i=1}^{m} QOUT_i + QEFF + QCATU + QLAT - QTG - GLOSS - QIRRIG + QIR \quad \ldots\ldots\ldots\ldots\ldots (2.74)$

and EVAPV, QOUTC, QOUTF and VOL' are functions of the unknown h_2 defined by equations 2.57, 2.62, 2.63 and 2.72.

Using the Newton-Rhapson procedure, the $(i+1)^{th}$ approximation of h_2, h_2^{i+1}, is given by:

$$h_2^{i+1} = h_2^i - \frac{f(h_2^i)}{f'(h_2^i)}$$

$$= h_2^i - \frac{CONST - EVAPV(h_2^i) - VOL\ (h_2^i) - QOUTC(h_2^i) - QOUTF(h_2^i)}{-DEVAPV(h_2^i) - DVOL\ (h_2^i) - DQOUTC(h_2^i) - DQOUTF(h_2^i)}$$

$\ldots\ldots\ldots (2.75)$

where DEVAPV, DQOUTC, DQOUTF and $DVOL'$ are differentials with respect to h_2 of equations 2.57, 2.62, 2.63 and 2.72.

Differentiating equations 2.57 and 2.72 with respect to h_2 yields:

$$DEVAPV = ET2 \quad \ldots\ldots\ldots\ldots\ldots\ldots (2.76)$$

and $$DVOL' = VTH2 + 2 \cdot VTH3 \cdot h_2 \quad \ldots\ldots\ldots\ldots\ldots\ldots (2.77)$$

The differential of equation 2.62 with respect to h_2 is given by:

$$DQOUTC = \left[\frac{CUMEC \cdot SLOPE^{\frac{1}{2}}}{AMANC \cdot NSTEP}\right] \cdot \left[AXC \cdot \frac{d}{dh_2}\left[\left(\frac{AXC}{PC}\right)^{2/3}\right] + \left(\frac{AXC}{PC}\right)^{2/3} \cdot \frac{d}{dh_2}(AXC)\right]$$

$$= \left[\frac{CUMEC \cdot SLOPE^{\frac{1}{2}}}{AMANC \cdot NSTEP}\right] \cdot \left[AXC \cdot \frac{2}{3} \cdot \left(\frac{AXC}{PC}\right)^{-1/3} \cdot PC^{-2} \cdot PC \cdot \frac{d}{dh_2}(AXC) - AXC \cdot \frac{d}{dh_2}(PC) + \left(\frac{AXC}{PC}\right)^{2/3} \cdot \frac{d}{dh_2}(AXC)\right]$$

$$= \left[\frac{CUMEC \cdot SLOPE^{\frac{1}{2}}}{AMANC \cdot NSTEP}\right] \cdot \left(\frac{AXC}{PC}\right)^{2/3} \cdot \left[\frac{5}{3} \cdot \frac{d}{dh_2}(AXC) - \frac{2}{3} \cdot \frac{AXC}{PC} \cdot \frac{d}{dh_2}(PC)\right]$$

$$= \left[\frac{CUMEC \cdot SLOPE^{\frac{1}{2}}}{AMANC \cdot NSTEP}\right] \cdot \left(\frac{AXC}{PC}\right)^{2/3} \cdot \left[\frac{5}{6} \cdot AXCH2 + \frac{5}{3} \cdot AXCH3 \cdot (h_1 + h_2) - \frac{2}{6} \cdot \left(\frac{AXC}{PC}\right) \cdot PCH2\right] \quad \ldots\ldots\ldots (2.78)$$

Similarly DQOUTF is given by:

$$DQOUTF = \left[\frac{CUMEC \cdot SLOPE^{\frac{1}{2}}}{AMANF \cdot NSTEP}\right] \cdot \left(\frac{AXF}{PF}\right)^{2/3} \cdot \left[\frac{5}{6} \cdot AXFH2 + \frac{5}{3} AXFH3 \cdot (h_1 + h_2) - \frac{2}{6} \cdot \left(\frac{AXF}{PF}\right) \cdot PFH2\right] \quad \ldots\ldots\ldots (2.79)$$

Successive estimates of h_2 are made using equation 2.75 until ERR_1, the absolute difference between h_2^{i+1} and h_2^i, is less than ERROR (m), the specified maximum permissible error.

When discontinuities in the river reach cross-section are encountered the solution procedure can become unstable, resulting in divergence. A check is therefore incorporated to switch to a more stable, although slower, convergence procedure (the method of False Position) if ERR_1 exceeds ERR_{i-1}, the absolute error of the preceding iteration.

The $(i+1)^{th}$ approximation of h_2 is then given by:

$$h_2^{i+1} = h_2^i - \frac{(h_2^o - h_2^i) \cdot f(h_2^i)}{f(h_2^o) - f(h_2^i)} \quad \ldots\ldots\ldots\ldots\ldots (2.80)$$

where h_2^o is some earlier choice of h_2 and f is the function of h_2 given in equation 2.72.

The method of False Position is first order convergent. It is still possible, although less likely, that this procedure can also become unstable when discontinuities in channel cross-section are encountered. Should this occur, the computational time step for the current day is halved and the computation for the day is repeated using starting conditions as at the start of the day.

The user may limit the maximum number of iterations during any time step to NQMAX iterations. Should convergence not have occurred after NQMAX iterations, then the computational error may be unacceptably high. Alternatively, a systematic gain or loss of water due to allowable computational errors could occur. A check calculation is therefore made at the end of every day to ensure that the water mass balance is preserved. This is done by first summating the storage at the start of the day and the total inflow into the reach during the day. This value, $DIFFV_o$, is then given by:

$$DIFFV_o = VOL + \left[\sum_{i=1}^{m} QOUT_i + QEFF + QCATU + QLAT + QIR\right] \cdot NSTEP \quad \ldots\ldots\ldots (2.81)$$

Each of the losses of water from the reach is then successively subtracted from $DIFFV_o$:

$$DIFFV_j = DIFFV_{j-1} - LOSS_j \quad \ldots\ldots\ldots\ldots\ldots\ldots (2.82)$$

where $LOSS_i$ = computed loss during the day

i.e. $LOSS_1 = \sum_{k=1}^{NSTEP} (EVAPV_k)$

$LOSS_2 = QTG \cdot NSTEP$

$LOSS_3 = GLOSS \cdot NSTEP$

$LOSS_4 = QIRRIG \cdot NSTEP$

$LOSS_5 = \sum_{k=1}^{NSTEP} (QOUTC_k)$

and $LOSS_6 = \sum_{i=1}^{NSTEP} (QOUTF_k)$

where k refers to the k^{th} time step.

Equation 2.82 is thus applied six times. If $DIFFV_j \geq 0$ no adjustment is made, but if $DIFFV_j < 0$, then $LOSS_j$ is adjusted to:

$$LOSS_j = DIFF_{j-1} \qquad \text{.....(2.83)}$$

and $LOSS_{j+1}$ .....$LOSS_6$ are set equal to zero.

(j) Internal water mass balance

Having solved the overall continuity equation for the reach it now becomes necessary to determine the fluxes between channel and flood plain.

Fig. 2.16 depicts the movement of water through the reach.

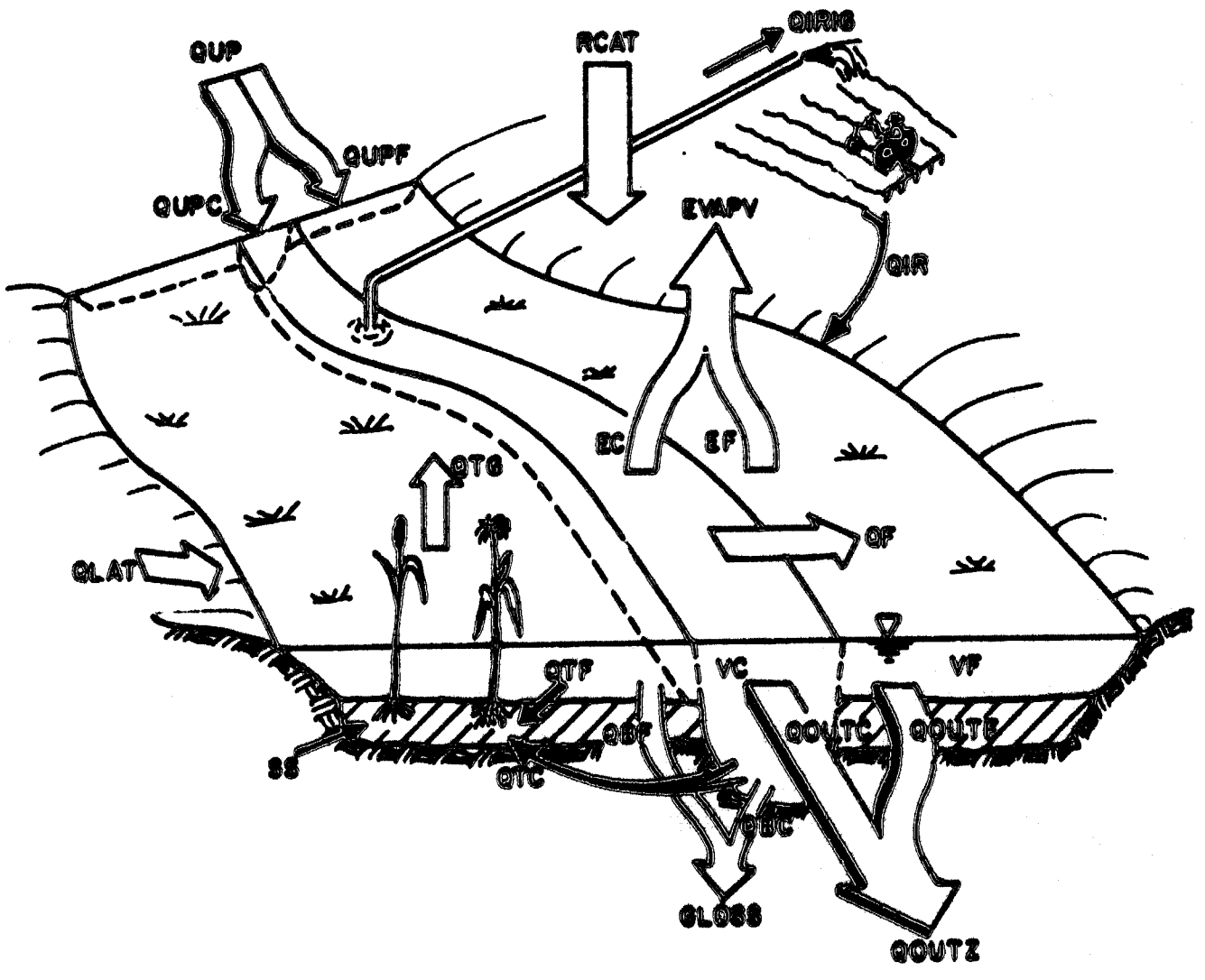

Fig. 2.16: Generalised channel reach.

The inflow at the upstream end of the reach, QUP (m^3x10^6), is distributed between the flood plain and the channel in proportion to QOUTC and QOUTF: Hence:

$$QUPC = \frac{QOUTC}{QOUTZ} \cdot QUP \qquad \text{.....(2.84)}$$

and $$QUPF = QUP - QUPC \qquad \text{.....(2.85)}$$

where $$QUP = \sum_{i=1}^{m} QOUT_i + QEFF + QCATU \cdot NSTEP$$

QUPC = inflow to upstream end of flood plain (m^3x10^6)
QUPF = inflow to upstream end of channel (m^3x10^6)
QOUTZ = QOUTC + QOUTF (m^3x10^6)

Evaporation, evapotranspiration and bed seepage losses are assumed to be derived from channel and flood plain storage in proportion to the corresponding water surface areas.

Thus:

$$EC = \frac{AC}{AT} \cdot LOSS_1 \qquad \text{.....(2.86)}$$

$$QTC = \frac{AC}{AT} \cdot LOSS_2 \qquad \text{.....(2.87)}$$

$$QBC = \frac{AC}{AT} \cdot LOSS_4 \qquad \text{.....(2.88)}$$

and:

$$EF = LOSS_1 - EC \qquad \text{.....(2.89)}$$

$$QTF = LOSS_2 - QTC \qquad \text{.....(2.90)}$$

$$QBF = LOSS_4 - QBC \qquad \text{.....(2.91)}$$

where EC, QTC and QBC are evaporation, evapotranspiration and bed seepage losses from the channel and EF, QTF and QBF are the corresponding losses from the flood plain.

Making the assumption that irrigation demands are pumped from the channel while irrigation return flows and lateral inflows from the surrounding catchment enter the flood plain allows QF, the transverse flow from the channel to the flood plain during the day (m^3x10^6), to be calculated as:

$$QF = VC-VC'+QUPC-QIRRIG-EC-QTC-QBC-QOUTC \quad \text{.....(2.92)}$$

where VC = channel storage at start of day (m^3x10^6)
VC′= channel storage at end of day (m^3x10^6)
= $AXC_L \cdot CHAIN \cdot 10^{-3}$

where AXC_L is the wetted cross-sectional area of the channel (as given by equation 2.64) at the end of the last computational time step of the current day.

VF′, the flood plain storage at the end of the day (m^3x10^6), is then calculated as:

$$VF' = VOL'_L - VC' \quad \text{.....(2.93)}$$

where VOL'_L = total reach storage at end of last computational time step of the current day (m^3x10^6).

2.3.2 Channel routing model : salt mass balance

All the water and salt entering the upstream end of the channel during each day is aggregated to form a new cell. The cells are advected through the reach with no allowance for dispersion between cells. Dispersion was ignored, as the simplicity of the model does not warrant such sophistication. Dispersion effects are to some extent accounted for by the interchange between the central channel and the flood plain. For tributary systems with more than one river reach a significant amount of dispersion is achieved when the entire day's outflow from each reach is mixed before being introduced into the following reach.

The assumption is made that the flood plain can be treated as a single, completely mixed cell. This assumption is tenable due to the relatively long detention time of the flood plain storage compared with that of the channel.

(a) Salt fluxes between channel and flood plain

The volume of the new cell created at the upstream end of the channel, vc_N, is set equal to QUPC. The salt load entering cell N, sc_N (t), is given as:

$$SC_N = SUP \cdot \frac{QUPC}{QUP} \quad \text{.....(2.94)}$$

where $$SUP = \left[\sum_{i=1}^{m} (QOUT_i \cdot COUT_i) + QEFF \cdot CEFF + QCATU \cdot CCAT\right] \cdot NSTEP \quad \text{.....(2.95)}$$

and $COUT_i$ = salinity of outflow from i^{th} upstream reach (mg/ℓ)

CEFF = salinity of effluent point inflow (mg/ℓ)

CCAT = salinity of catchment runoff (mg/ℓ)

The salt load entering the upstream end of the flood plain is then calculated as:

$$SQUPF = SUP - SC_N \quad \text{.....(2.96)}$$

The salt load returned from irrigated lands during the day, SQIR (t), is given by:

$$SQIR = SQI_o \ (1-FIX) \quad \text{..... ..(2.97)}$$

where SQI_o = salt load applied to irrigated land during previous day (t)

FIX = proportion of applied salt load retained on irrigated land ($0 < FIX < 1$)

The catchment washoff salt load entering the reach laterally, SLAT (t), is given by:

$$SLAT = QLAT \cdot CCAT \quad \text{.....(2.98)}$$

The salt load flushed out of the swamp "sponge" storage during the day, SFLUSH (t), is given by:

$$SFLUSH = FLEACH \cdot SS \cdot \tfrac{1}{2}(VP+VP') \quad \text{.....(2.99)}$$

where FLEACH = leaching factor for salts stored in the swamp sponge

SS = swamp sponge salt storage at start of day (t)

VP = flood plain water storage at start of day ($m^3 \times 10^6$)

If SFLUSH as calculated by equation 2.99 is greater than SS, then SFLUSH is set equal to SS.

There are two possible flow conditions that need to be considered:

Case I: $QF \leq 0$

In this case the salt mass balance for the flood plain is first computed. Pre-mixing all inflows to the flood plain yields:

$$SF'' = SF+SQIR+SLAT+SQUPF+SFLUSH \quad \ldots\ldots\ldots\ldots\ldots\ldots (2.100)$$

where SF'' = intermediate flood plain salt storage (t)
SF = flood plain salt storage at start of day (t)

The salt load moving from the flood plain to the channel, SQF (t), is then given by:

$$SQF = SF'' \cdot \frac{QF}{VF''} \quad \ldots\ldots\ldots\ldots\ldots\ldots (2.101)$$

where $VF'' = VF+QIR+QLAT+QUPF \quad \ldots\ldots\ldots\ldots\ldots\ldots (2.102)$

The lateral inflow to the reach is then apportioned to each cell according to its storage. Thus for cell i the adjusted storage vc_i'' is given by:

$$vc_i'' = vc_i + \frac{vc_i}{VCT} \cdot (-QF) \quad \ldots\ldots\ldots\ldots\ldots\ldots (2.103)$$

where vc_i = cell volume at start of day ($m^3 x 10^6$)
$VCT = VC + QUPC$

The corresponding adjusted cell salt load, sc_i (t), is given by:

$$sc_i'' = sc_i + \frac{vc_i}{VCT} \cdot (-SQF) \quad \ldots\ldots\ldots\ldots\ldots\ldots (2.104)$$

where sc_i = cell salt load at start of day (t).

The implicit assumption is that the entire upstream inflow enters the reach at the beginning of the day, whereas in fact cell N grows from zero volume at the start of the day to its full volume at the day's end. The lateral inflow to cell N will therefore be over-estimated. Similarly, at the downstream end of the reach, the lateral inflow to those cells leaving the reach will also be over-estimated. This approximation is satisfactory provided the inflow at the upstream end is small relative to the total reach storage.

The second implied assumption is that the channel is uniform, with uniform lateral inflow along its length (i.e. the lateral inflow to any cell is proportional to the cell volume). Catchment and channel irregularities reduce the validity of this assumption, however. In view of the limitations of this second assumption, there is little purpose to be served by applying the complex equations required to modify the first assumption. The effects of these approximations are considered to be of little consequence compared with those resulting from the other assumptions that have had to be made.

Channel losses are next deducted from each cell in proportion to the adjusted cell volume vc_i''. The new adjusted cell volume vc_i' and the adjusted cell storage sc_i are given by:

$$vc_i' = vc_i'' - (QTC+QBC+EC+QIRRIG) \cdot \frac{vc_i''}{VCT-QF} \quad \ldots\ldots\ldots\ldots (2.105)$$

$$sc_i' = sc_i'' - SQBC_i - SQTC_i - SQI_i \quad \ldots\ldots\ldots\ldots (2.106)$$

where $$SQBC_i = sc_i'' \cdot \frac{QBC}{(VCT-QF)} \quad \ldots\ldots\ldots\ldots (2.107)$$

$$SQTC_i = sc_i'' \cdot \frac{QTC}{(VCT-QF)} \quad \ldots\ldots\ldots\ldots (2.108)$$

$$SQI_i = sc_i'' \cdot \frac{QIRRIG}{(VCT-QF)} \quad \ldots\ldots\ldots\ldots (2.109)$$

Case II: $QF > 0$

In this case the losses from each cell are first deducted. The new volume V_i' and the new cell storage sc_i' are then given by:

$$vc_i' = vc_i - (QTC+QBC+EC+QIRRIG+QF) \cdot \frac{vc_i}{VCT} \quad \ldots\ldots\ldots\ldots (2.110)$$

$$sc_i' = sc_i - SQBC_i - SQTC_i - SQI_i - SQF_i \quad \ldots\ldots\ldots\ldots (2.111)$$

where $$SQBC_i = sc_i \cdot \frac{QBC}{VCT} \quad \ldots\ldots\ldots\ldots (2.112)$$

$$SQTC_i = sc_i \cdot \frac{QTC}{VCT} \quad \ldots\ldots\ldots\ldots (2.113)$$

$$SQI_i = sc_i \cdot \frac{QIRRIG}{VCT} \quad \text{.....(2.114)}$$

$$SQF_i = sc_i \cdot \frac{QF}{VCT} \quad \text{.....(2.115)}$$

Pre-mixing all inflows to the flood plain yields:

$$SF'' = SF+SQIR+SLAT+SQUPF+SFLUSH+\sum_{i=1}^{N}(SQF_i) \quad \text{.....(2.116)}$$

and $$VF'' = VF+QIR+QLAT+QUPF+QF \quad \text{.....(2.117)}$$

After SF'' has been computed by equation 2.100 or 2.116 the final salt storage at the end of the day SF' is computed as:

$$SF' = SF''-SOUTF-SQBF-SQTF \quad \text{.....(2.118)}$$

where $$SOUTF = SF''.\frac{QOUTF}{VF''} \quad \text{.....(2.119)}$$

$$SQBF = SF''.\frac{QBF}{VF''} \quad \text{.....(2.120)}$$

$$SQTF = SF''.\frac{QTF}{VF''} \quad \text{.....(2.121)}$$

(b) Salt balance in the swamp sponge

The salt mass balance equation for the swamp sponge can now be solved as:

$$SS' = SS-SFLUSH+SQTF+\sum_{i=1}^{N}(SQTC_i) \quad \text{.....(2.122)}$$

where SS' = swamp sponge salt storage at end of day (t).

(c) Salt loss to bed seepage

The total bed seepage salt loss during the day, SGLOSS (t), is given by:

$$SGLOSS = SQBF+\sum_{i=1}^{N}(SQBC_i) \quad \text{.....(2.123)}$$

(d) Advection of salt from the reach

Finally to be accounted for is advection out of the downstream end of the reach. The salt load SOUTF leaving the downstream end of

the channel section is calculated thus:

$$SOUTZ = SOUTF + \sum_{i=1}^{n-1}(sc_i') + sc_n' \cdot \left[QOUTC - \sum_{i=1}^{n-1} vc_i'\right] \quad \ldots\ldots(2.124)$$

The first n-1 cells are completely drained and discarded, while cell n is partially drained, its new volume vc_i'' being given by:

$$vc_n'' = vc_n' - \left[QOUTC - \sum_{i=1}^{n-1} vc_i'\right] \quad \ldots\ldots\ldots\ldots\ldots(2.125)$$

The water leaving the downstream end of the reach then forms part of the inflow to the next downstream reach. The steps involved in the cell advection process are illustrated in Fig. 2.17.

A maximum allowable number of cells per reach, NMAX, is introduced to prevent the number of cells from becoming unmanageable when for prolonged periods outflow remains much smaller than the total reach storage. The number of cells is controlled as follows:

If the number of cells reaches NMAX, the first NMIX cells are mixed to form a new cell of volume vc_1^*:

$$vc_1^* = \sum_{i=1}^{NMIX} (vc_i) \quad \ldots\ldots\ldots\ldots\ldots\ldots\ldots(2.126)$$

and salt storage sc_1^*:

$$sc_1^* = \sum_{i=1}^{NMIX} (sc_i) \quad \ldots\ldots\ldots\ldots\ldots\ldots\ldots(2.127)$$

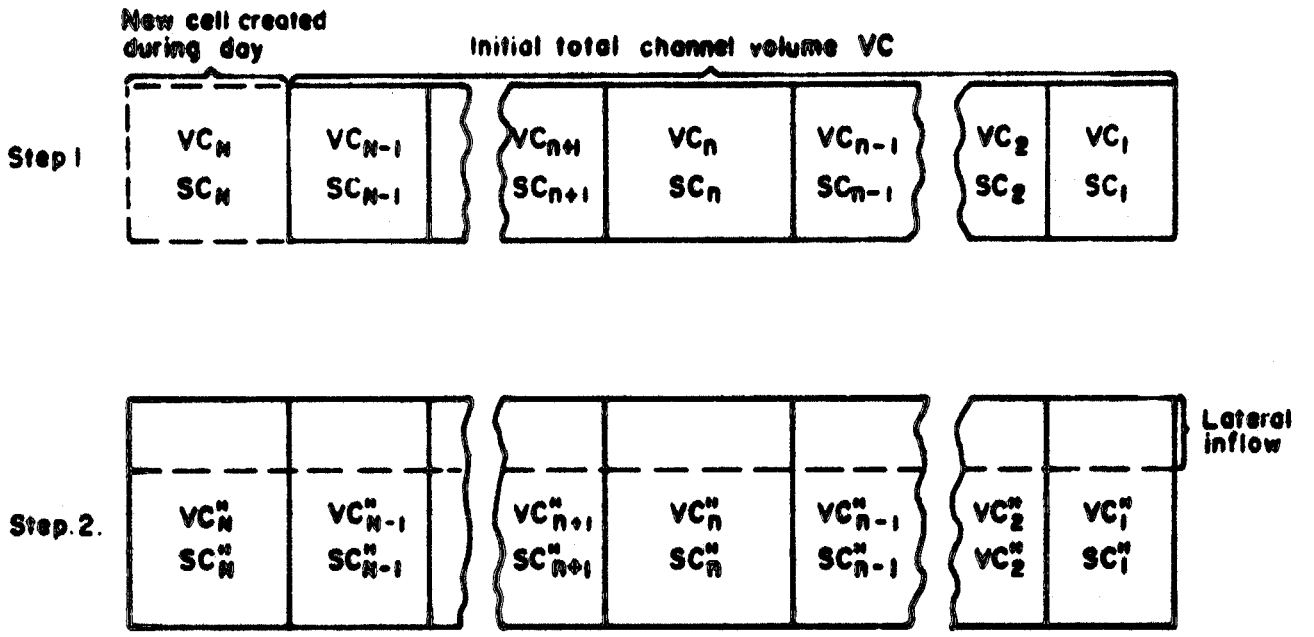

Fig.2.17: Description of cell advection progress.

CHAPTER 3 TESTING OF THE MODEL

This chapter describes the tests made to ensure that the model described in chapter 2 works satisfactorily. Before testing the ability of the model to simulate daily discharges and salt loadings accurately it was first carefully checked manually for programming errors and internal stability. Programs NACLØ1 and NACLØ2 print out as a matter of course cumulative total inputs and outputs as well as initial and final storage states for both water and salt. These enable the user, if he so desires, to check the integrity of the mass balance equations every time the programs are run. The capability of the model to reproduce observed daily flows and salinities successfully serves as further proof of the internal consistency of the programs. Any serious undetected error would render satisfactory calibration of the models impossible.

The remainder of the chapter describes the catchments used to test the models and gives details of the results obtained.

3.1 Objective functions

The following criteria have been adopted for judging the goodness-of-fit between modelled and observed daily flows, TDS and salt loads:

a) Daily mean

Observed and modelled mean daily values should be as close as possible, i.e. E_1 in the following expression must be minimised:

$$E_1 = \left| \frac{\bar{x}_m - \bar{x}_o}{\bar{x}_o} \right| \cdot 100 \qquad \text{.....(3.1)}$$

where E_1 = percentage error of mean daily values

$\bar{x}_m$ = modelled mean daily value

$\bar{x}_o$ = observed mean daily value

b) Standard deviation

The standard deviation of modelled monthly salt loads should be as close as possible to that of the observed loads, i.e. E_2 in the equation 3.2 must be minimised:

$$E_2 = \left| \frac{S_m - S_o}{S_o} \right| \cdot 100 \qquad \text{.....(3.2)}$$

where E_2 = percentage error in standard deviations
S_m = standard deviation of modelled daily values
S_o = standard deviation of observed daily values

c) Linear correlation coefficient

The linear correlation coefficient, r, of modelled and observed daily values should be as near to unity as possible.

d) Visual fit

The visual fit between plotted modelled and observed daily values should be good, i.e. modelled and observed peaks and troughs should coincide as closely as possible in both magnitude and time.

e) Parameter stability

There should be no long-term instability of the model parameters. In particular, there should be a reasonable balance between the initial and final catchment surface salt storages. During any simulation the total surface salt recharge should be of the same order of magnitude as the total surface salt wash-off.

Criterion (d), although practically impossible to quantify, is extremely important and demands close attention. When the visual fit is good, the other criteria are usually also satisfied.

There are three reasons for not attempting to combine the quantifiable criteria, (a) - (c), into a single objective function:

(i) A single, multi-purpose objective function is inevitably far less sensitive than the individual functions. For instance, it is highly desirable that E_1 should be as near zero as possible, and it should therefore be heavily weighted. To do so, however, makes the combined function much less sensitive to changes in E_2 and r. By keeping the functions separate it is always possible to satisfy criterion (a) without in any way impairing the sensitivity of the other criteria.

$$E_2 = \left| \frac{S_m - S_o}{S_o} \right| \cdot 100 \qquad \text{.....(3.2)}$$

where E_2 = percentage error in standard deviations
S_m = standard deviation of modelled daily values
S_o = standard deviation of observed daily values

c) Linear correlation coefficient

The linear correlation coefficient, r, of modelled and observed daily values should be as near to unity as possible.

d) Visual fit

The visual fit between plotted modelled and observed daily values should be good, i.e. modelled and observed peaks and troughs should coincide as closely as possible in both magnitude and time.

e) Parameter stability

There should be no long-term instability of the model parameters In particular, there should be a reasonable balance between the initial and final catchment surface salt storages. During any simulation the total surface salt recharge should be of the same order of magnitude as the total surface salt wash-off.

Criterion (d), although practically impossible to quantify, is extremely important and demands close attention. When the visual fit is good, the other criteria are usually also satisfied.

There are three reasons for not attempting to combine the quantifiable criteria, (a) - (c), into a single objective function:

(i) A single, multi-purpose objective function is inevitably far less sensitive than the individual functions. For instance, it is highly desirable that E_1 should be as near zero as possible, and it should therefore be heavily weighted. To do so, however, makes the combined function much less sensitive to changes in E_2 and r. By keeping the functions separate it is always possible to satisfy criterion (a) without in any way impairing the sensitivity of the other criteria.

(ii) No mathematical objective function can incorporate criterion (d).

(iii) The only real justification for a single objective function would be to permit automatic calibration procedures to be introduced but these have certain drawbacks - viz. they require numerous iterations before convergence and they often converge upon a poor fit. Perhaps most serious of all, they encourage blind use of the model by persons who are not familiar with hydrological processes and the modelling assumptions and are therefore not in a position to interpret the results.

It is often the case that records of daily streamflow and TDS are intermittent, due to defective or inadequate equipment or infrequent sampling. In applying criteria a) to d) therefore, it is important to know how representative the records are of actual flow conditions.

When, for example, a streamflow recorder measures only low flows, then the modelled flows inevitably tend to exhibit a higher mean and standard deviation than those observed and the correlation coefficient deteriorates. This results from the fact that very often modelled floods are slightly out of phase with those observed. Fig. 3.1 serves to illustrate the point.

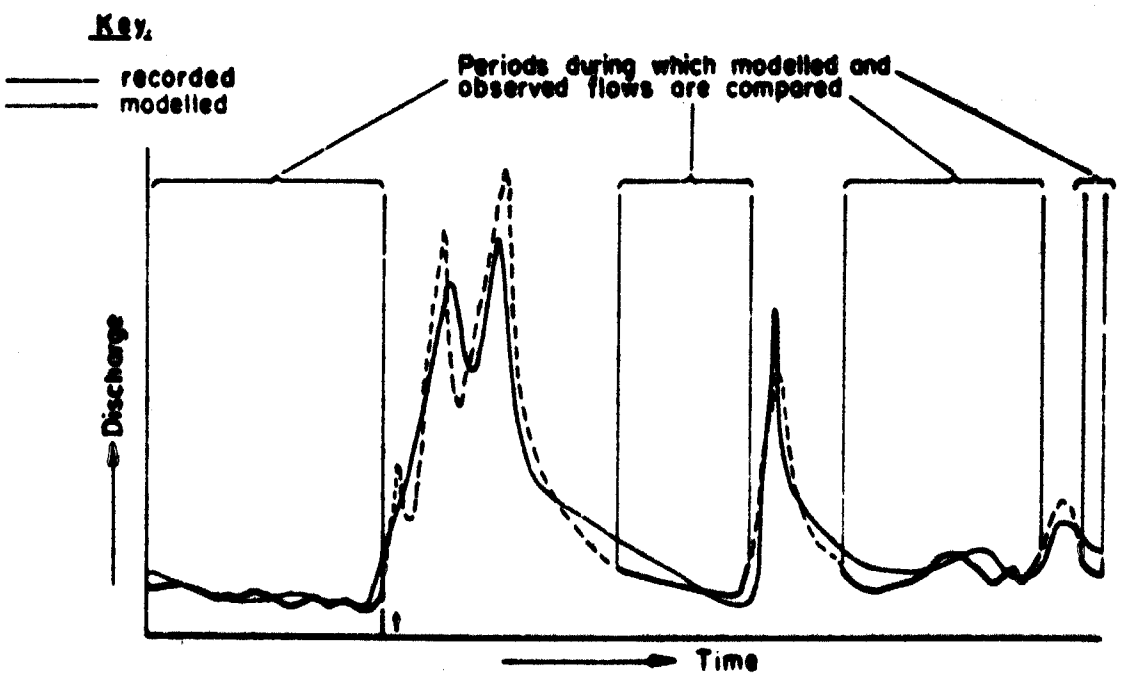

Fig. 3.1: Example of poorly representative stream flow record.

In the figure the broken black line represents the actual stream-flows which were not recorded. A statistical comparison of observed and modelled flows for the periods when the recorder is in operation would in this instance prove highly misleading. At time t, for instance, the modelled discharge is much higher than that observed; this insignificant error would lead to the conclusion that the modelled standard deviation is much too high, whereas in fact it is nearly correct.

A "significance factor", SF, has been devised to give an indication of the representativeness of the sample for the period simulated:

$$SF = 1 - \left[\frac{|\bar{x}_N - \bar{x}_n|}{\bar{x}_N + \bar{x}_n} + \frac{|S_N - S_n|}{S_N - S_n} \right] \quad \ldots\ldots\ldots\ldots (3.3)$$

in which $\bar{x}$ and S are the means and standard deviations of the modelled values and the subscripts refer:

N to the entire period simulated and
n to the days on which observed data were available.

A significance factor approaching unity would [illegible]e a representative sample; the smaller the value of SF t[illegible]r the sample. Values of SF can vary between -1 and +1.

3.2 Model tests

The model was tested using stream-flow and TDS data obtained at several points in the southern PWVS region. The region was divided into 12 subcatchments as indicated in Fig. 3.2 on which are shown also the locations of streamflow gauging stations and water quality sampling points. Each subcatchment is in turn divided into one or more river reaches to facilitate routing of water and dissolved solids through the tributary system. The river reaches are indicated in Fig.3.3.

Model calibration proceeded in two steps. First, all available daily streamflow data at each monitoring point up to August 1978 were used to calibrate the rainfall/runoff parameters of the model for each subcatchment. Secondly, water quality parameters were established for each subcatchment for the period 1977.09 to 1978.08.

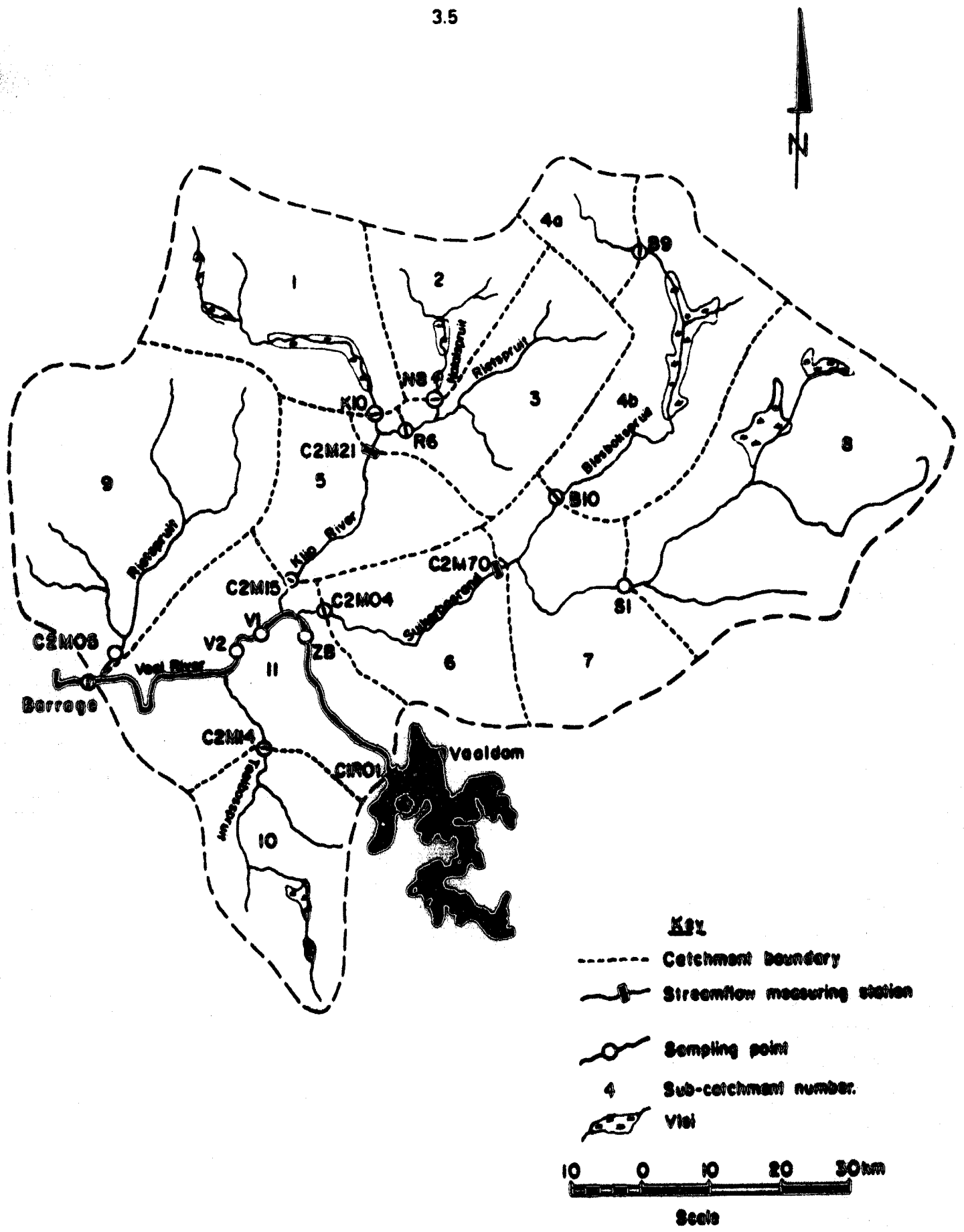

Fig.3.2: Map showing sub-catchments and monitoring points.

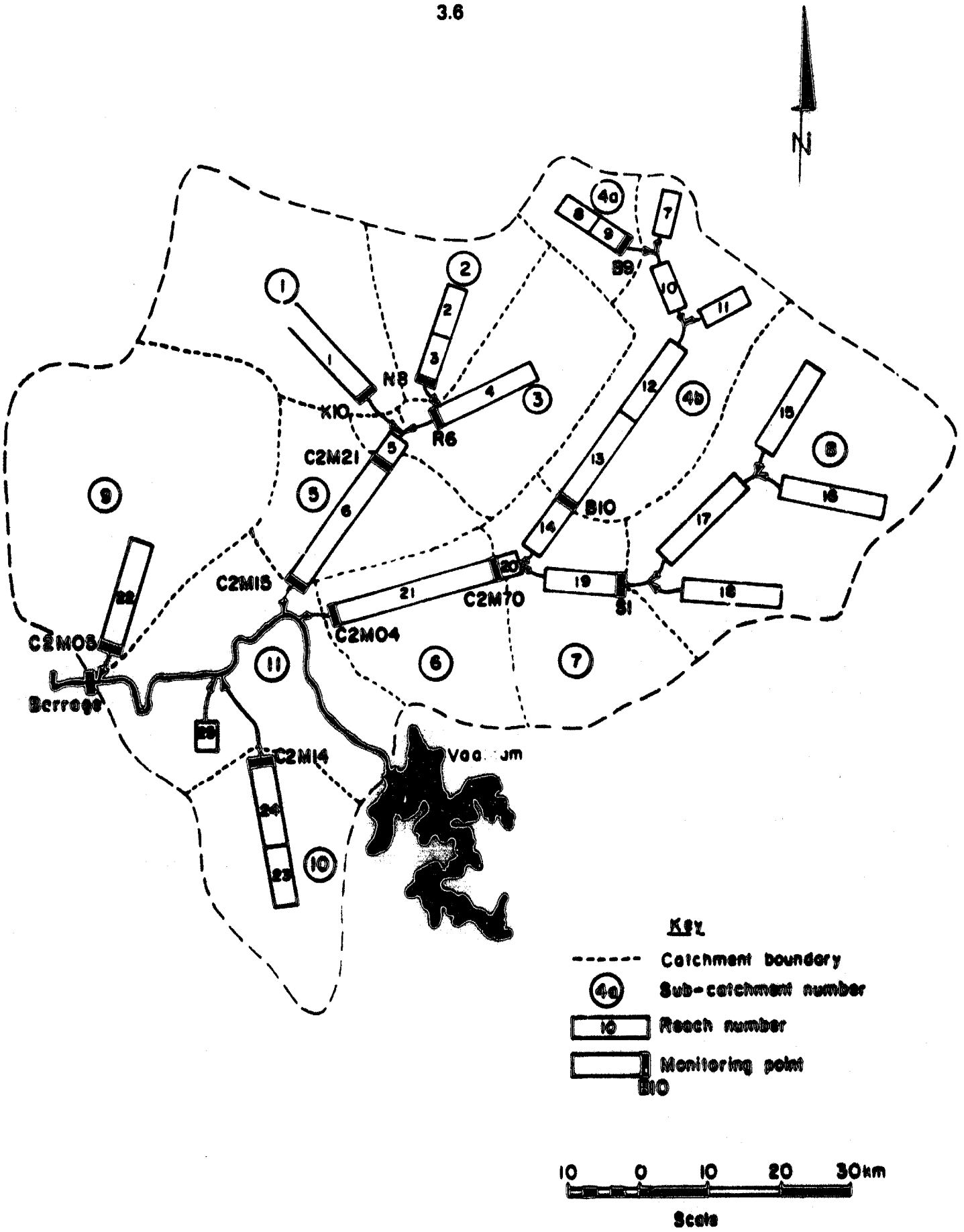

Fig. 3.3: Map showing tributary reaches.

This latter period was limited to one year because prior to that date river quality sampling was at weekly (in some cases monthly) intervals. Since 12 September 1977 the sampling frequency at several key points has been increased to daily intervals thereby enabling good estimates of salt loads to be made at those locations where streamflow records are reliable. Point flow data in earlier years are also less accurate, especially mine pumpage values. Moreover it is reasonable to assume that the rates at which diffuse-source salt is generated have increased with time as human activities have proliferated and that therefore the non-stationarity of the parameter values could adversely affect calibration results for a longer simulation period.

Data for the period 1978.09 to 1979.08 were reserved for purposes of verification of the calibrated model parameters (see section 3.4).

3.2.1 Streamflow modelling

Parameters controlling the synthesization of catchment runoffs were calibrated for each of the 12 subcatchments shown in Fig. 3.2 by comparing modelled with observed flows at each monitoring point and adjusting parameter values until acceptable agreement was reached. Best-fit parameter values thus obtained for each subcatchment are given in Table 3.1 while Table 3.2 shows calibrated parameter values for each of the channel reaches indicated in Fig. 3.3. The statistical properties of the modelled and observed flows are given in Table 3.3.

The results for each monitoring point are now discussed.

Station K10: Monitoring station K10 is situated on the Klip river downstream of a vlei 13 km^2 in extent into which effluent discharges from the Klipspruit and Olifantsvlei sewage works of the Johannesburg municipality. Base flows are therefore dominated by effluent discharges. At K10 the stream is divided by a low island which is submerged during floods. Both channels are controlled by weirs, each with a water level recorder. The weirs are rated only for low flows. The presence of rapids just upstream of the main channel, on the eastern side of the island, leads to unfavourable approach conditions. The reliability of flow records is further undermined

by the presence of thick undergrowth further downstream which often traps fallen tree trunks and other debris. The resultant backwater often submerges the main weir even during low flows. The streamflow record is therefore of value only for checking base flows (comprising predominantly point source influents) and even then is not reliable. Little effort was therefore made to calibrate the model against this record; greater weight was given to the record at station C2M21. Fig. 3.4 is a plot of modelled and observed discharges at K10 for the period September 1975 to August 1978, while Fig. 3.5 shows the corresponding duration curves.

Table 3.1: Runoff component model parameters used in Program NACLØ1

Parameter	Subcatchment number											
	1	2	3	4a	4b	5	6	7	8	9	10	11
AREA	861	392	442	231	1119	541	409	608	1118	1116	829	948
POW	3	3	3	3	3	3	3	3	3	3	3	3
SL	0	0	0	0	0	0	0	0	0	0	250	200
SE	130	138	140	100	180	130	120	200	200	72	300	250
ST	410	400	400	400	400	400	400	400	400	300	400	400
FT	0,40	0,40	0,40	0,10	0,07	0,20	0,40	0,05	0,10	0,10	0,05	0,20
AI	0,037	0,089	0,020	0,059	0,014	0,007	0	0	0,003	0,006	0	0,029
ZMINN	1	1	1	1	3	1	1	3	3	2	3	0
ZMAXN	10	12	12	12	11	11	14	15	15	10	10	10
PI	1,5	1,5	1,5	1,5	1,5	1,5	1,5	1,5	1,5	1,5	1,5	1,5
TL	0,5	0,5	0,5	0,5	0,5	0,5	0,5	0,5	0,5	0,6	1,0	0,8
LAG	2	1	0	0	0	0	0	0	0	1	1	0
GL	5	5	5	3	5	5	3	3	3	5	2	5
QOBS	0,10	0,05	0,05	0,05	0,05	0,05	0,05	0,05	0,05	0,05	0,01	0,05
DGL	0	0	0	0	0	0	0	0	0	0	0	0

Table 3.2: Model parameters used in program MACLØ2

Reach No.	Parameter														
	AVLEI	AIRRIG	CHAIN	RETURN	FIX	FLEACH	PLAT	PUP	HSTART	CONSU	CONSL	GLOSS	SLOPE	AMANC	AMANF
1	13,0	23,0	49,0	0,2	0,7	0,5	0,74	0,26	1,50	450	500	0	0,0022	0,04	0,10
2	1,0	0	7,5	0,2	0,7	0,5	0,40	0,14	1,50	1500	1500	10	0,0024	0,04	0,06
3	6,9	3,0	17,0	0,2	0,7	0,5	0,46	0	1,50	700	800	0	0,0024	0,08	0,10
4	0	20,0	40,0	0,2	0,7	0,5	0,90	0,10	1,50	1000	1000	0	0,0020	0,04	0,06
5	0	4,0	1,0	0,2	0,7	0,5	0,04	0	1,50	600	600	0	0,0011	0,04	0,06
6	0	9,0	45,0	0,2	0,7	0,5	0,96	0	1,50	600	600	0	0,0011	0,04	0,06
7	8,6	0,8	20,0	0,2	0,7	0,5	0,11	0,05	1,50	1000	1050	0	0,0015	0,06	0,12
8	0	0	16,0	0,2	0,7	0,5	0,52	0,38	2,00	400	400	24	0,0020	0,10	99,00
9	0	0,3	2,0	0,2	0,7	0,5	0,10	0	2,00	825	825	0	0,0020	0,04	99,00
10	4,1	1,0	9,5	0,2	0,7	0,5	0,10	0	1,50	1050	1100	0	0,0009	0,06	0,12
11	11,9	3,9	12,0	0,2	0,7	0,5	0,07	0,06	1,50	1000	1050	0	0,0007	0,06	0,12
12	19,9	0	16,0	0,2	0,7	0,5	0,22	0	1,50	1080	1300	6	0,0016	0,06	0,12
13	0	0,8	27,5	0,2	0,7	0,5	0,39	0	1,50	1300	1300	0	0,0016	0,04	0,06
14	0	2,1	18,0	0,2	0,7	0,5	0,24	0	1,00	1300	1300	0	0,0019	0,04	0,06
15	8,4	0	17,0	0,2	0,7	0,5	0,12	0,12	1,50	150	150	0	0,0011	0,04	0,10
16	16,4	0	30,0	0,2	0,7	0,5	0,33	0,08	1,50	150	150	0	0,0009	0,04	0,10
17	7,9	0,2	24,0	0,2	0,7	0,5	0,13	0	0,50	150	150	0	0,0022	0,04	0,10
18	10,9	0	26,0	0,2	0,7	0,5	0,16	0,03	0,50	150	150	0	0,0024	0,04	0,10
19	0	1,7	36,5	0,2	0,7	0,5	0,76	0	1,00	150	150	0	0,0017	0,04	0,06
20	0	0	1,5	0,2	0,7	0,5	0	0	1,00	600	600	0	0,0009	0,04	0,06
21	0	7,8	52,5	0,2	0,7	0,5	1,00	0	1,00	600	600	0	0,0009	0,04	0,06
22	0	4,0	17,0	0,2	0,7	0,5	0,28	0,72	1,00	800	800	0	0,0015	0,04	0,10
23	12,8	0	53,0	0,2	0,7	0,5	0,40	0,11	0,20	1000	1000	0	0,0011	0,04	0,10
24	0	0	10,0	0,2	0,7	0,5	0,12	0,37	0,20	1000	1000	0	0,0005	0,04	0,10
25	0	0	5,0	0,2	0,7	0,5	1,00	0	1,00	800	800	0	0,0010	0,04	0,10

Table 3.3: Statistical properties of modelled and observed discharges (units: m^3/s)

Tributary	Station number	Period	Sample size	Observed		Modelled		Linear correlation coefficient	SF
				$\bar{x}$	S	$\bar{x}$	S		
Klip river	K10	1975.10-78.08	788	4,510	1,319	5,677	3,682	0,407	0,264
	N8	1975.10-78.08	884	,863	2,637	2,773	2,620	0,781	0,932
	R6	1975.10-78.08	1096	2,675	0,656	3,068	2,643	0,292	0,580
	C2M21	1977.10-78.08	317	14,896	19,863	15,527	18,612	0,902	0,974
	C2M15	1970.09-78.08	1655	3,515	1,472	,222	3,123	0,327	0,065
Suikerbosrand	B9	1976.07-78.08	724	0,500	0,282	0,730	0,561	0,635	0,106
	B10	1975.10-78.08	775	2,530	4,064	2,101	3,742	0,422	0,149
	C2M70	1977.06-78.08	409	10,248	33,124	12,520	42,086	0,841	0,929
	C2M04	1970.09-78.08	2674	7,357	28,033	7,191	30,596	0,802	0,986
Rietspruit	C2M05	1970.09-78.08	2746	1,667	6,320	1,653	6,322	0,689	0,988
Taaibosspruit	C2M14	1970.09-78.08	2446	0,382	1,086	0,968	4,001	0,477	0,295
Vaal river	Barrage	1970.09-78.08	2922	82,064	291,221	81,143	258,994	0,984	1,000

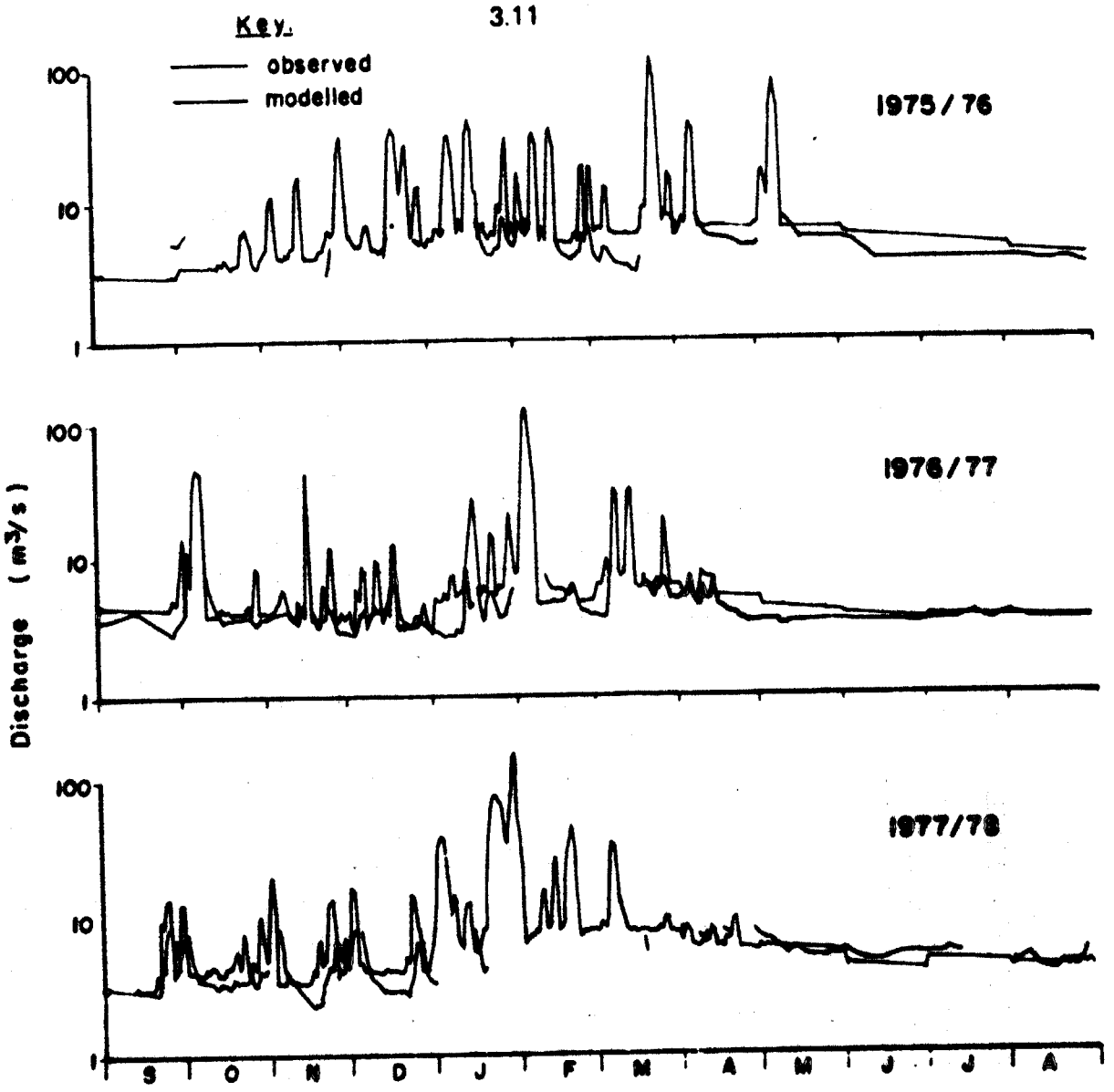

Fig.3.4: Modelled and observed daily discharges at station K10 for period 1975-09 - 1978-08.

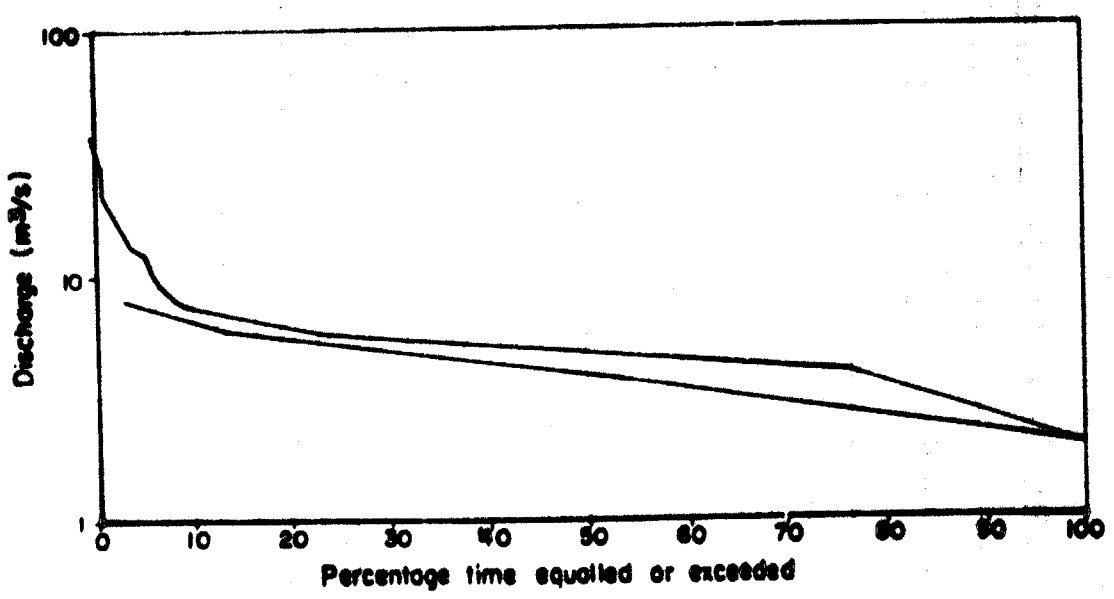

Fig.3.5: Duration curve of modelled and observed daily discharges at station K10 for period 1975-09 - 1978-08.

Station N8: The streamflow record at station N8 on the Natalspruit is generally good except for periods during which the level recorder failed to operate. The water levels are recorded upstream of a Parshall flume located in a disused causeway at the downstream end of a 8-km^2 vlei. As the station had not been rated, water levels were calculated for a wide range of discharges using the flood plain model developed by Weiss (1976). The streamflow record is reliable and efforts were therefore made to obtain a good fit between modelled and observed discharges. From Table 3.3 and Figs. 3.6 and 3.7 it can be seen that a reasonably good fit has been achieved.

Station R6: Upstream of this station the Rietspruit bifurcates around a small, low island. Two weirs control discharges in the channels at the downstream end of the island but water levels are recorded only upstream of the weir in the larger of the channels. Thus even for low flow conditions only part of the discharge is monitored. For higher discharges the flow spreads over a wide flood plain. The discharge record is therefore of little value and was largely disregarded when calibrating the model. Parameter values similar to those used for subcatchment number 2 were adopted. Fig. 3.8 is a plot of modelled and observed daily discharges while Fig. 3.9 shows the corresponding duration curves for the period September 1975 to August 1978.

Station C2M21: A reach of the Klip river controlled by a bridge opening has been rated for a wide range of discharges by the Directorate of Water Affairs (Murphey, 1978) and in October, 1977, a level recorder was installed.

The record, although short, is reliable. The model parameters used for subcatchment number 1 were calibrated to yield a best fit between modelled and observed discharges at this station. From Table 3.3 and Fig. 3.10 and 3.11 it can be seen that a good fit has been obtained.

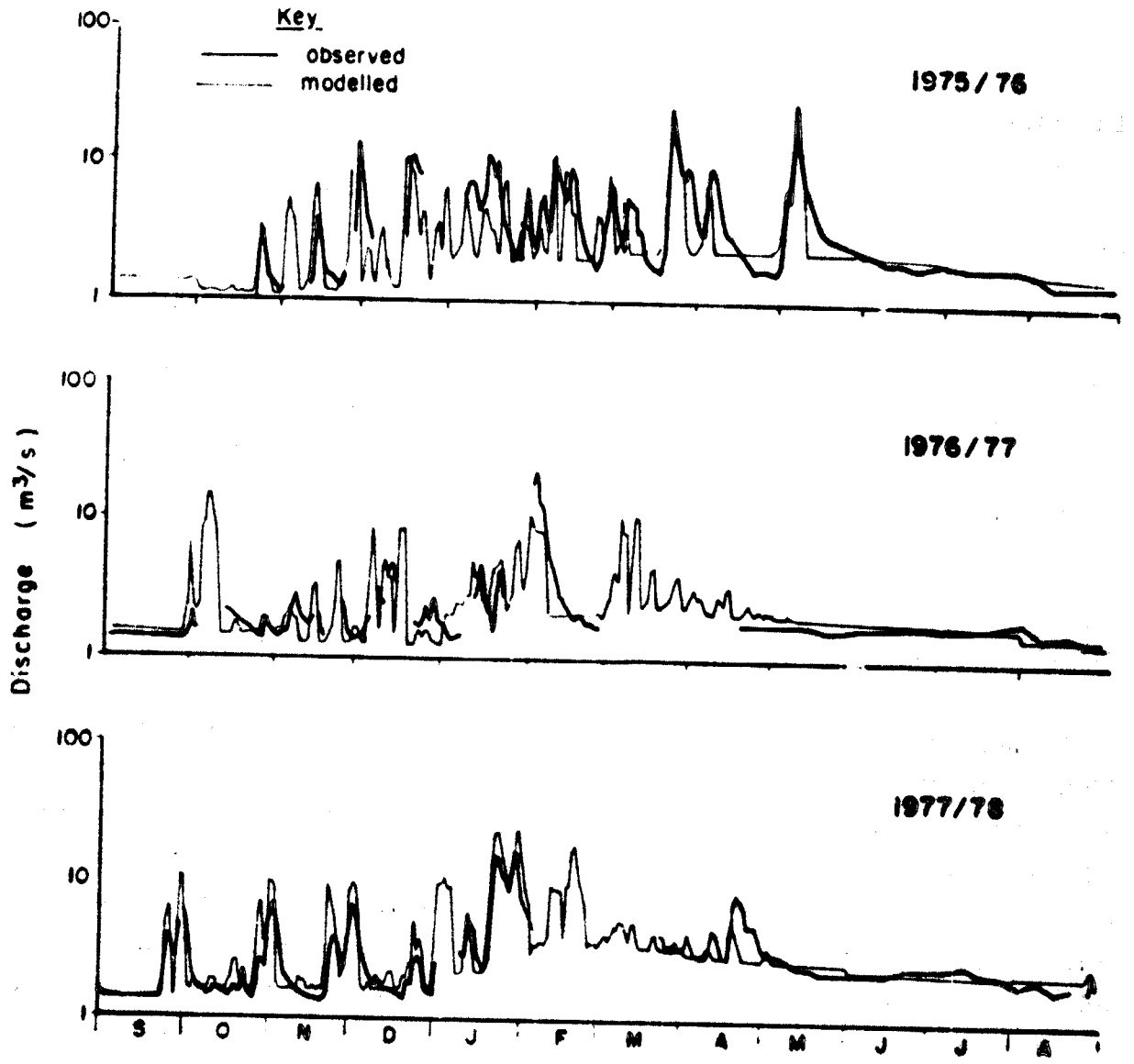

Fig.3.6 : Modelled and observed daily discharges at station N8 for period 1975-09 - 1978-08

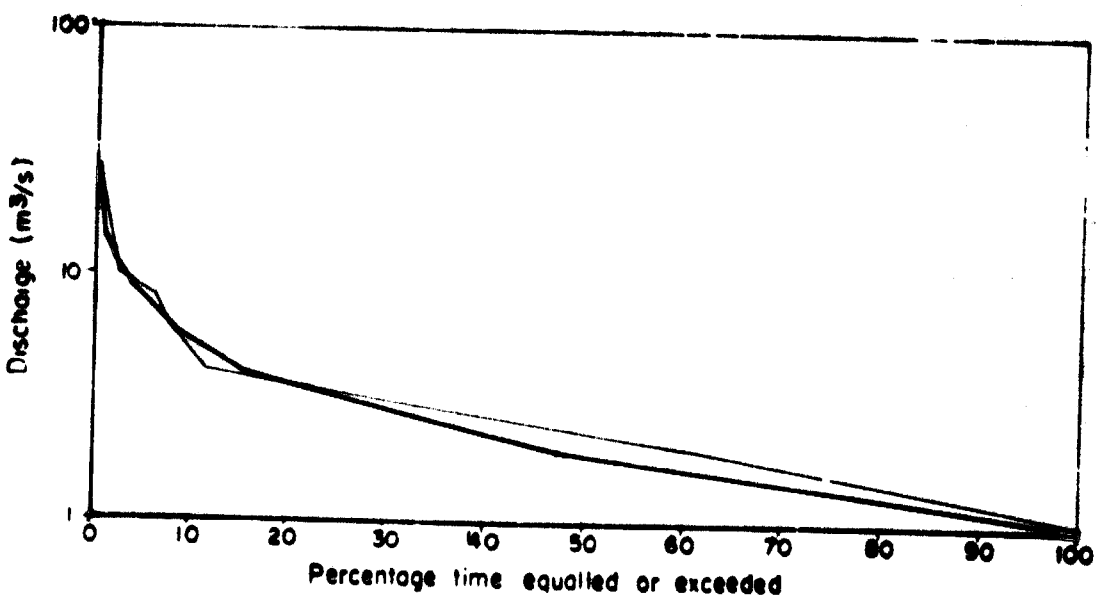

Fig.3.7: Duration curve of modelled and observed daily discharges at station N8 for period 1975-09 - 1978-08

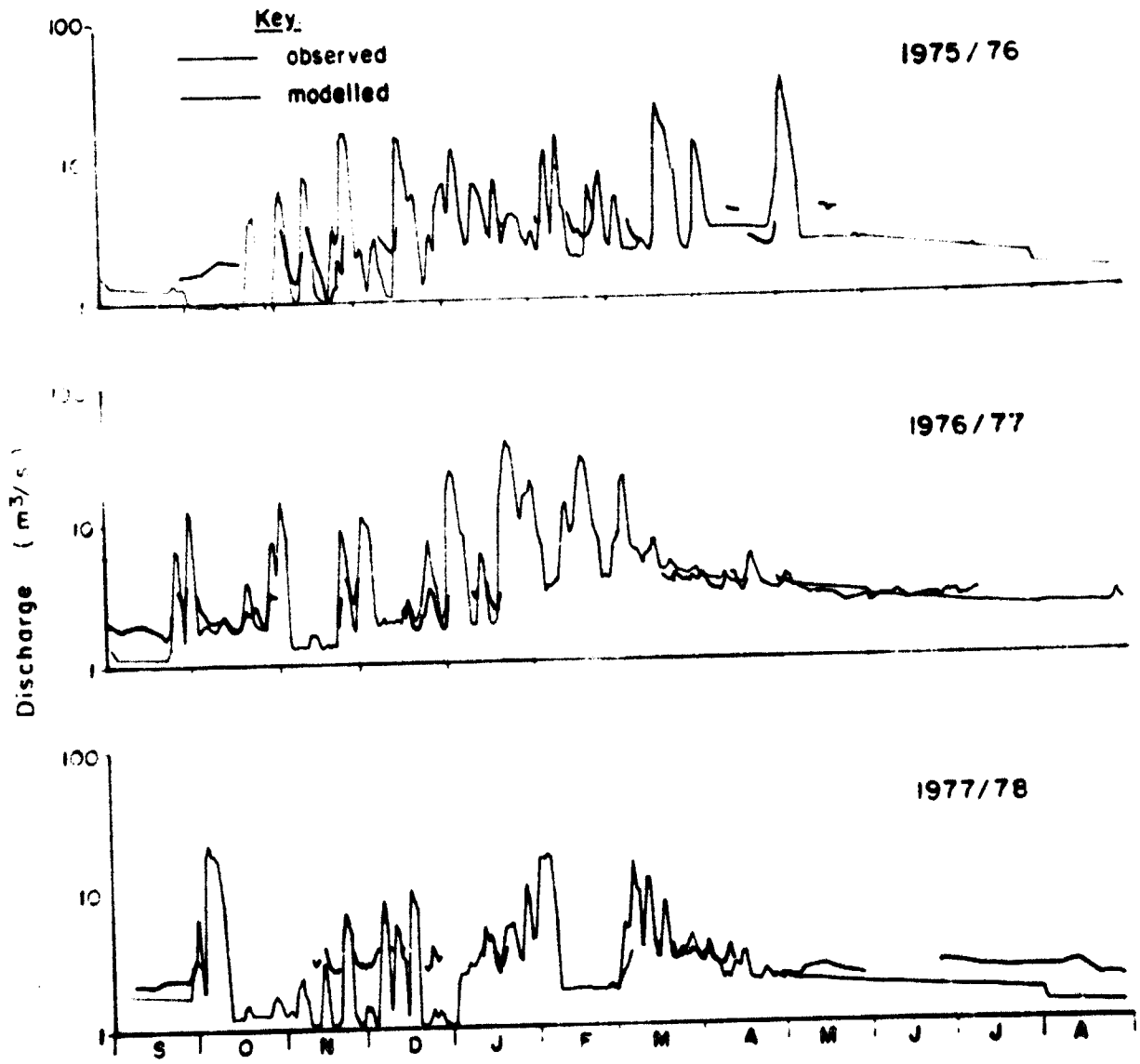

Fig.3.8: Modelled and observed daily discharges at station R6 for period 1975-09 - 1978-08

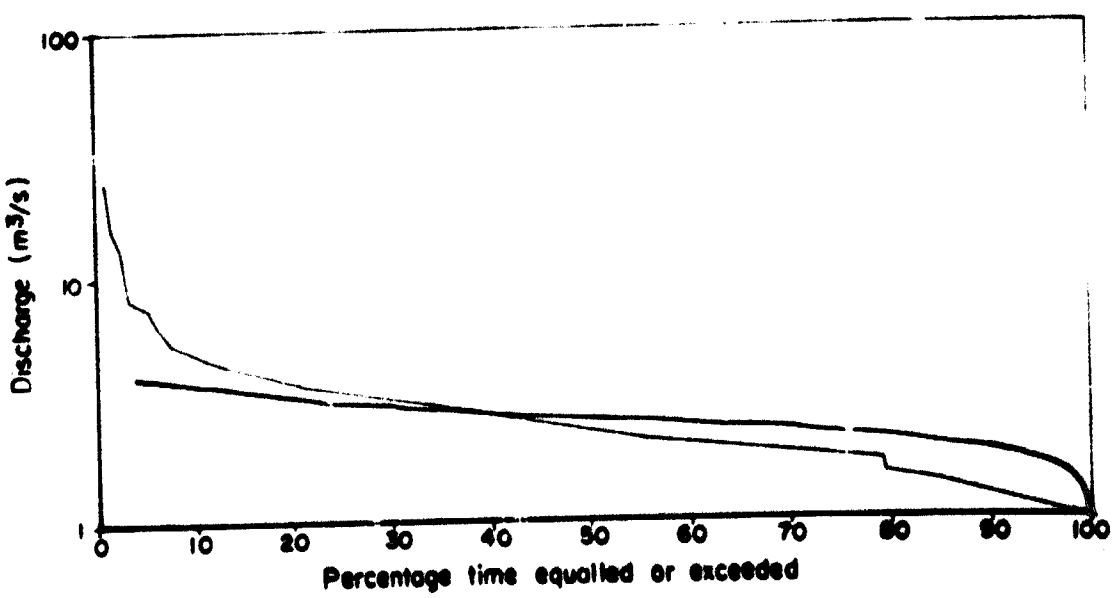

Fig.3.9: Duration curve of modelled and observed daily discharges at station R6 for period 1975-09 - 1978-08.

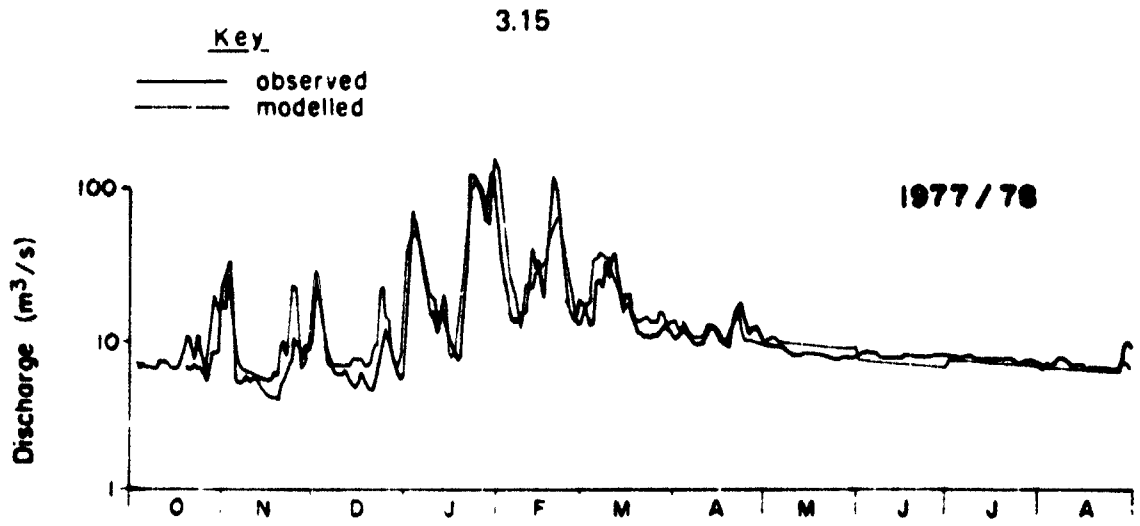

Fig. 3.10: Modelled and observed daily discharges at station C2M21 for period 1977-09 - 1978-08

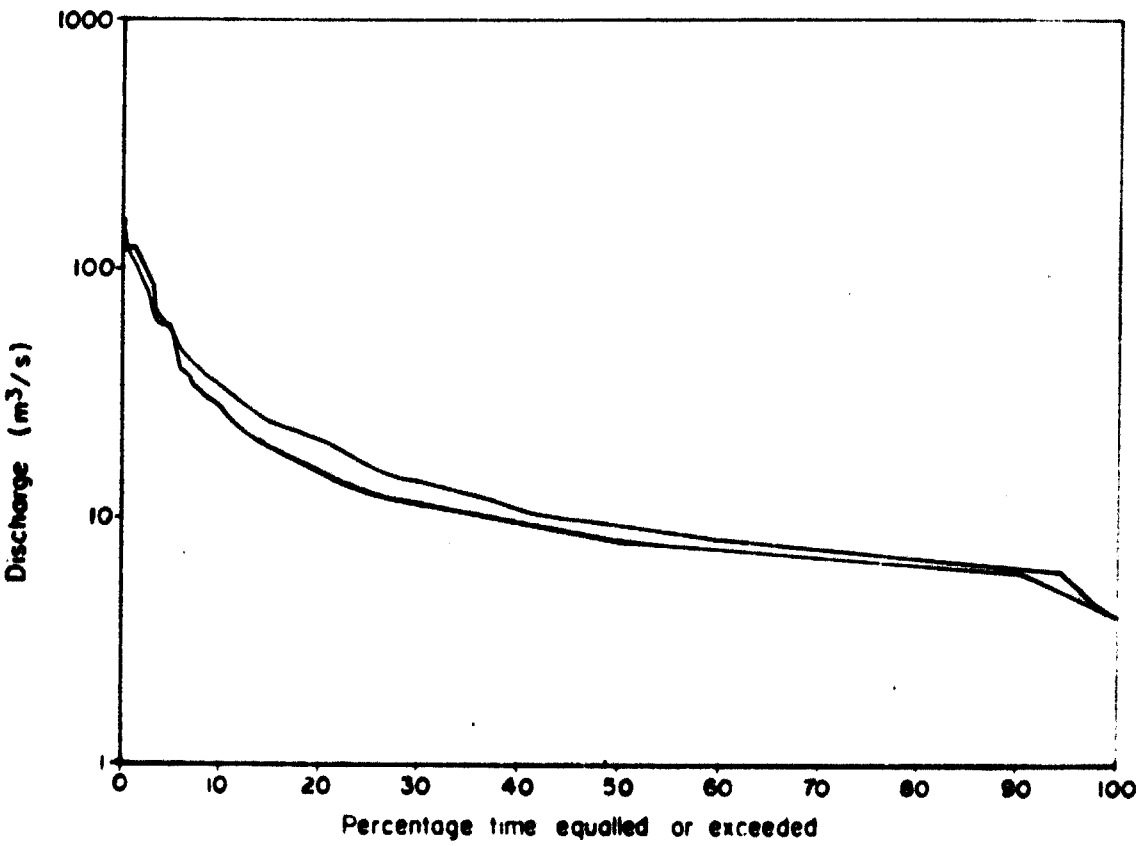

Fig. 3.11: Duration curve of modelled and observed daily discharges at station C2M21 for period 1977-09 - 1978-08

Station C2M15: C2M15 is a low level weir in the Klip river near its confluence with the Vaal. It is submerged even during moderate flows, and towards the end of the simulation period submergence even occurs during base flow conditions. This is attributable to increasing effluent inputs to the upper reaches of the Klip river. On occasion the weir is also submerged by backwater from the Vaal Barrage. The record was therefore of use only for checking the modelled base flows. Table 3.3 indicates a very low significance factor for the data sample. The inevitable consequence is a tendency for the modelled mean and standard deviation to be higher than those observed (see section 3.1). This is apparent in Fig. 3.13. Fig. 3.12 does, however, reveal a tendency for the modelled base flows to be a little high during the 1971 and 1973 dry seasons. The point flow data for these earlier years is extremely inaccurate and could contribute to the poor fit. This uncertainty, together with the absence of streamflow records for any of the other monitoring points on the Klip river during this period, precluded further refinement of the calibrations.

Station B9: Station B9 is the outflow weir from a lake, Cowles dam, on the upper reaches of the Blesbokspruit. Estimates of discharge are made daily by staff of SAPPI Fine Papers (Pty) Ltd. Only relatively small discharges are recorded. A feature of the catchment upstream of B9 is the cascade of several small dams and lakes. Details of the cross-sectional geometry of these lakes is not available and it was therefore impossible to model the catchment with acceptable accuracy. Instead, the catchment was modelled by dividing the channel into two reaches each with assumed geometry representative of a lake.

Fig. 3.14 is a plot of modelled and observed daily discharges and Fig. 3.15 gives the corresponding duration curves for the period September 1976 to August 1978.

As can be seen from Fig. 3.14 this simplified model does partially achieve the desired lag and attenuation of the flood peaks. Effluents from various municipalities enter the lakes upstream of Cowles dam, while Cowles dam itself receives effluent from the SAPPI paper factory. Evaporative loss from the lakes is not sufficient to account for the low base flows leaving Cowles dam. It therefore

Station C2M15: C2M15 is a low level weir in the Klip river near its confluence with the Vaal. It is submerged even during moderate flows, and towards the end of the simulation period submergence even occurs during base flow conditions. This is attributable to increasing effluent inputs to the upper reaches of the Klip river. On occasion the weir is also submerged by backwater from the Vaal Barrage. The record was therefore of use only for checking the modelled base flows. Table 3.3 indicates a very low significance factor for the data sample. The inevitable consequence is a tendency for the modelled mean and standard deviation to be higher than those observed (see section 3.1). This is apparent in Fig. 3.13. Fig. 3.12 does, however, reveal a tendency for the modelled base flows to be a little high during the 1971 and 1973 dry seasons. The point flow data for these earlier years is extremely inaccurate and could contribute to the poor fit. This uncertainty, together with the absence of streamflow records at any of the other monitoring points on the Klip river during this period, precluded further refinement of the calibrations.

Station B9: Station B9 is the outflow weir from a lake, Cowles dam, on the upper reaches of the Blesbokspruit. Estimates of discharge are made daily by staff of SAPPI Fine Papers (Pty) Ltd. Only relatively small discharges are recorded. A feature of the catchment upstream of B9 is the cascade of several small dams and lakes. Details of the cross-sectional geometry of these lakes is not available and it was therefore impossible to model the catchment with acceptable accuracy. Instead, the catchment was modelled by dividing the channel into two reaches each with assumed geometry representative of a lake.

Fig. 3.14 is a plot of modelled and observed daily discharges and Fig. 3.15 gives the corresponding duration curves for the period September 1976 to August 1978.

As can be seen from Fig. 3.14 this simplified model does partially achieve the desired lag and attenuation of the flood peaks. Effluents from various municipalities enter the lakes upstream of Cowles dam, while Cowles dam itself receives effluent from the SAPPI paper factory. Evaporative loss from the lakes is not sufficient to account for the low base flows leaving Cowles dam. It therefore

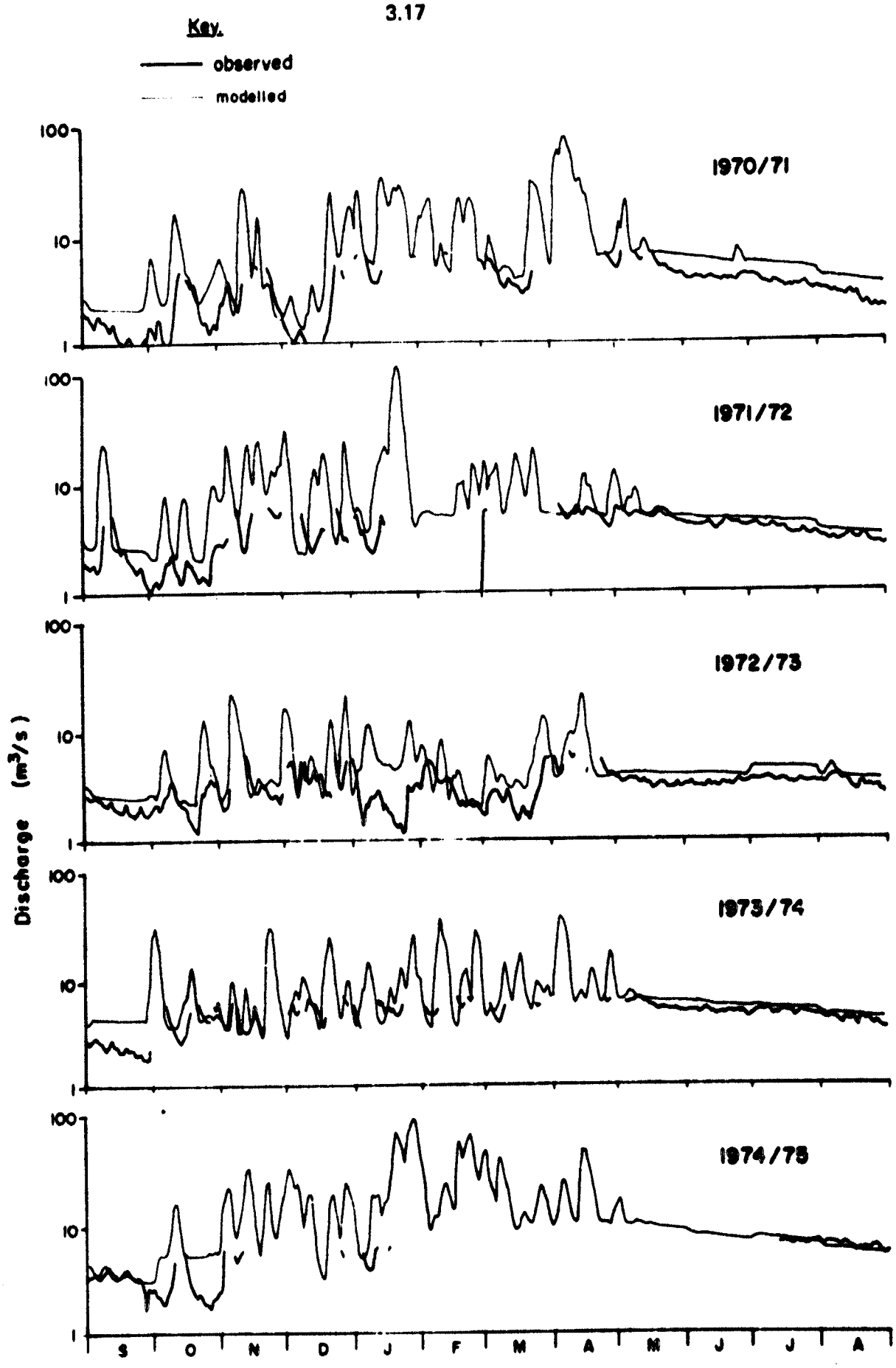

Fig. 3.12 : Modelled and observed daily discharges at station C2M15 for period 1970-09 - 1978-08

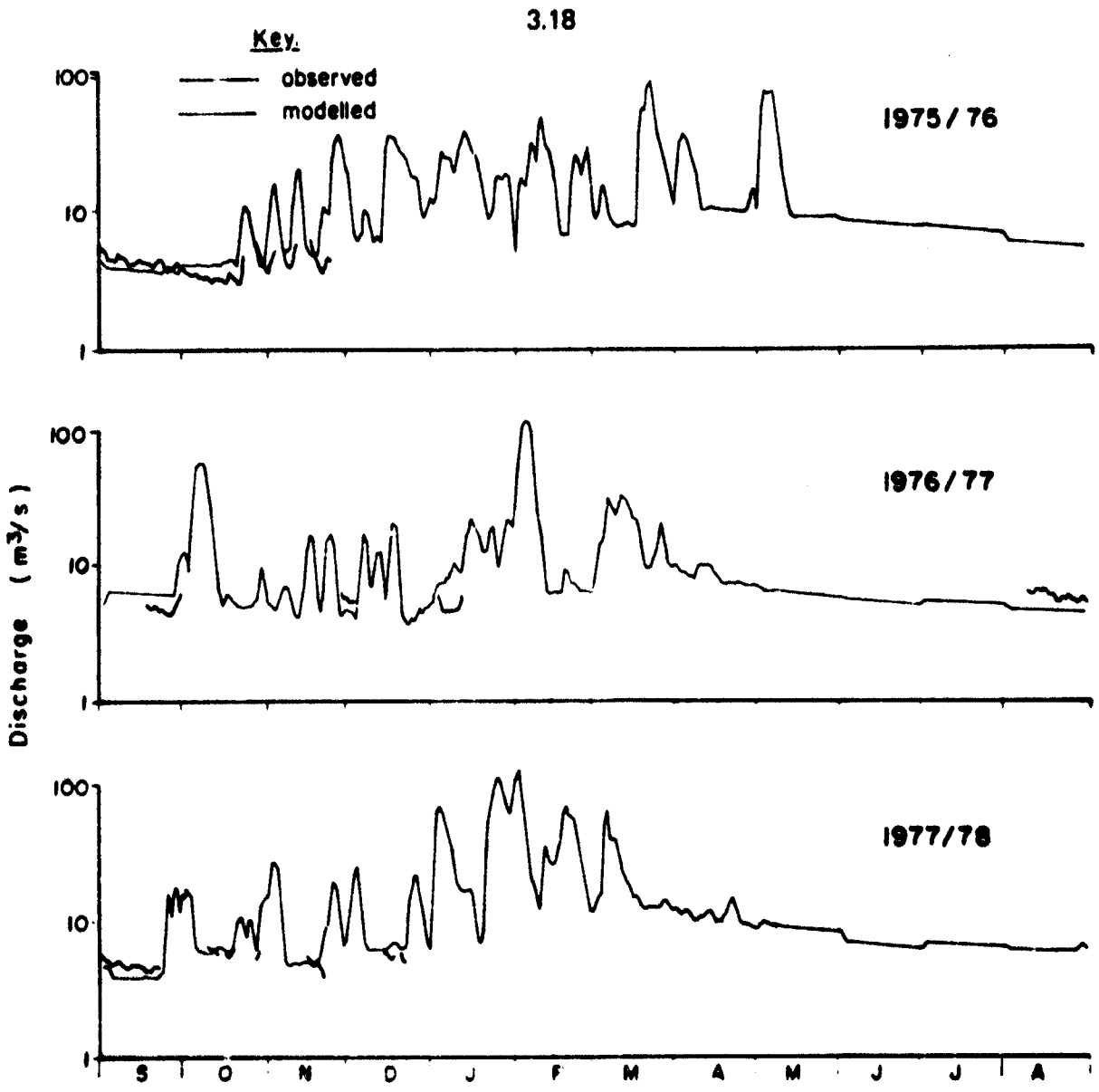

Fig.3.12: Modelled and observed daily discharges at station C2M15 for period 1970-09 - 1978-08

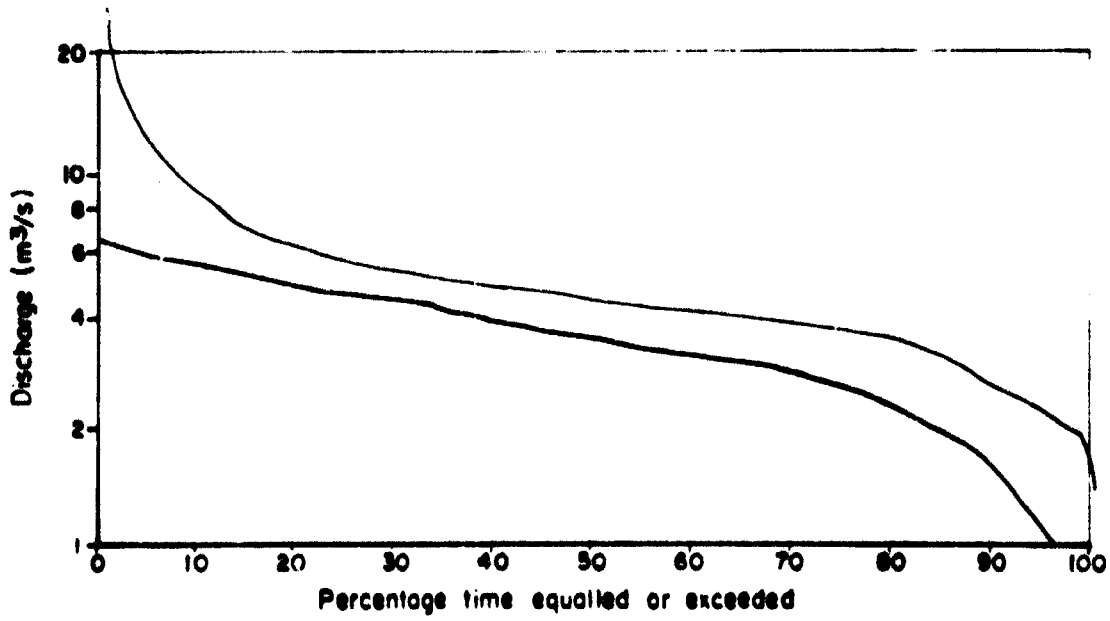

Fig.3.13: Duration curve of modelled and observed daily discharges at station C2M15 for period 1970-09 - 1978-08

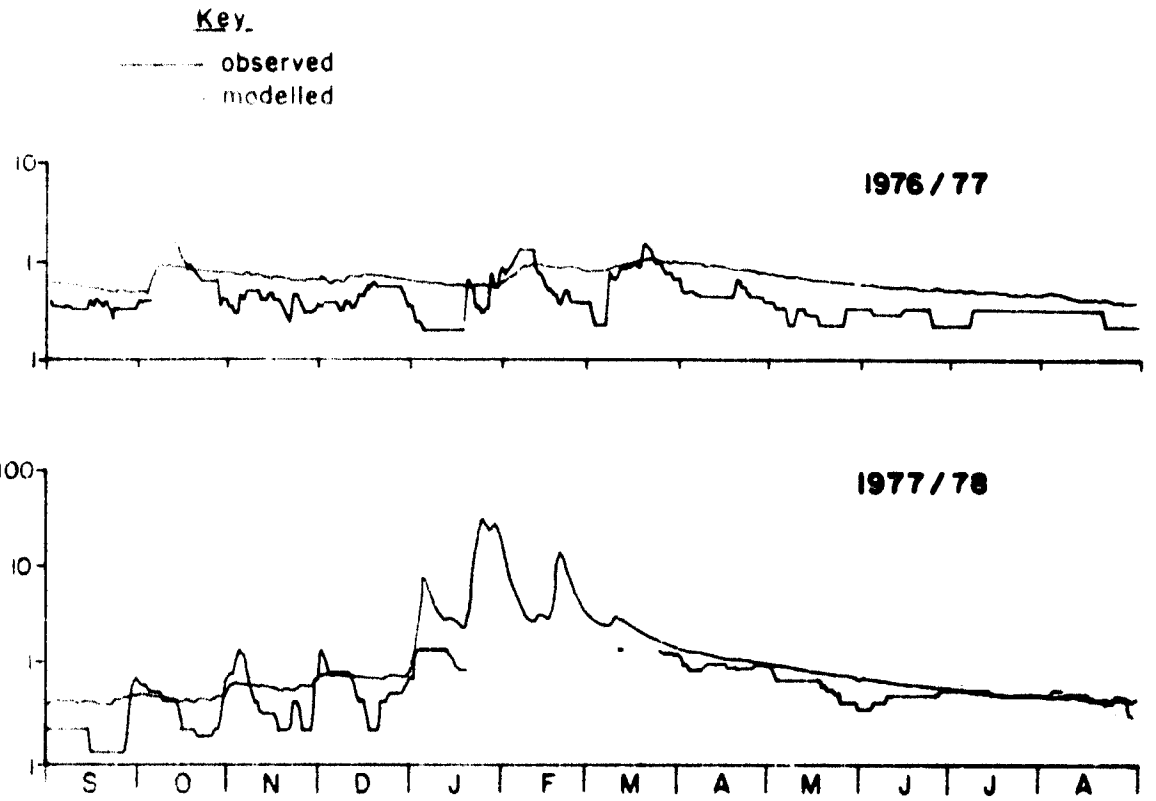

Fig. 3.14: Modelled and observed daily discharges at station B9 for period 1976-09 - 1978-08

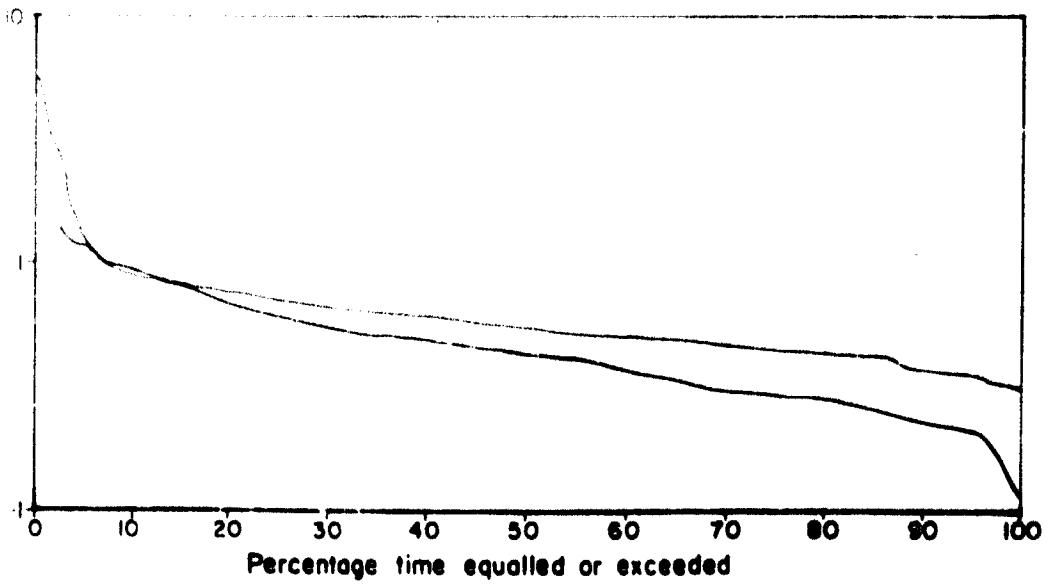

Fig. 3.15: Duration curve off modelled and observed daily discharges at station B9 for period 1976-09 - 1978-08

became necessary to hypothesise a considerable seepage loss from reach number 8 (i.e. the lakes upstream of Cowles Dam). This is not unreasonable as the underlying dolomitic rock strata have been extensively de-watered by gold mining activities. As with station C2M15 the significance factor is low and a poor fit is to be expected. The uncertainties in the lake storages and outlet controls further reduce the goodness of fit which could be achieved. Although the fit is not particularly good, the effect of the inaccuracies is not too serious in terms of the entire Suikerbosrand catchment as is evidenced by the good fit further downstream at station C2M70 and C2M04.

Station B10: The weir at B10 is located in a well defined, stable section of the Blesbokspruit and forms a good control. It was therefore possible to interpret the water level record for a wide range of discharges using Weiss's flood plain model. Unfortunately the record is short and the level recorder is prone to jam. Between stations B9 and B10 lies a vast vlei 45 km^2 in extent which in places is up to 1200m wide. The cross-sectional geometry is unknown and had to be assumed (Herold, 1981). It can be expected that during high flows the reeds will be flattened by flowing water with a resultant drastic change in the roughness coefficient. This makes calibration extremely difficult. Changes such as burning of the reeds, dredging of channels and changes to bridge openings compound these difficulties. The fit obtained is nevertheless adequate as may be seen by the good fit at stations C2M70 and C2M04. Fig. 3.16 is a plot of modelled and observed daily discharges and Fig. 3.17 shows the corresponding duration curves.

Station C2M70: C2M70 is an unstable bridge section of the Suikerbosrand downstream of the confluence with the Blesbokspruit which has been rated for a wide range of flows by the Directorate of Water Affairs (Murphy, 1978). From Fig. 3.2 it can be seen that a large portion of the Suikerbosrand catchment lies between gauges B10 and C2M70. Due to the poor runoff record at B10 it was not possible to differentiate accurately between runoff from the Blesbokspruit and that from the upper reaches of the Suikerbosrand. Despite these difficulties it was possible to obtain a reasonably good fit at C2M70.

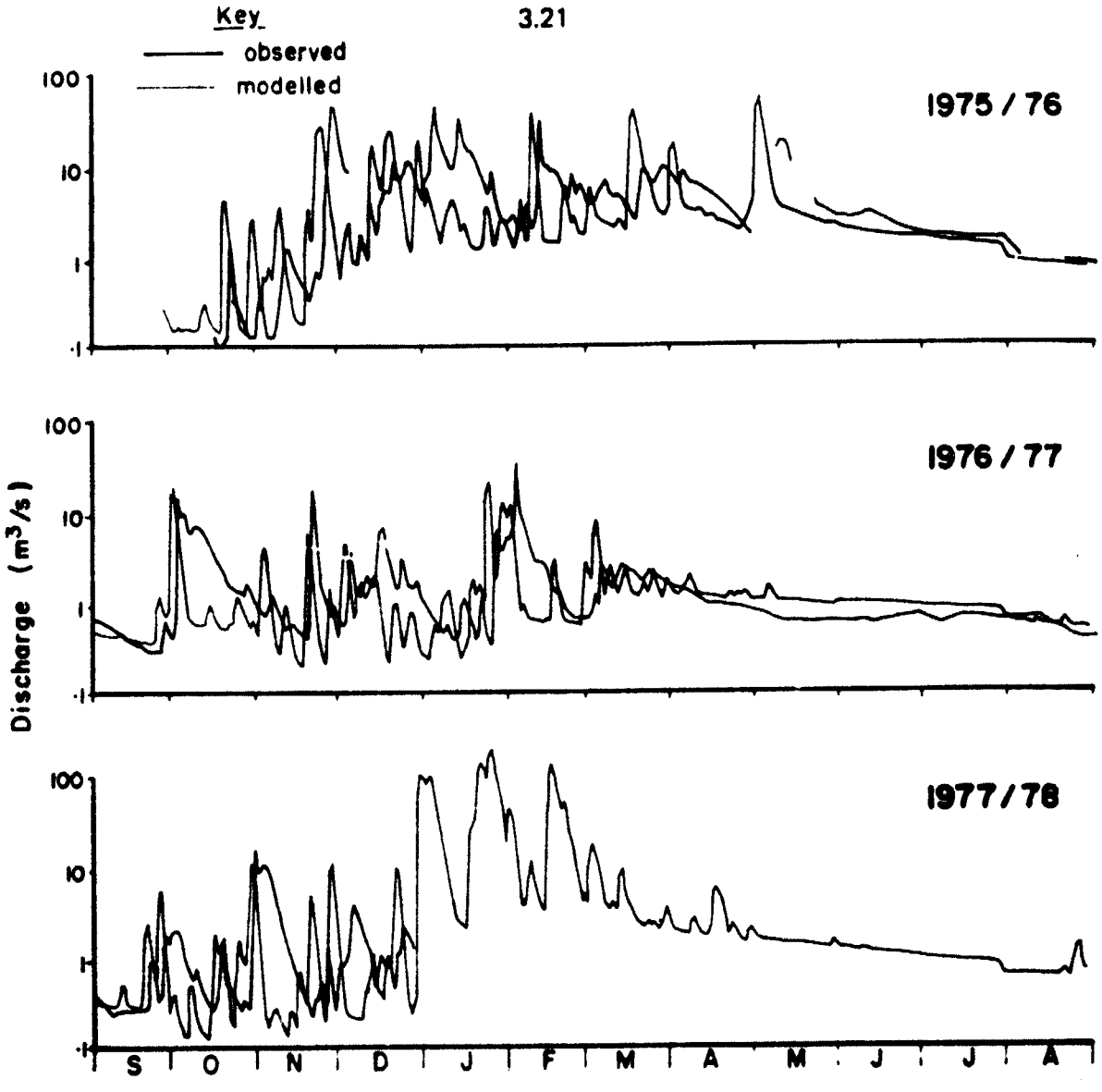

FIG. 3.16: Modelled and observed daily discharges at station B10 for period 1975-10 - 1978-08.

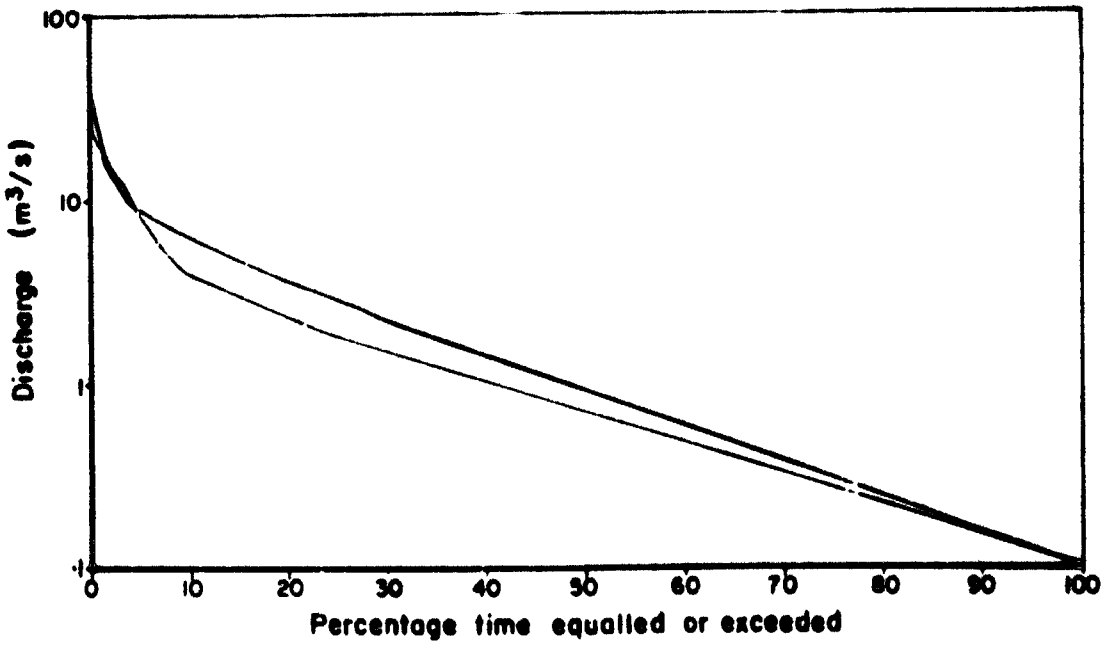

FIG. 3.17: Duration curve of modelled and observed daily discharges at station B10 for period 1975-10 - 1978-08.

Fig. 3.18 is a plot of modelled and observed daily discharges while Fig. 3.19 shows the corresponding duration curves.

From Fig. 3.18 it can be seen that the modelled discharges during the dry season of 1977 are somewhat lower than those observed. This is in conflict with the situation at C2M04 (see Fig. 3.20) where modelled and observed values are seen to be more closely in agreement. Attempts to improve the fit at C2M70 lead to a deterioration at C2M04 and necessitate the assumption of high seepage losses between the two stations which cannot readily be justified by the geology. Greater emphasis was therefore placed upon the longer and more accurate record at station C2M04.

Station C2M04: C2M04 is a well constructed weir situated in a well defined valley. The channel section forms a good control and it was possible to rate the station for a wide range of discharges using the Weiss flood plain model. The flow record is both long and reliable. Table 3.3 and Figs. 3.20 and 3.21 show that a good fit between modelled and observed discharges has been obtained.

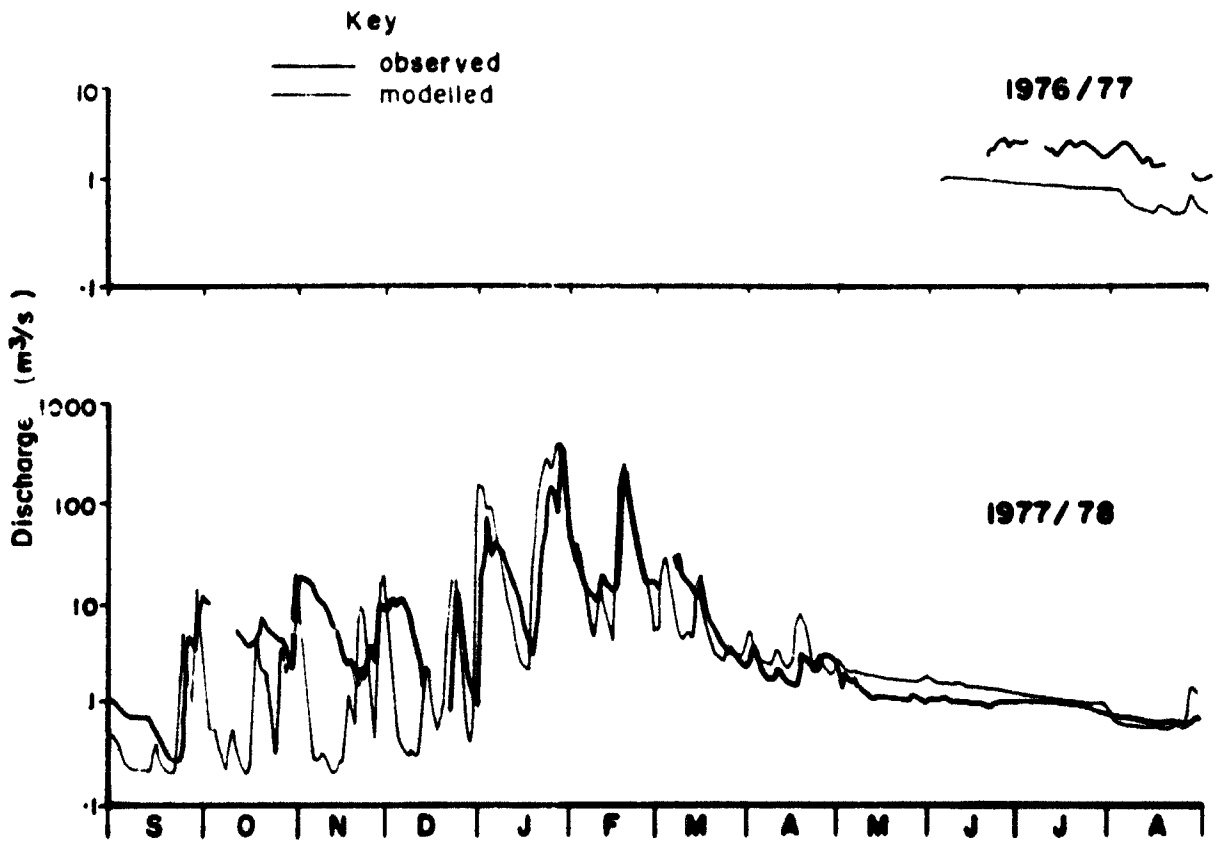

FIG. 3.18: Modelled and observed daily discharges at station C2M70 for period 1977-06 - 1978-08.

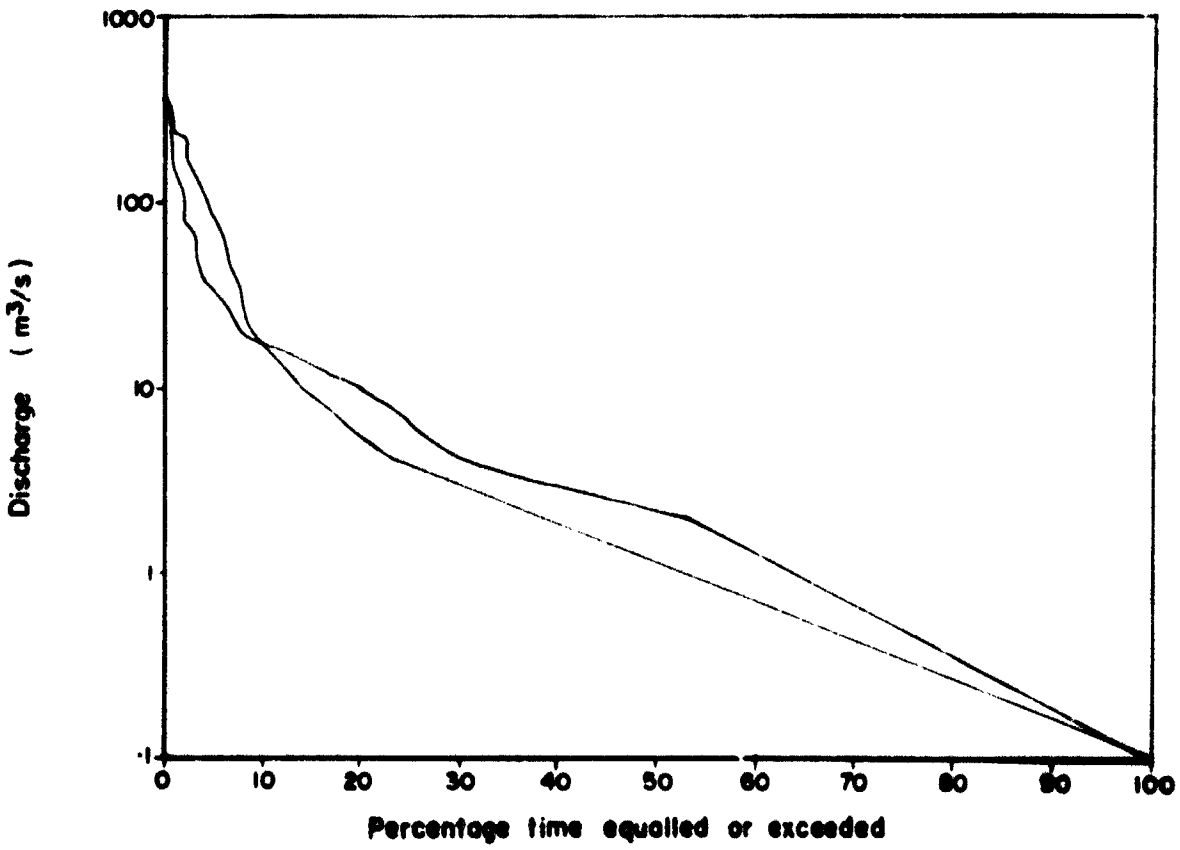

Fig. 3.19: Duration curve of modelled and observed daily discharges at station C2M70 for period 1977-06 - 1978-08.

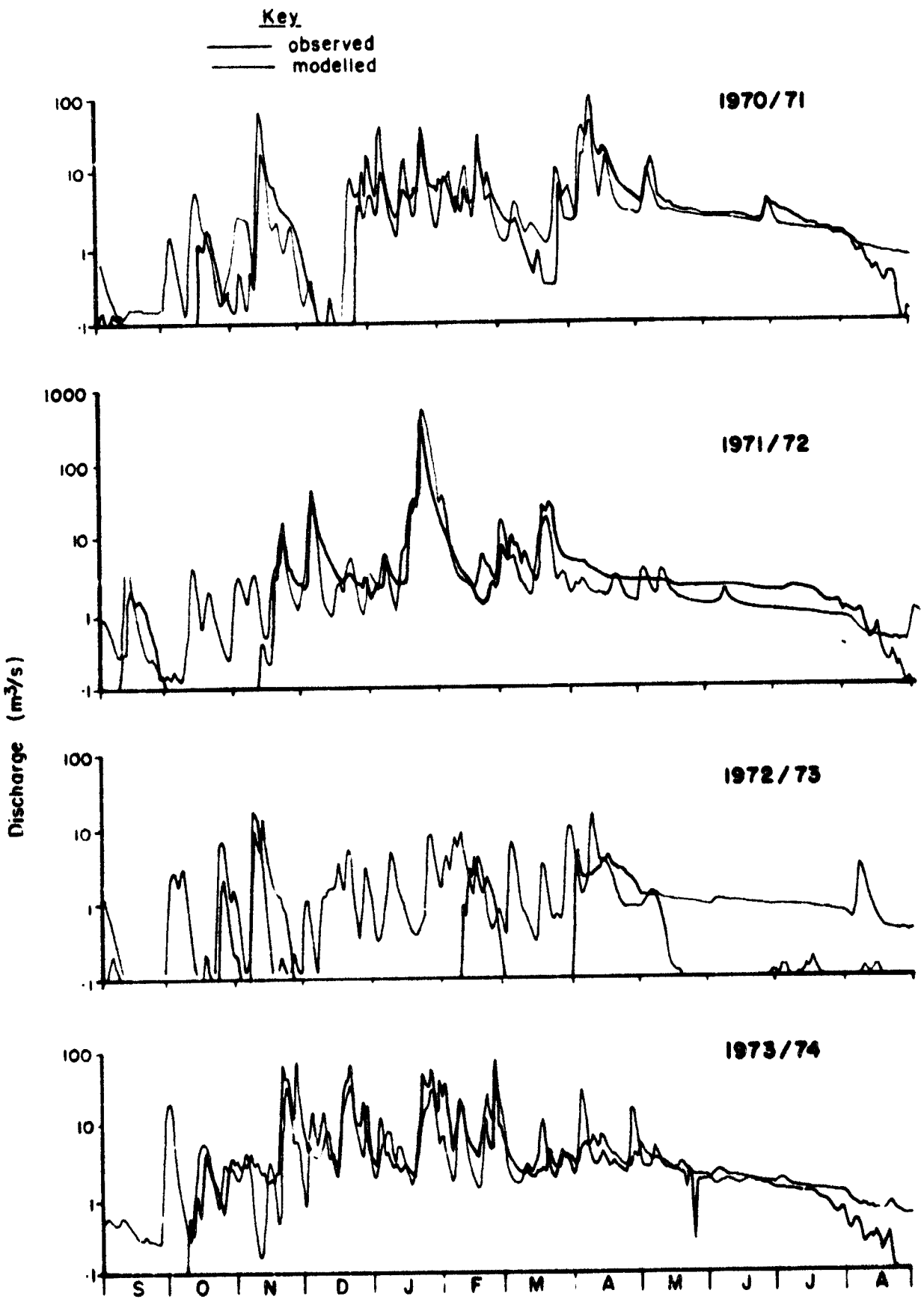

Fig. 3.20: Modelled and observed daily discharges at station C2M04 for period 1970-09-1978-08.

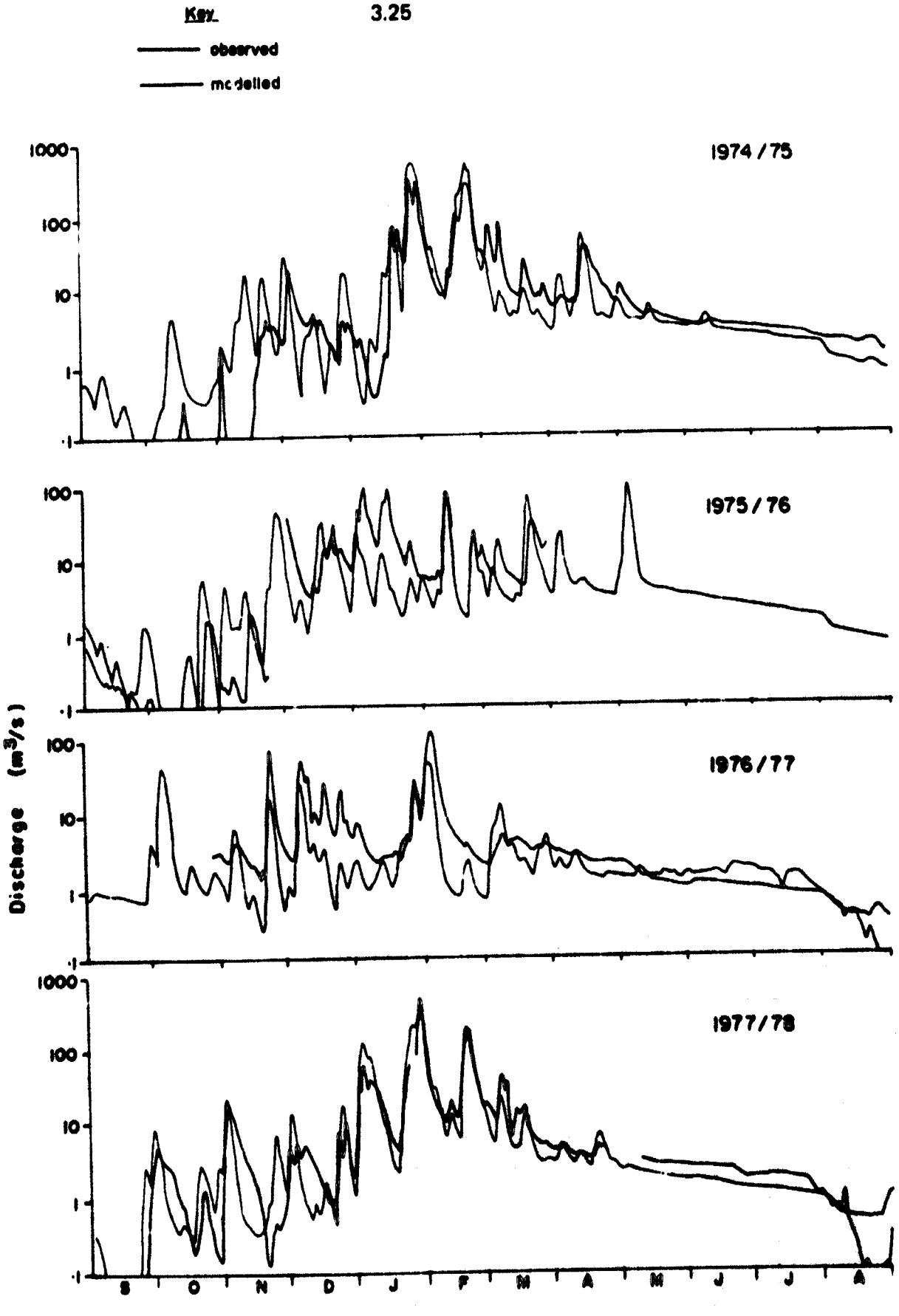

Fig. 3.20 : Modelled and observed daily discharges at station C2M04 for period 1970-09 -- 1978-08

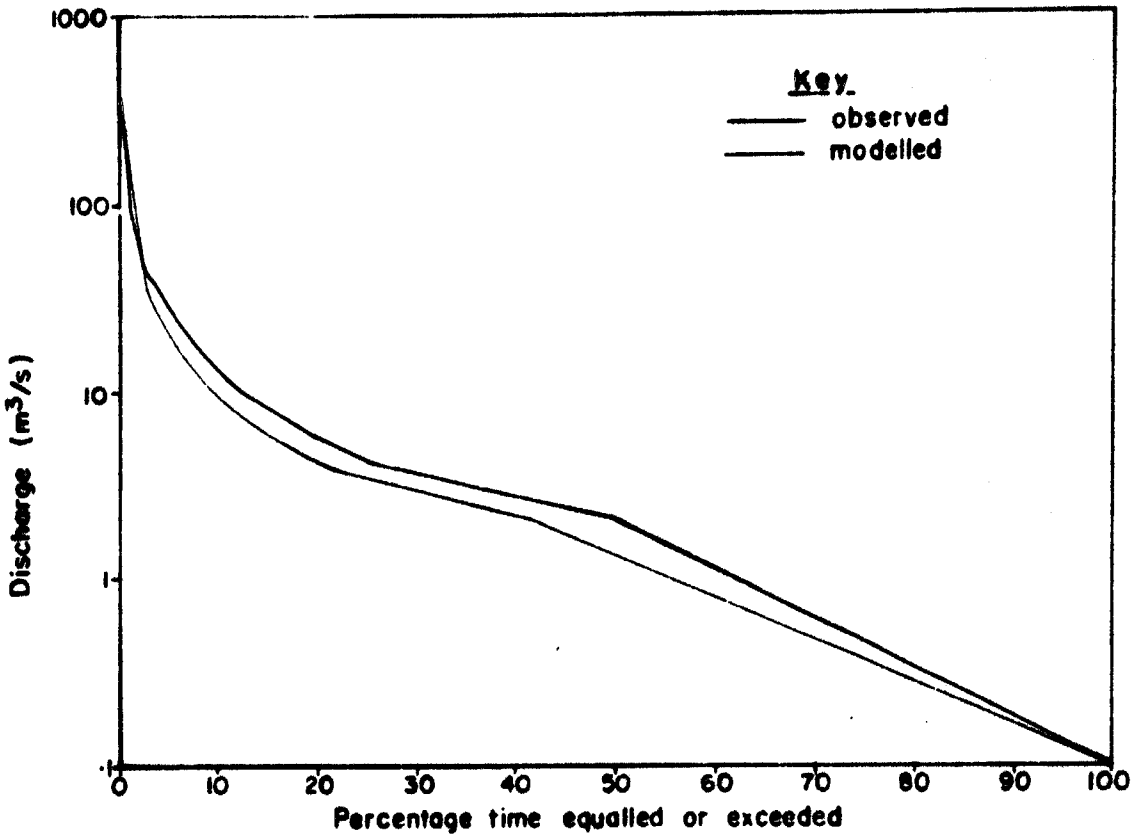

Fig. 3.21: Duration curve of modelled and observed daily discharges at station C2M04 for period 1970-09 - 1978-08.

Station C2M05: C2M05 is a low level weir located in the Rietspruit (not to be confused with the Rietspruit which is a tributary of the Klip river) near its confluence with the Vaal. The channel is not stable and the weir, being situated in a wide, flat flood plain, is not a particularly good control. The Weiss flood plain model was used to interpret the water level record for a wide range of discharges but it must be emphasised that the margin of error in the rating curve is appreciable, particularly for higher discharges. However, from Table 3.3 and Figs. 3.22 and 3.23 it can be seen that a reasonably good fit was obtained.